15. Deutsches LS-Dyna Forum 2018

Integration neuer graphischer Auswertemethoden zur verbesserten Erkennung von Blechversagen unter dem Einfluss nicht-linearer Dehnungspfade

P. Hora, L. Tong, N. Manopulo

Experiments n.l. FLC: W. Volk, Ch. Gaber, UTG

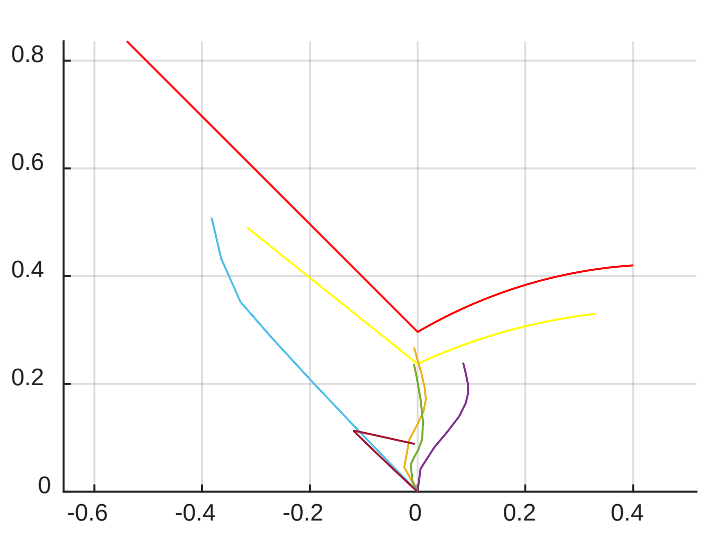

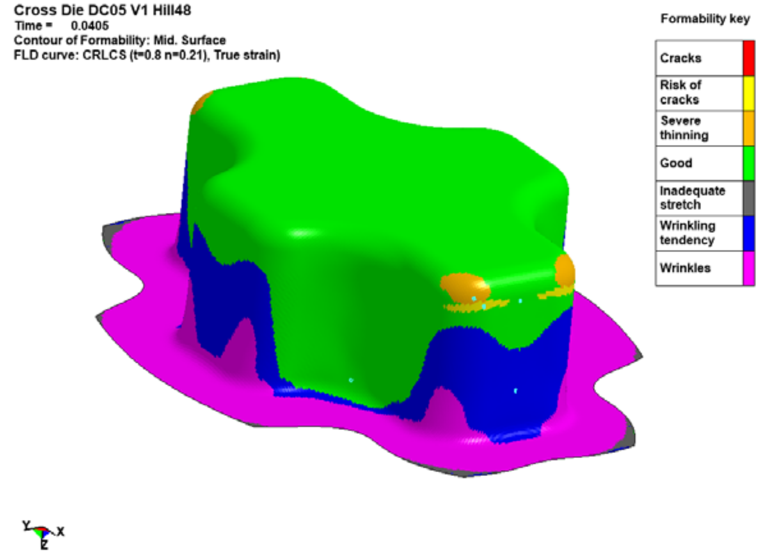

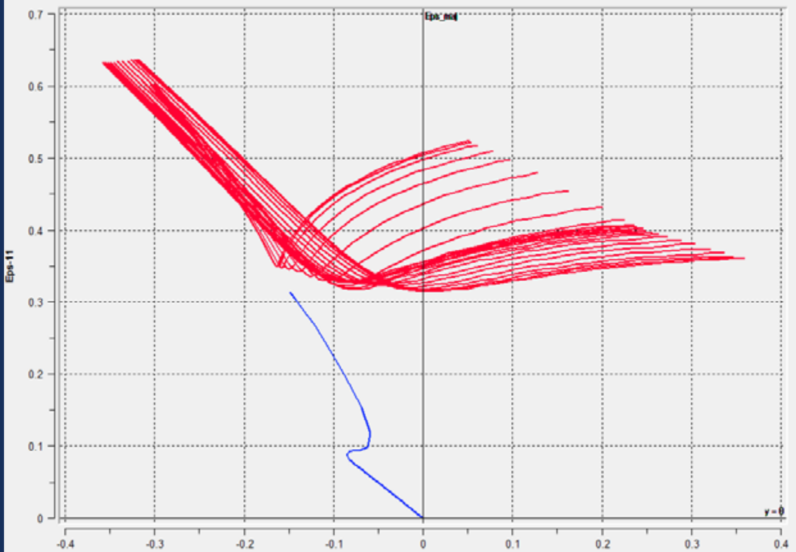

Content

IVP research fields

IVP-FEM
Special purpose
ALE

Planning tools
- FEINTOOL
- ETG
- HydroPlan

Material models
- TRIP
- ETG
- PH
- HAH
- LD-FLC

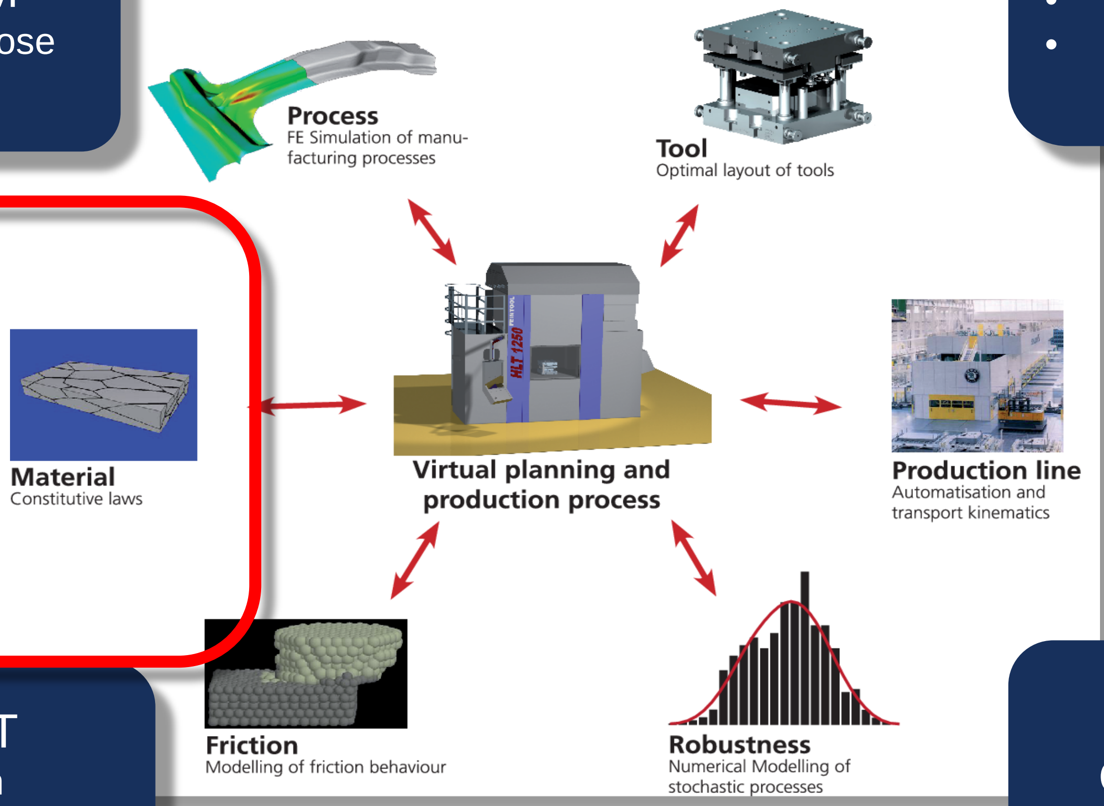

Sensors
- EC-Mat
- DB-Force

CTT
- Friction models
- New test

Q-Guard

IVP's LS-Dyna developments

- Development of stainless steel material models (MAT_TRIP Hänsel model)
- Development of press hardening material models (22MnB5)
- Implementation of YLD2000 and HAH with distortional hardening
- Development of combined neckig-crack failure models for multilayer Al-sheets (FUSION)
- Implementation of non associated flow rules (NAFR) in combination with YLD2000
- ……..
- Application in many «engineering» cases

1.4301 metastable behavior

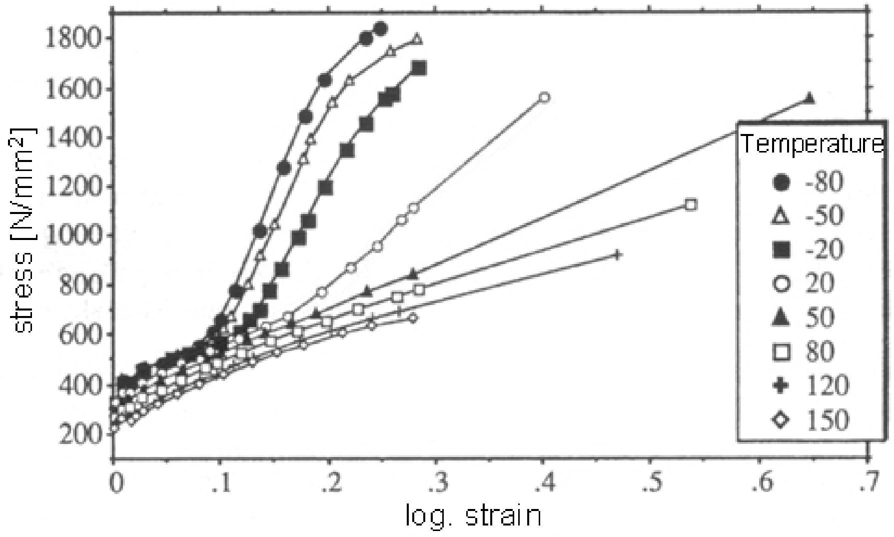

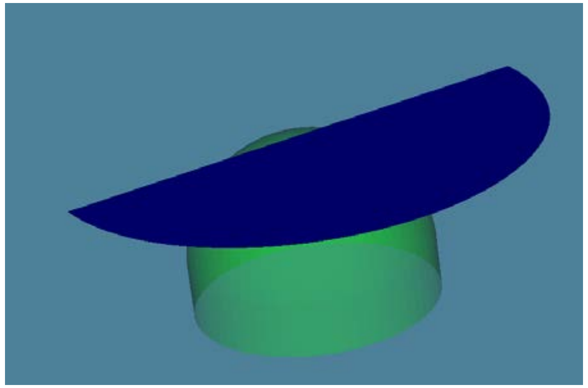

$$k_f^{ges} = \left[B_{HS} - \left(B_{HS} - A_{HS}\right)\cdot \exp\left(-m\cdot\varepsilon^n\right)\right]\cdot f_2(T) + \Delta k_f^{\gamma\rightarrow\alpha'}\cdot V_M$$

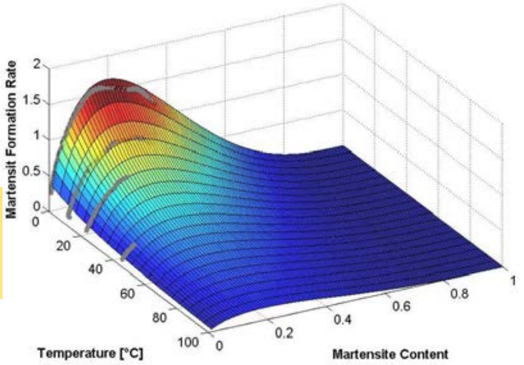

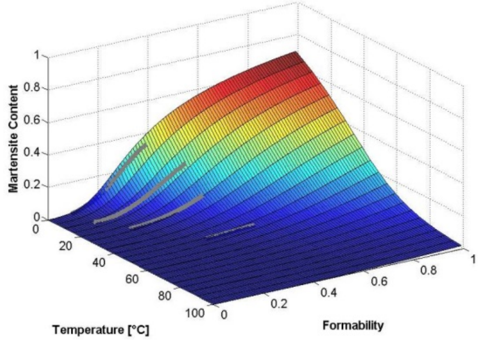

$$\frac{dV_M}{d\varepsilon} = \frac{B}{A}\cdot e^{\frac{Q}{T}}\cdot\left(\frac{1-V_M}{V_M}\right)^{\frac{1+B}{B}}\cdot V_M{}^p\cdot\left[0.5\cdot\left(1-\tanh\left(C+D\cdot T\right)\right)\right]$$

$$V_M = \int_0^{\varepsilon}\frac{dV_M}{d\varepsilon}\,d\varepsilon$$

Source: J.Krauer Diss. ETH 2010
A.Hänsel, Diss. ETH 1998

Hänsel Model (MAT_TRIP)

- Description by Hänsel

Hardening curve	A_{HS}	B_{HS}	m	n	K
	297.5	1542.1	2.39	1.0	0.001827

Martensite parameters	A	B	C	D	p	Q	E_0
	0.83	0.168	-47.892	0.0	8.011	1376.15	0.2

$$k_f^{ges} = \left[B_{HS} - \left(B_{HS} - A_{HS}\right)\cdot \exp\left(-m\cdot\varepsilon^{n}\right)\right]\cdot f_2(T) + \Delta k_f^{\gamma\to}$$

Startbedingung für Hänsel-Funktion: if ($\varepsilon_{eq} > E_o$) t

***MAT_TRIP**

This is Material Type 113. This isotropic elasto-plastic material model applies to shell elements only. It features a special hardening law aimed at modelling the temperature dependent hardening behavior of austenitic stainless TRIP-steels. TRIP stands for Transformation Induced Plasticity. A detailed description of this material model can be found in Hänsel, Hora, and Reissner [1998] and Schedin, Prentzas, and Hilding [2004].

Card Format (I10, 7E10.0)

Card 1	1	2	3	4	5	6	7	8
Variable	MID	RO	E	PR	CP	T0	TREF	TA0
Type	A8	F	F					
Default								

Card Format (8E10.0)

Card 2	1	2	3	4	5	6	7	8
Variable	A	B	C	D	P	Q	E0MART	VM0
Type	F	F						
Default								

Card Format (8E10.0)

Card 3	1	2	3	4	5	6	7	8
Variable	AHS	BHS	M	N	EPS0	HMART	K1	K2
Type								
Default								

Complex constitutive models in metal forming

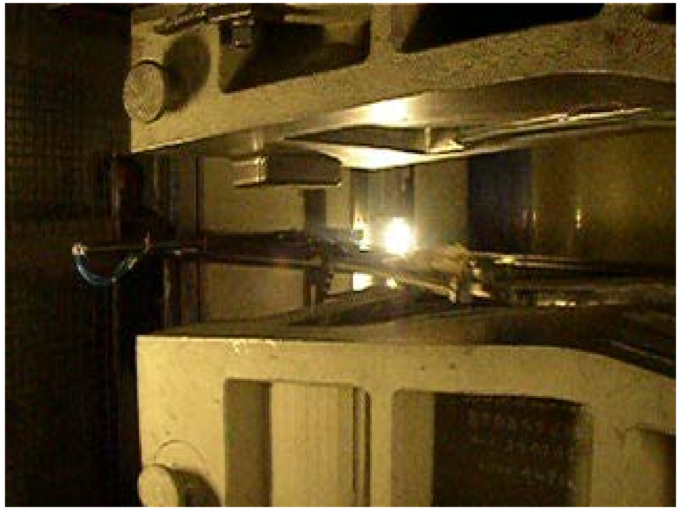

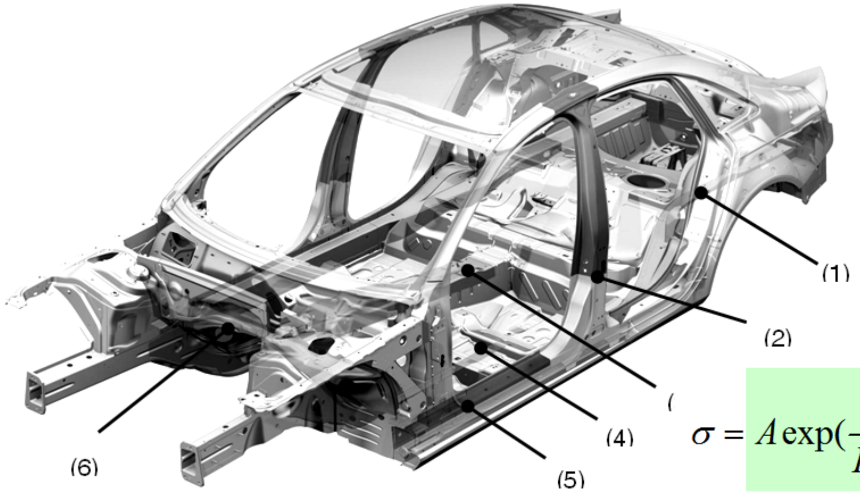

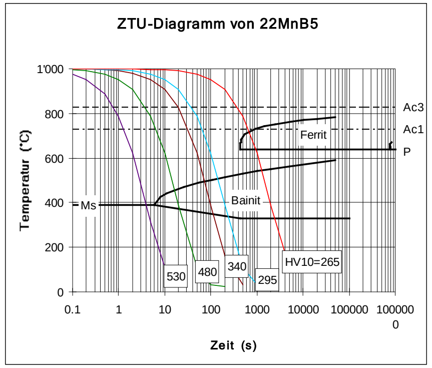

$$\sigma = A\exp(\frac{\tilde{Q}}{RT})\dot{\varepsilon}^m \left\{1+\alpha\exp\left[-c(\varepsilon-\varepsilon_o)^2\right]\right\}\left[1-\beta\exp(-N\varepsilon^n)\right]$$

Strain rate | Softening for $\varepsilon > \varepsilon_o$ | Strain hardening

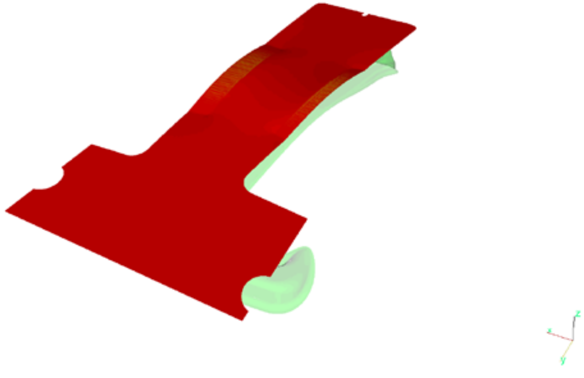

Prediction of “crash” material behavior

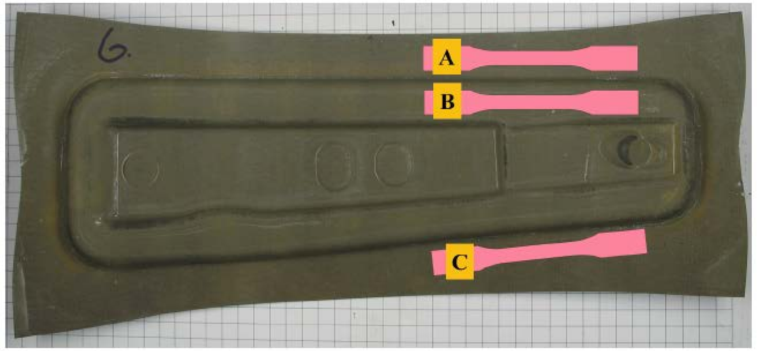

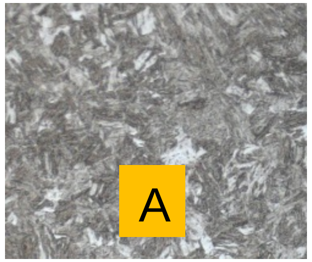

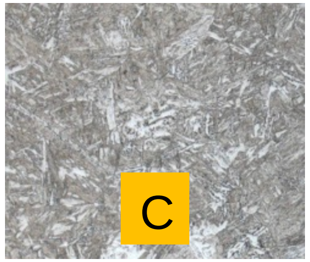

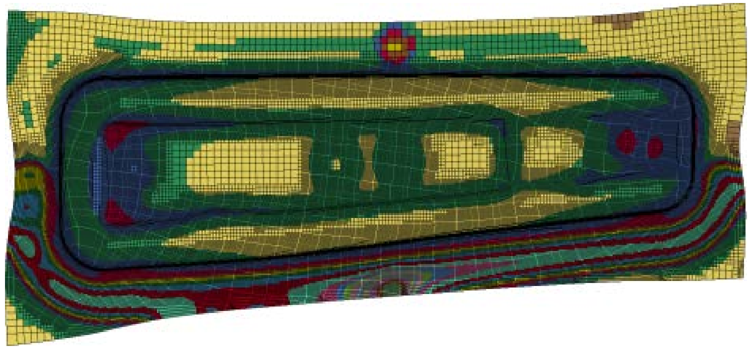

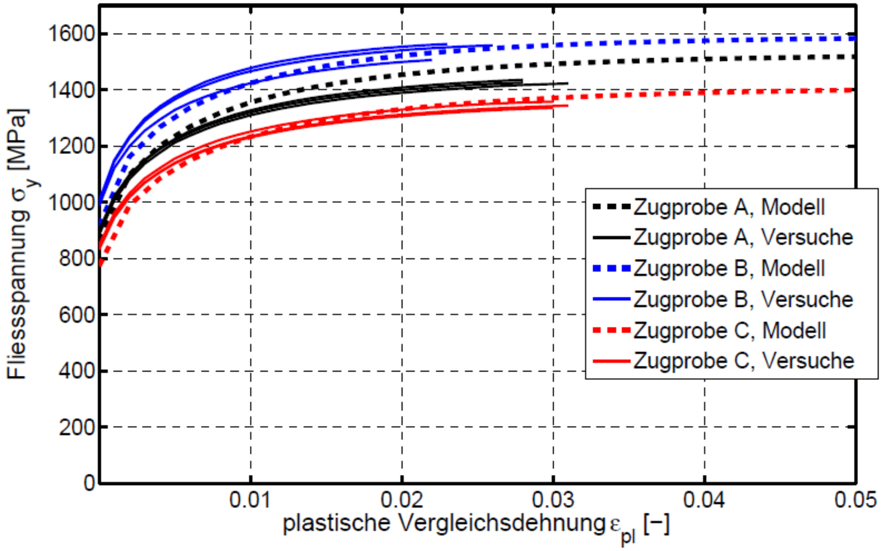

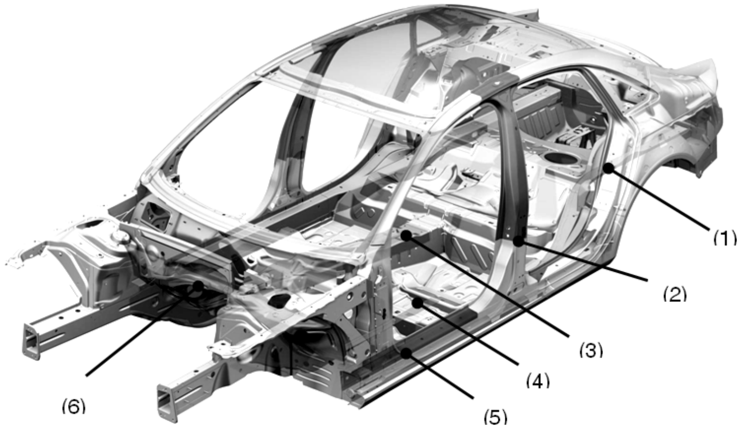

Source: B. Hochholdinger Diss. ETH 2012

Development of combined neckig-crack failure models for multilayer Al-sheets (FUSION)

Monolayer AC

FUSION

Source: M.Gorji Diss. ETH 2015

Monolayer AC170

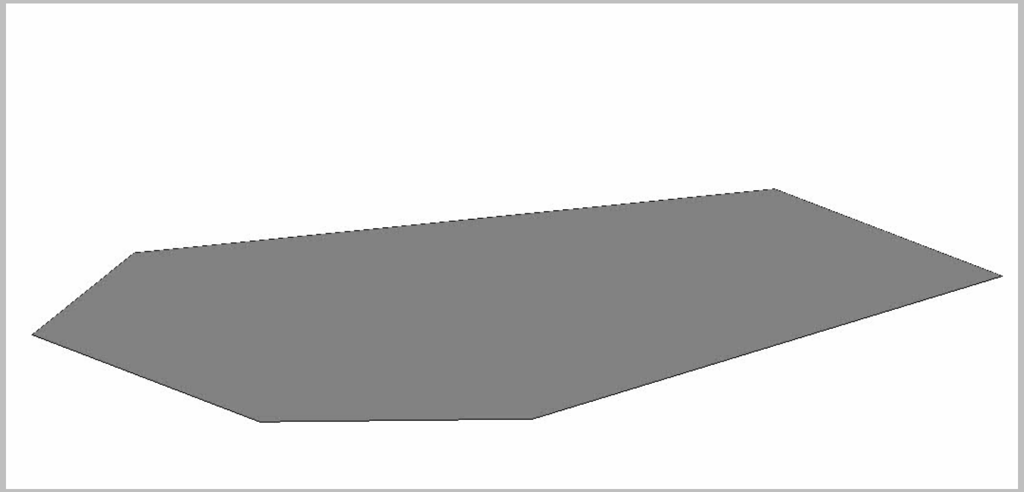

FUSION

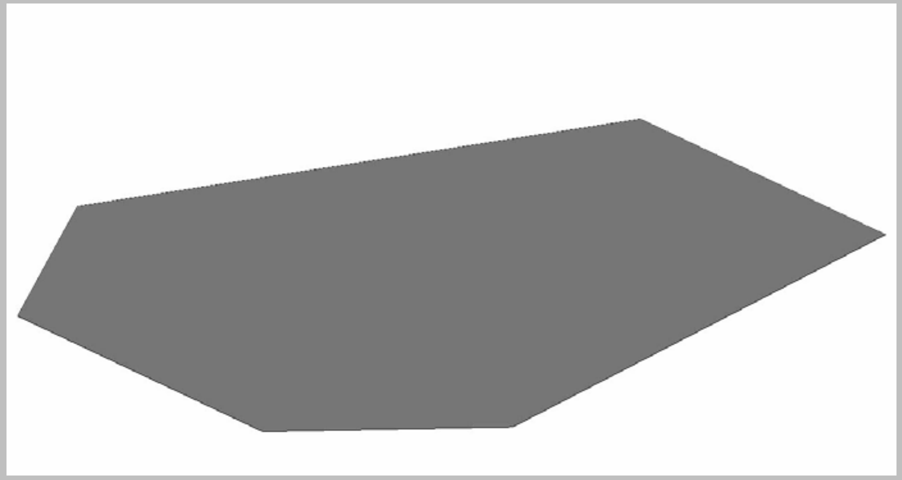

Source: M.Gorji Diss. ETH 2015

Impact of constitutive models on FEM results

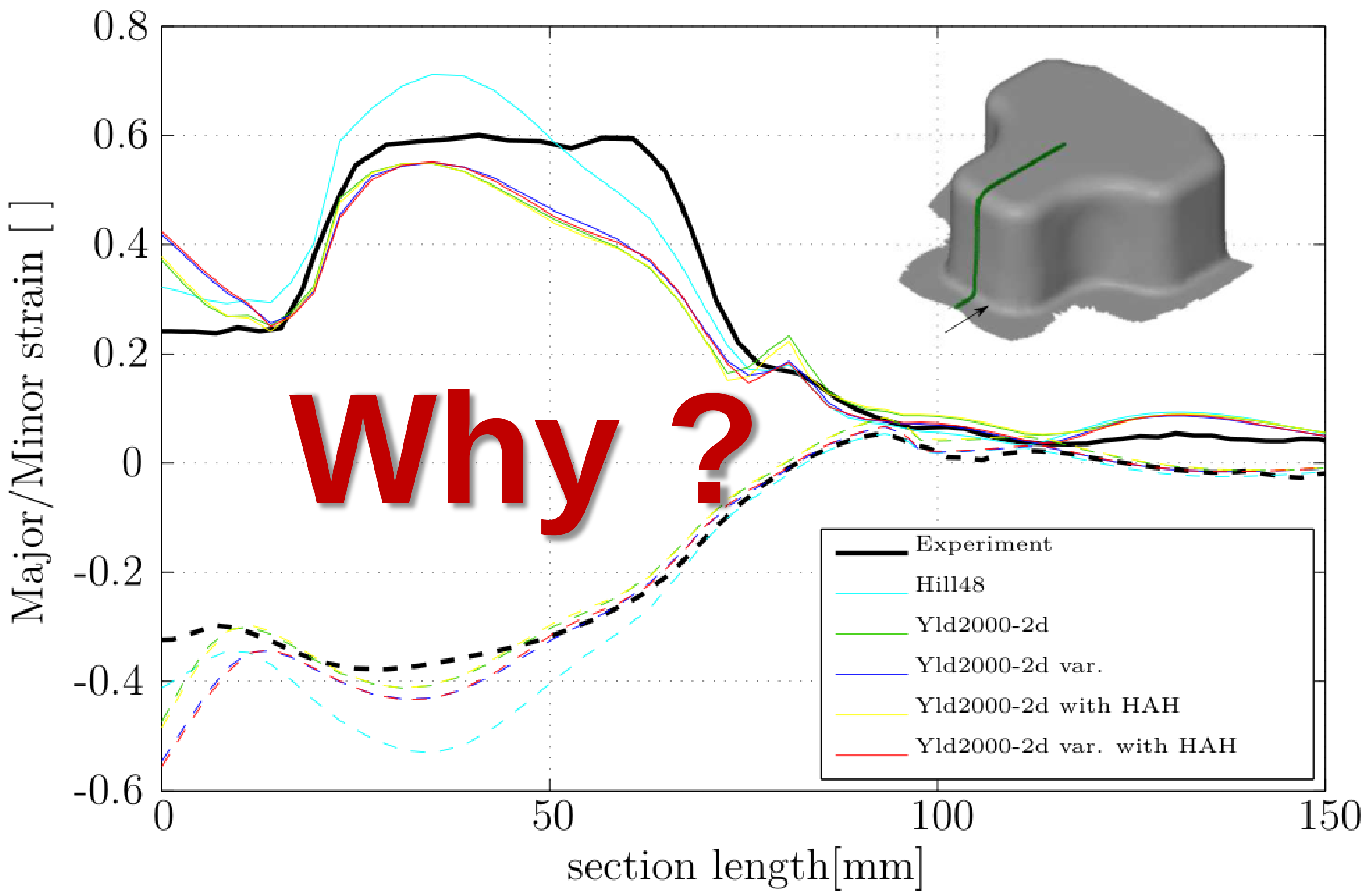

Accuracy of principal strain distributions
Cross-Die

Constitutive models

- **Hill'48**
- **Yld 2000-2d**
- **Yld 2000-2d var**
- **Yld 2000-2d with HAH**
- **Yld 2000-2d var with HAH**

Source: P.Peters. Diss. ETH 2015

Anisotropic Hardening

Strain dependent Barlat 2000 Model

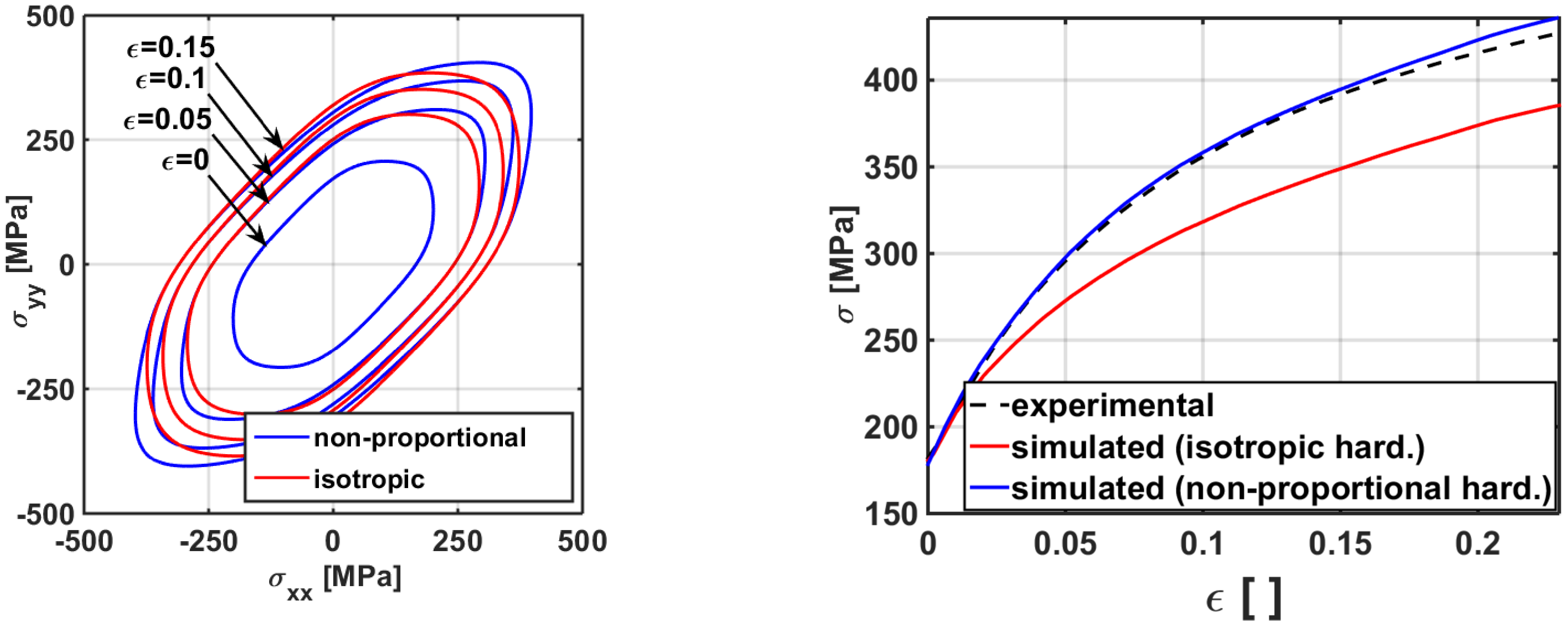

Anisotropic Hardening – YLD2000-var model

Strain dependent Barlat 2000 Model

$$\Phi = |X'_1 - X'_2|^a + |2X''_2 + X''_1|^a + |2X''_1 + X''_2|^a = 2\bar{\sigma}^a$$

$$\boldsymbol{X'} = \boldsymbol{C's} = \boldsymbol{C'T\sigma} = \boldsymbol{L'\sigma}$$
$$\boldsymbol{X''} = \boldsymbol{C''s} = \boldsymbol{C''T\sigma} = \boldsymbol{L''\sigma}$$

$$L'_{11} = \frac{2}{3}\alpha_1 \qquad L''_{11} = \frac{-2\alpha_3+2\alpha_4+8\alpha_5-2\alpha_6}{9}$$
$$L'_{12} = -\frac{1}{3}\alpha_1 \qquad L''_{12} = \frac{\alpha_3-4\alpha_4-4\alpha_5+4\alpha_6}{9}$$
$$L'_{21} = -\frac{1}{3}\alpha_2 \qquad L''_{21} = \frac{4\alpha_3-4\alpha_4-4\alpha_5+\alpha_6}{9}$$
$$L'_{22} = \frac{2}{3}\alpha_2 \qquad L''_{22} = \frac{-2\alpha_3+8\alpha_4+2\alpha_5-2\alpha_6}{9}$$
$$L'_{33} = \alpha_7 \qquad L''_{33} = \alpha_8$$

Strain dependent evolution of the YLD2000 parameters

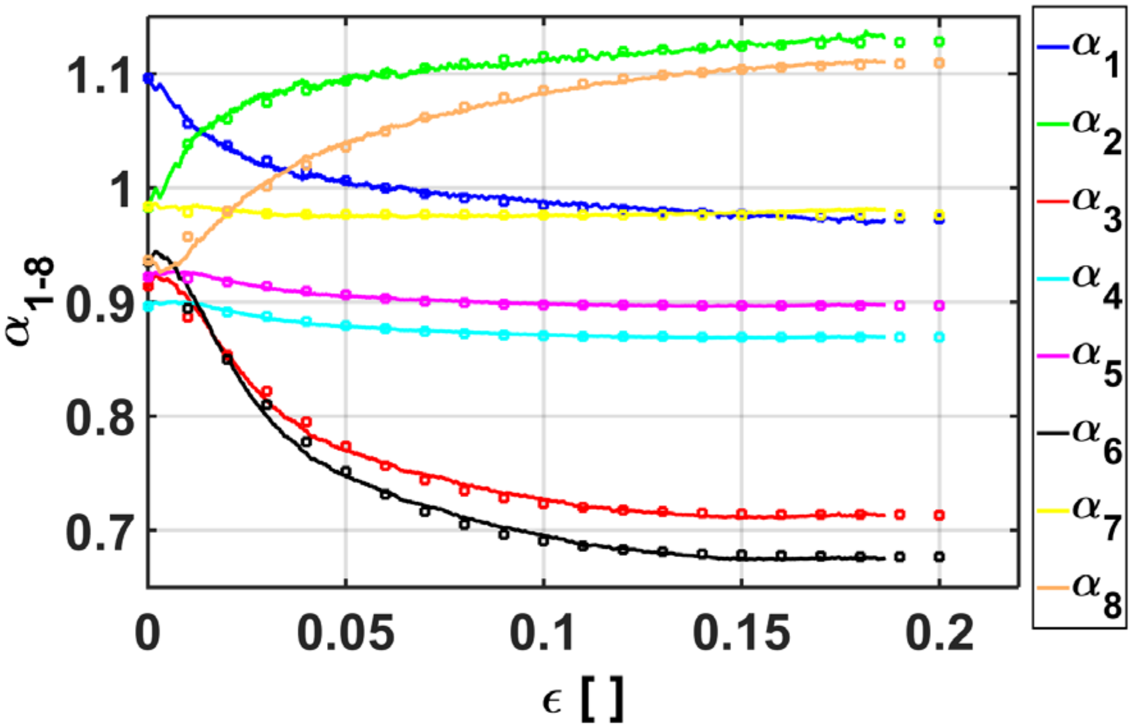

Source: P.Peters. Diss. ETH 2015

Applicability of NAFR models in combination with YLD2000

Check of the YL by Nakajima tests

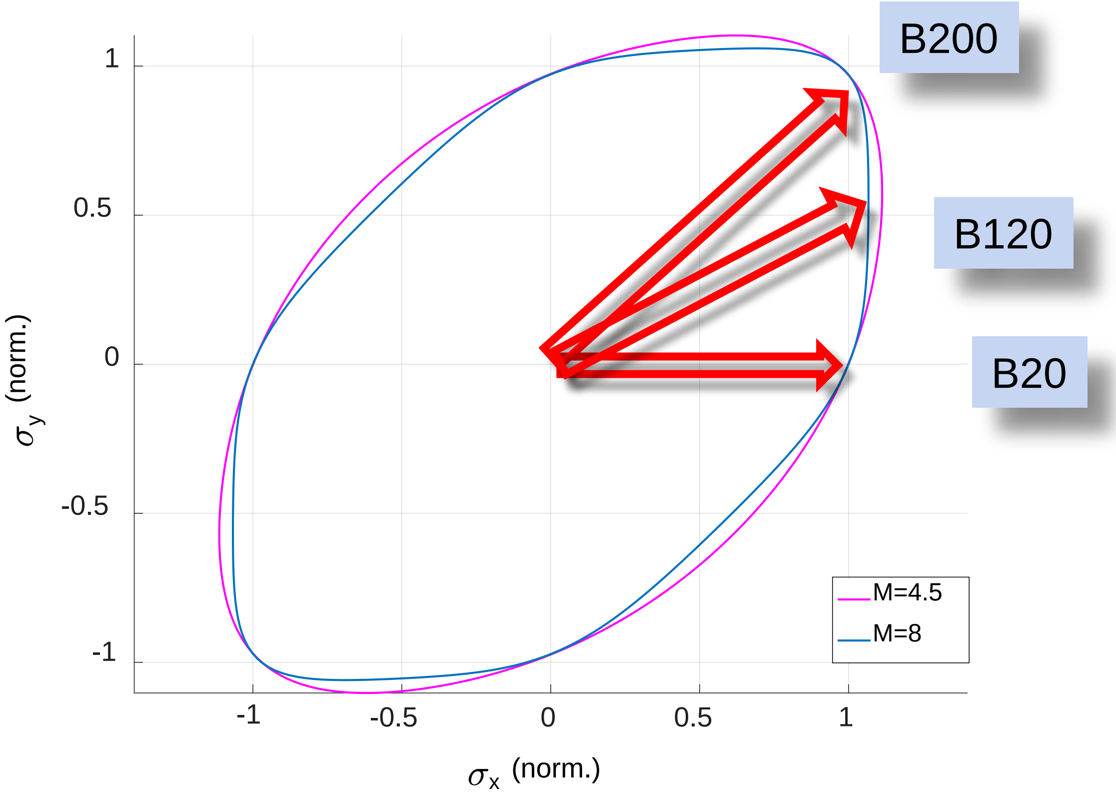

Introduction and Motivation
Limitations of non-quadratic yield loci

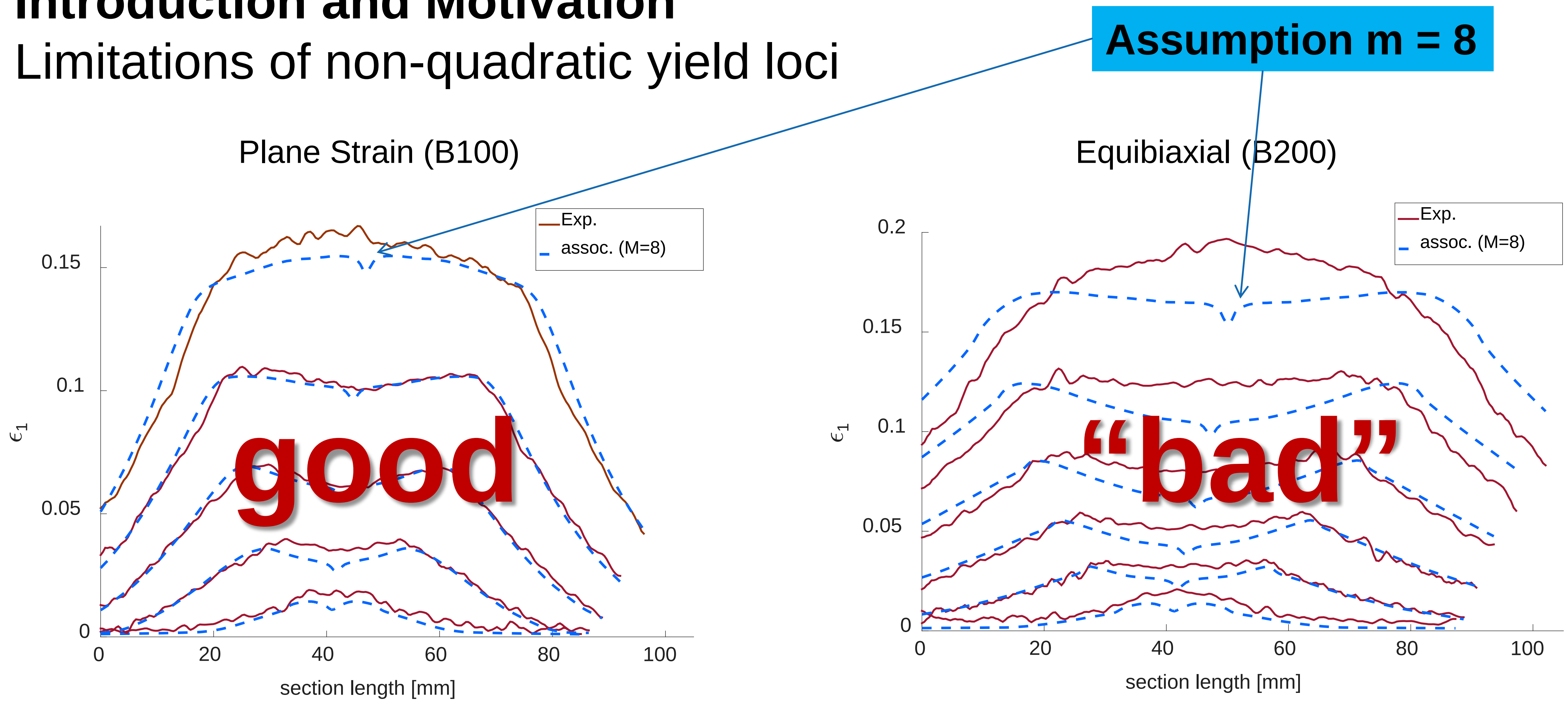

AA6016

Introduction and Motivation

Limitations of non-quadratic yield loci

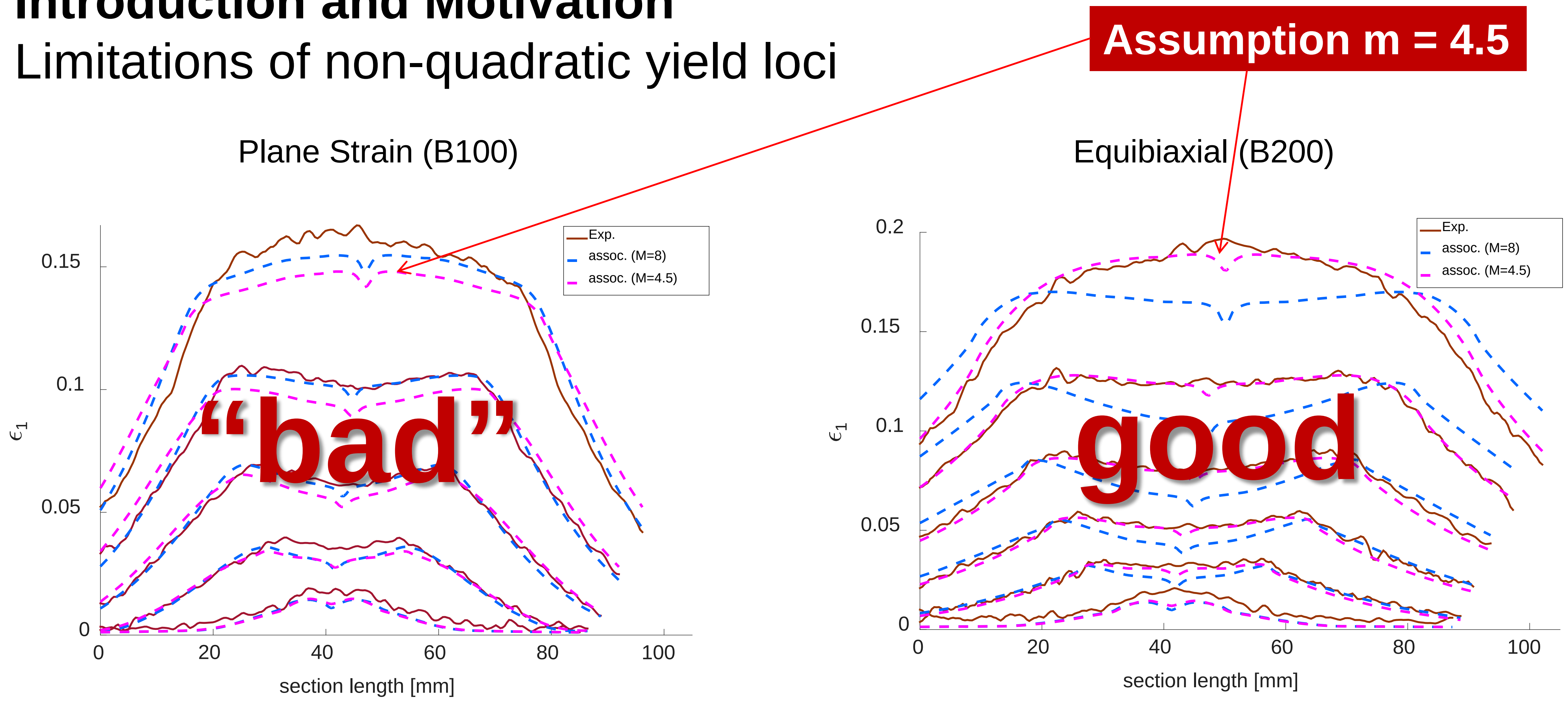

AA6016

YLD2000-2D-NAFR
Yield Locus and Plastic Potential

$\sigma_0 = 123.7$ MPa	$R_0 = 1.0$
$\sigma_{45} = 119.35$ MPa	$R_{45} = 1.0$
$\sigma_{90} = 120.27$ MPa	$R_{90} = 1.0$
$\sigma_b = 122.02$ MPa	$R_b = 1.0$

→ α_σ

$\sigma_0 = 123.7$ MPa	$R_0 = 0.686$
$\sigma_{45} = 123.7$ MPa	$R_{45} = 0.5$
$\sigma_{90} = 123.7$ MPa	$R_{90} = 0.666$
$\sigma_b = 123.7$ MPa	$R_b = 1.0$

→ α_p

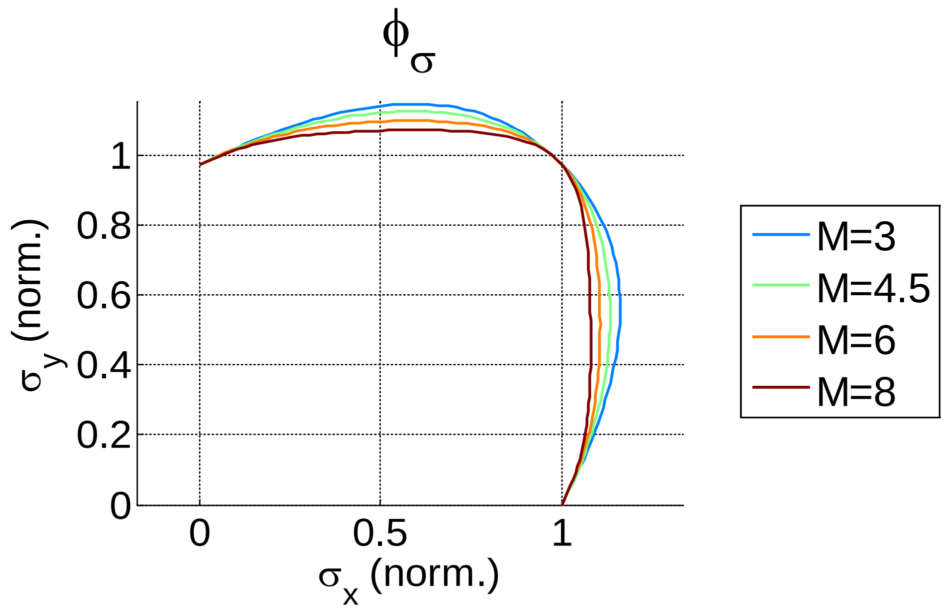

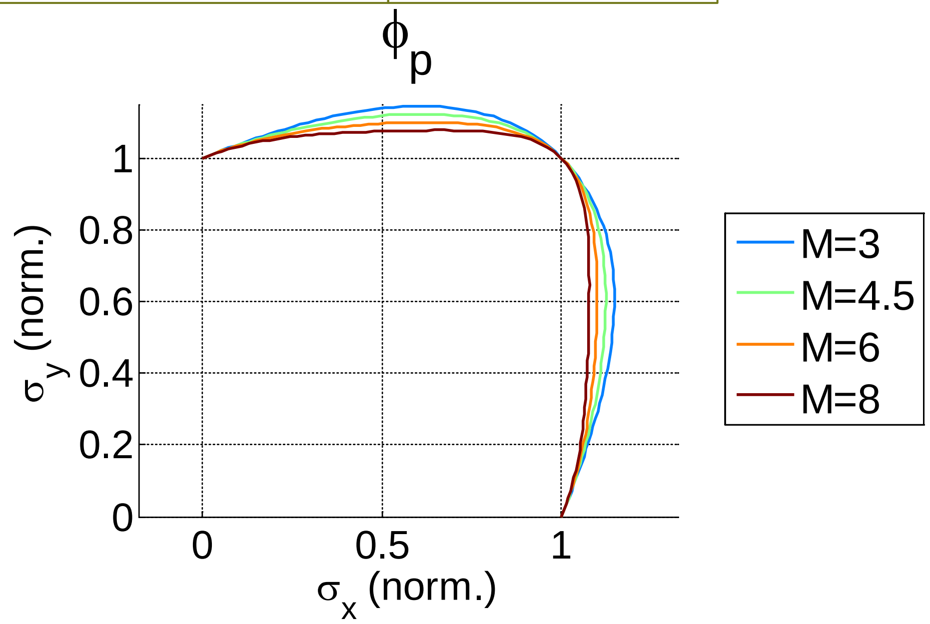

Optimum Search
Response Surface

- Two Nakajima configurations
  - B100
  - B200

- Full factorial design for the yield locus and plastic potential exponents

$$M_\sigma, M_p = \{3, 4.5, 6, 8\}$$

- Response surface based on error function values at the supports

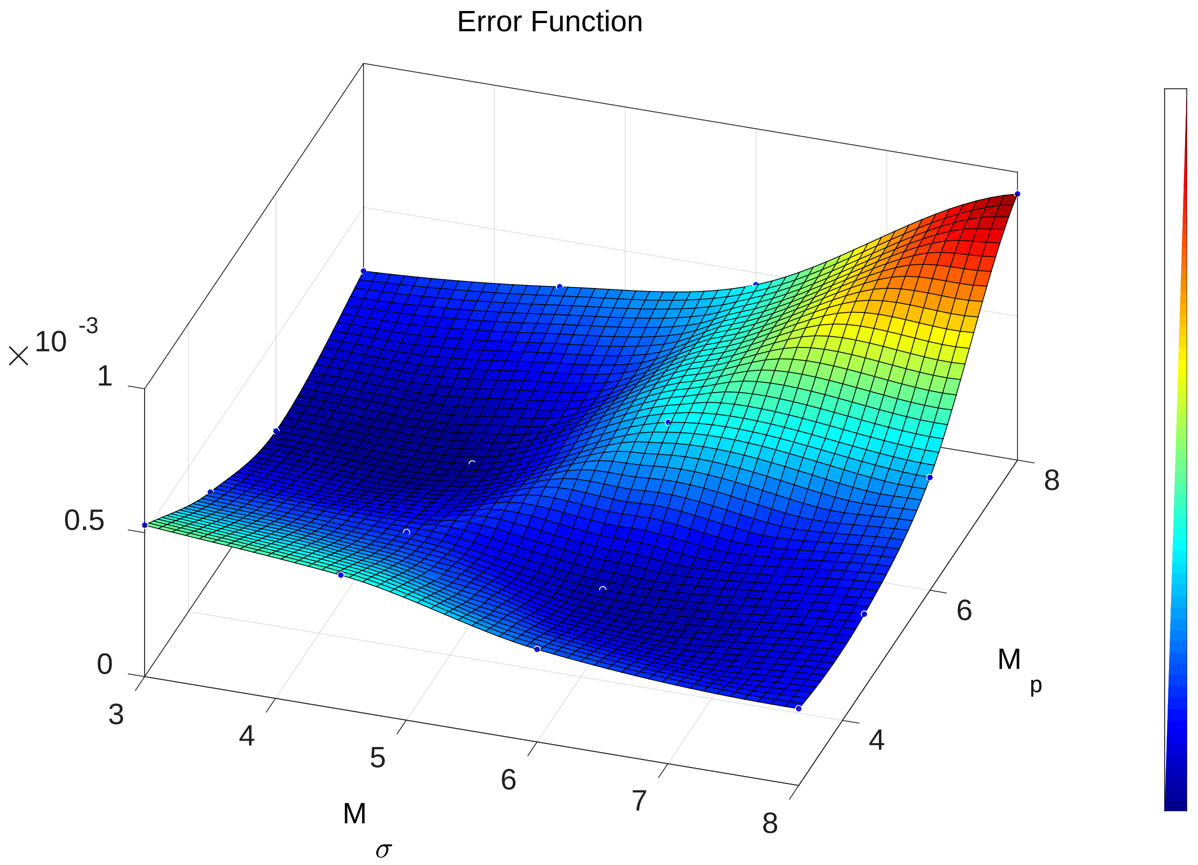

Yield criterion – General Idea

Source: Ch. Raemy, Diss ETH 2017

- Stress state parametrized by spherical coordinates r, φ, ψ
- A formally very compact criterion is proposed (FAY – Fourier Anisotropic Yield)

$$\bar{\sigma} = r \sqrt[q]{f(\varphi, \psi)}$$

- $f(\varphi, \psi)$ is a two-dimensional Fourier series of the angular coordinates

$$f(\varphi, \psi) = \sum_{m=0}^{\infty} \sum_{n=0}^{\infty} a_{m,n} \cos(m\varphi) \cos(n\psi) + \sum_{m=0}^{\infty} \sum_{n=1}^{\infty} b_{m,n} \cos(m\varphi) \sin(n\psi)$$
$$+ \sum_{m=1}^{\infty} \sum_{n=0}^{\infty} c_{m,n} \sin(m\varphi) \cos(n\psi) + \sum_{m=1}^{\infty} \sum_{n=1}^{\infty} d_{m,n} \sin(m\varphi) \sin(n\psi)$$

- Shape of yield surface adjustable through the coefficients of f

FAY Model
Convexity

Source: Ch. Raemy, Diss ETH 2017

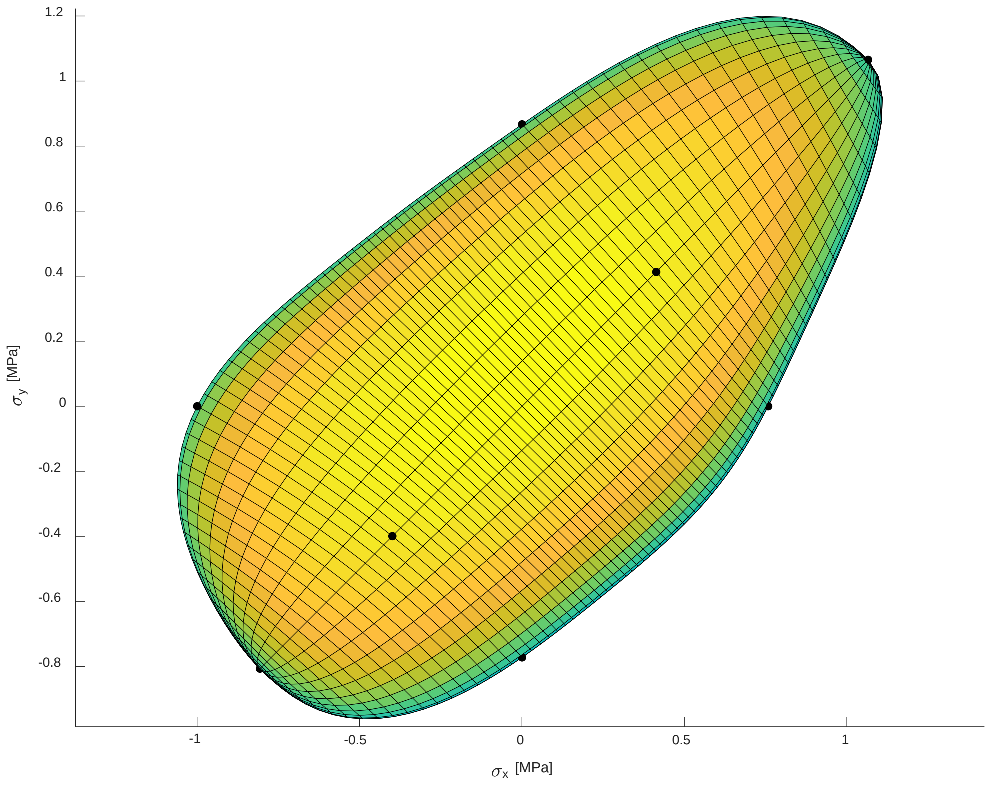

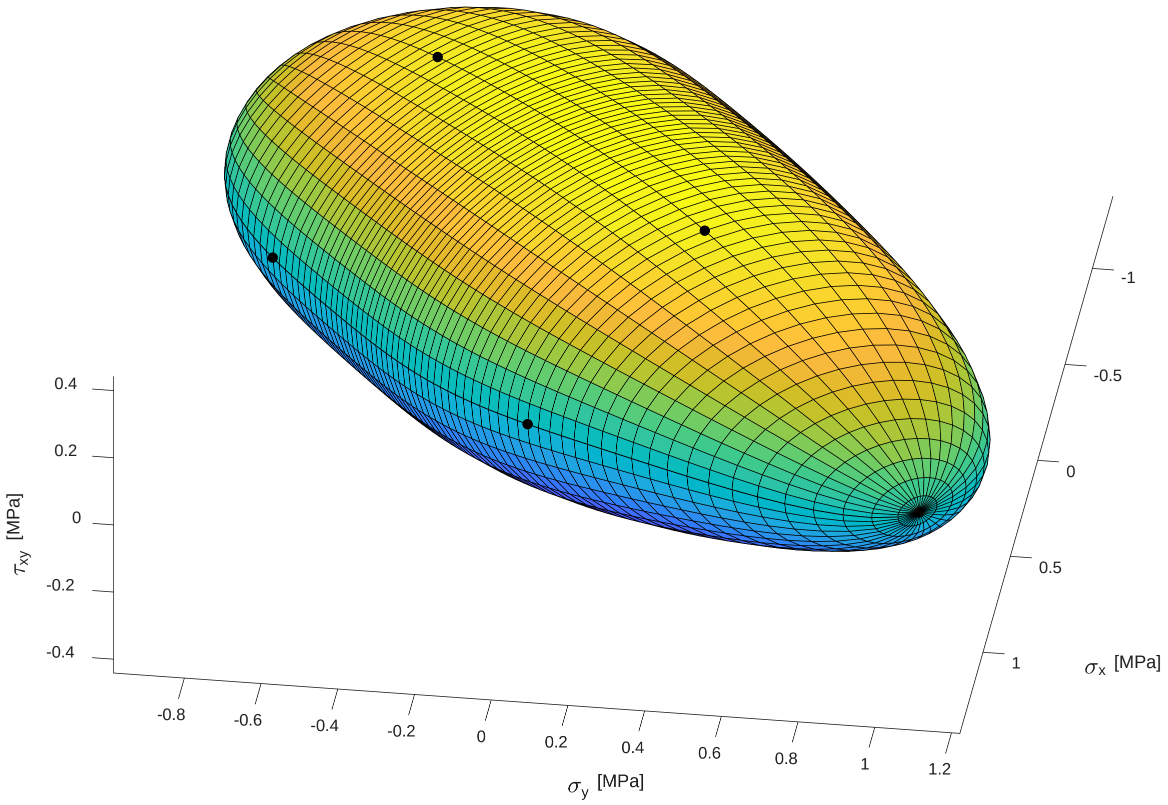

Comparison of non-AFR and FAY

Nakajima Results. Material AA6016

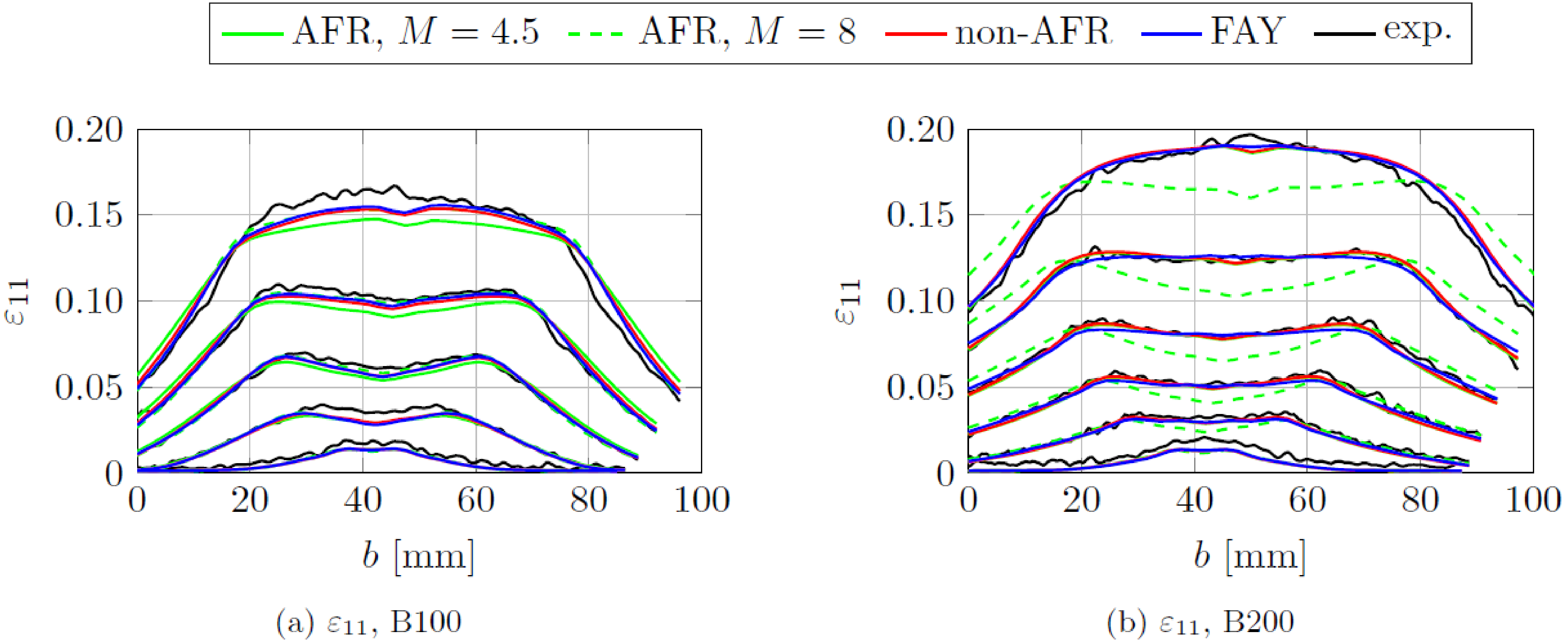

Figure 1: Measured and predicted strain distributions during Nakajima test of AA6016 at strokes of 5 mm, 10 mm, 15 mm, 20 mm and 25 mm; for B200 additionally at 30 mm.

Correct failure prediction – FLC based methods

- Time dependent evaluation method (Volk, Hora, 2010)
- MMFC Modiffied maximum force criterium (Hora-Tong)

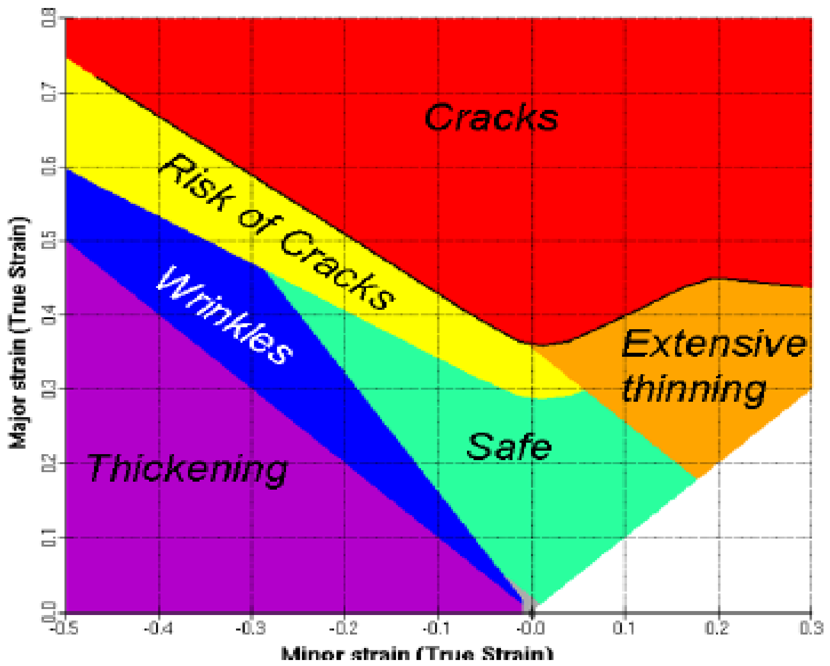

Conventional forming limit curve (FLC)

15. Deutsches LS-Dyna Forum 2018

Integration neuer graphischer Auswertemethoden zur verbesserten Erkennung von Blechversagen unter dem Einfluss nicht-linearer Dehnungspfade

P. Hora, L. Tong, N. Manopulo

Experiments n.l. FLC: W. Volk, Ch. Gaber, UTG

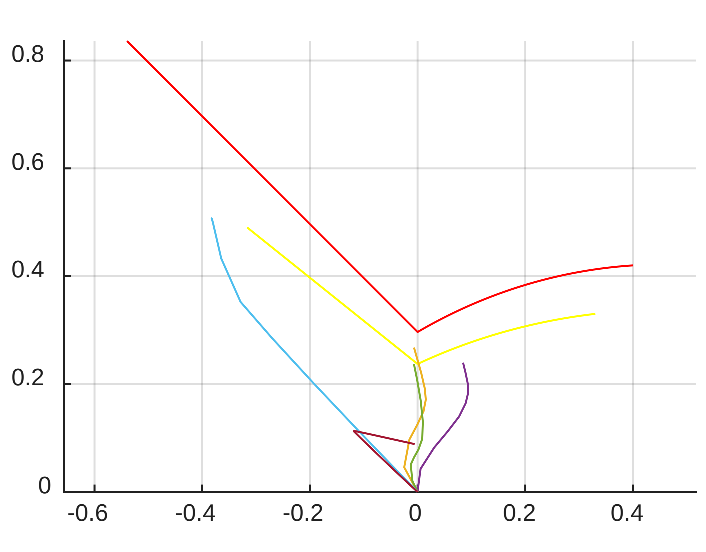

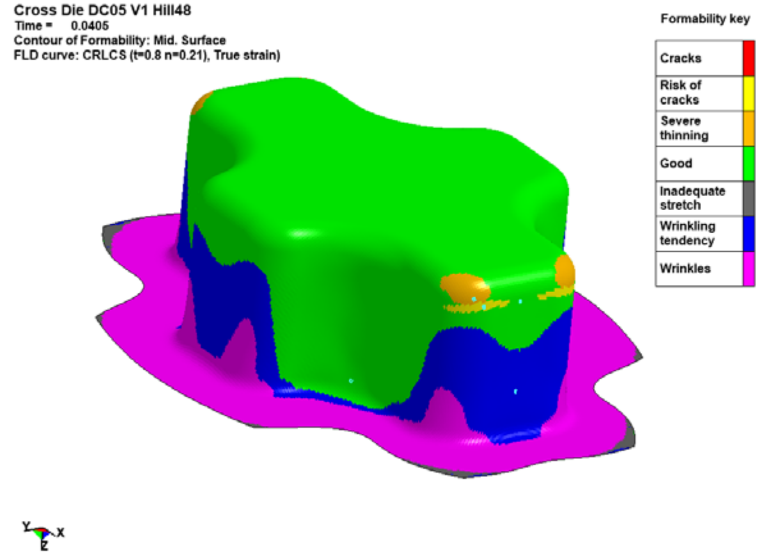

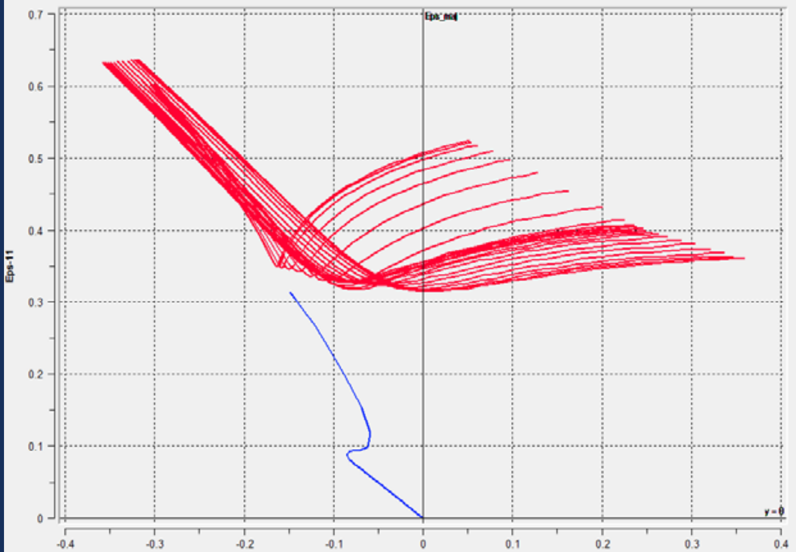

Content

Necking and fracture limits - X-FLC concept

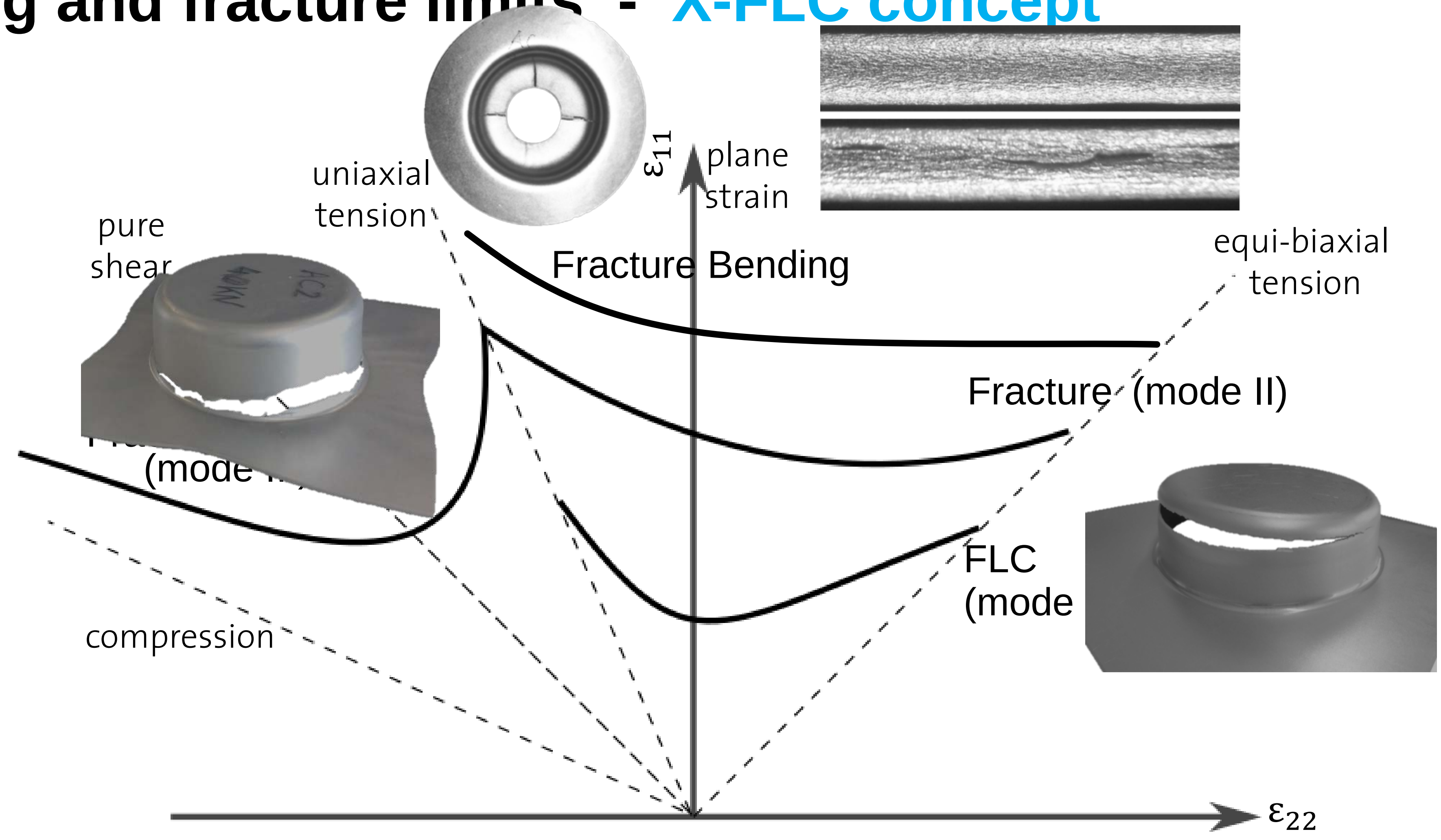

Schematic prediction of forming limits dependent on different failure modes

Failure detection models

	Experiments	Theoretical models	Output / Application
Necking	Nakajima test Marciniak test Cross line ev. Method Time dependent ev. Met.	M-K-Models eMMFC Models Stress Limit Curve GTN Models	FLC (linear) SLC GFLC (Volk) Nonlin FLC (eMMFC)
Ruptures / Cracks	Wierzbicki, Bai, … Nakajima + Cup (Gorji) Special Tests – tension torsion – rolling	GTN Models Stress Limit Curve (Mohr-Coulomb) Stress Limit Curve (3D-effective stress) GISSMO	Johnson Cook Mohr-Coulomb Triaxiality plots X-FLC

Failure detection models

	Experiments	Theoretical models	Output / Application
Necking	Nakajima test Marciniak test Cross line ev. Method Time dependent ev. Met.	M-K-Models eMMFC Models Stress Limit Curve GTN Models	FLC (linear) SLC GFLC (Volk) Nonlin FLC (eMMFC)
Ruptures / Cracks	Wierzbicki, Bai, … Nakajima + Cup (Gorji) Special Tests – tension torsion – rolling	GTN Models Stress Limit Curve (Mohr-Coulomb) Stress Limit Curve (3D-effective stress) GISSMO	Johnson Cook Mohr-Coulomb Triaxiality plots X-FLC

ETH zürich

PART I

NECKING PREDICTION

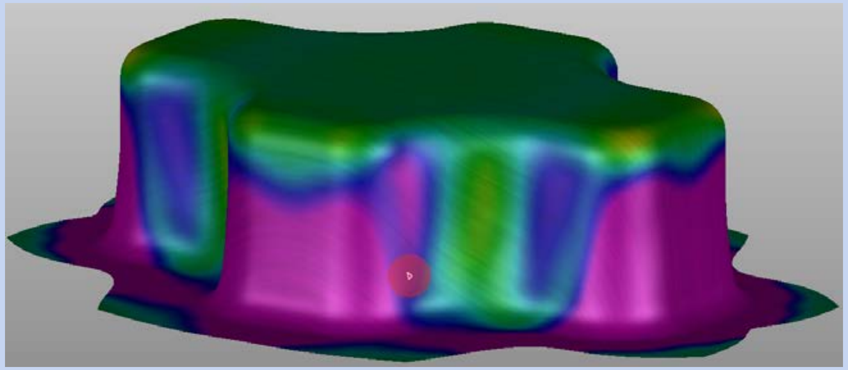

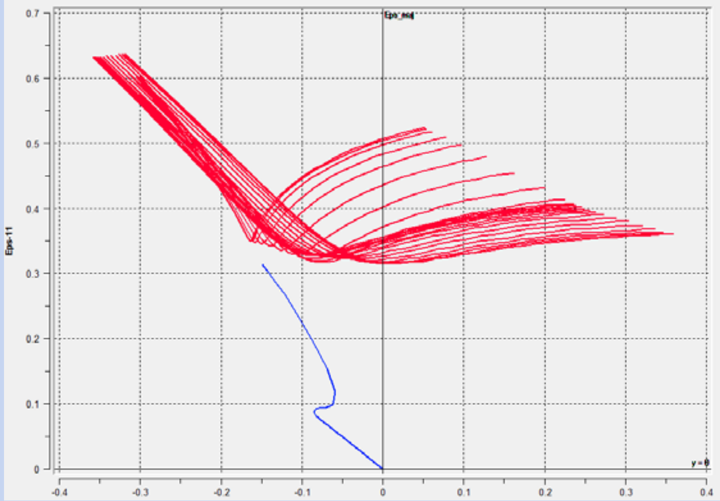

PART II

CRACK PREDICTION

Shear crack

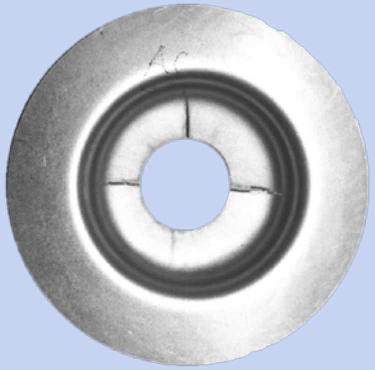

Edge crack

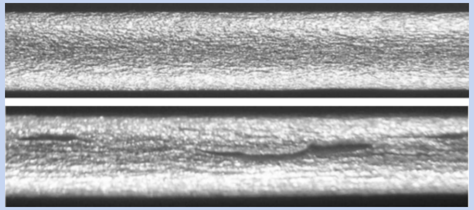

Bending crack

Content

1 **General topics in constitutive modeling**

2 **Necking prediction**

- Limitations of classical FLC based prediction methods
- FLC Limitations of Nakajima testing methods
- Advanced FLC methods (eMMFC)

3 **Crack prediction - Sheet specific fracture methods (X-FLC)**

- Different experimental methods
- Nakajima based experimental detection of crack (fracture) limits
- Application of X-FLC methods

4 **Conclusions**

Experimental evaluation of linear FLC

Sketch of the basic idea

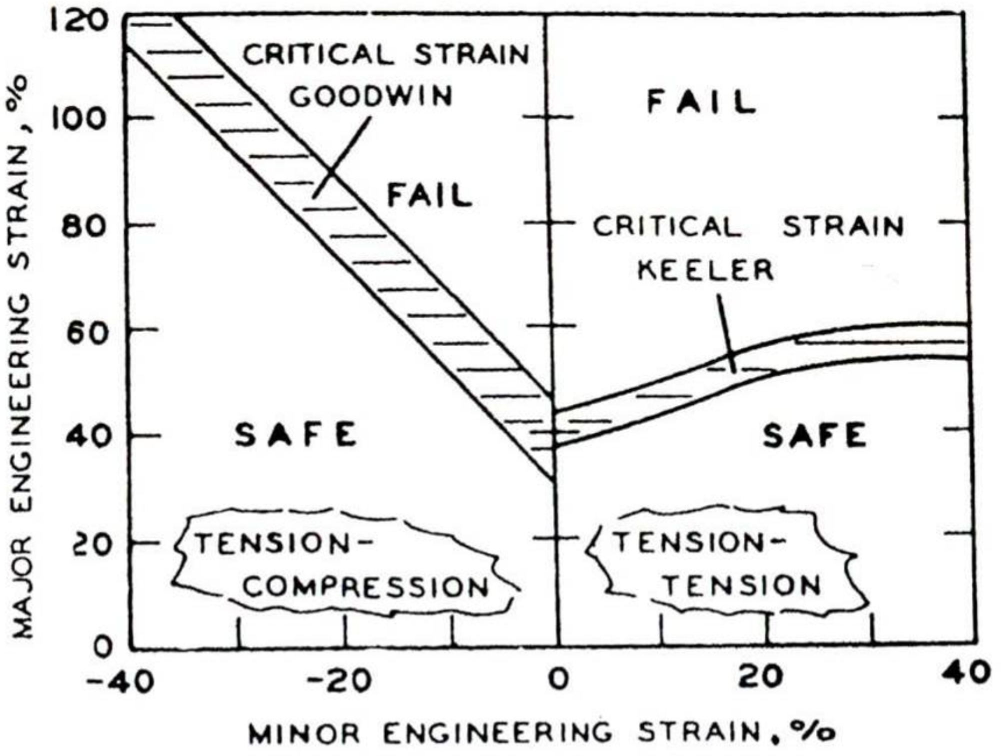

5.21 Forming limit diagrams defined by Keeler and Goodwin [5.75]

Strain history plot (AA6016)

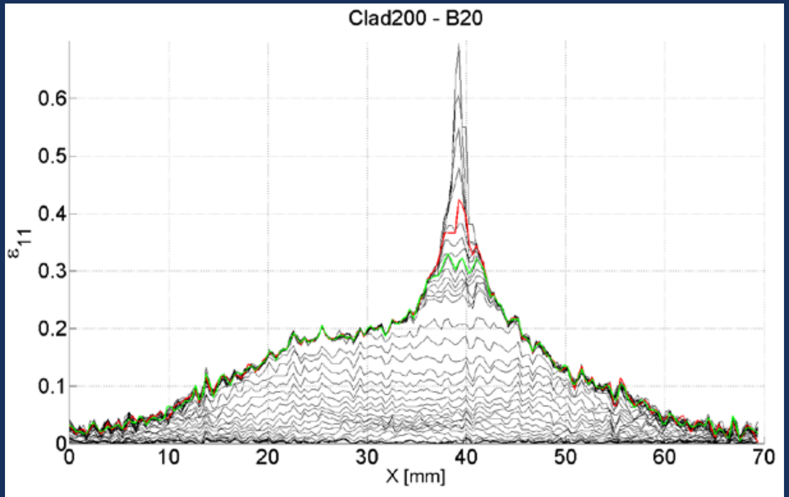

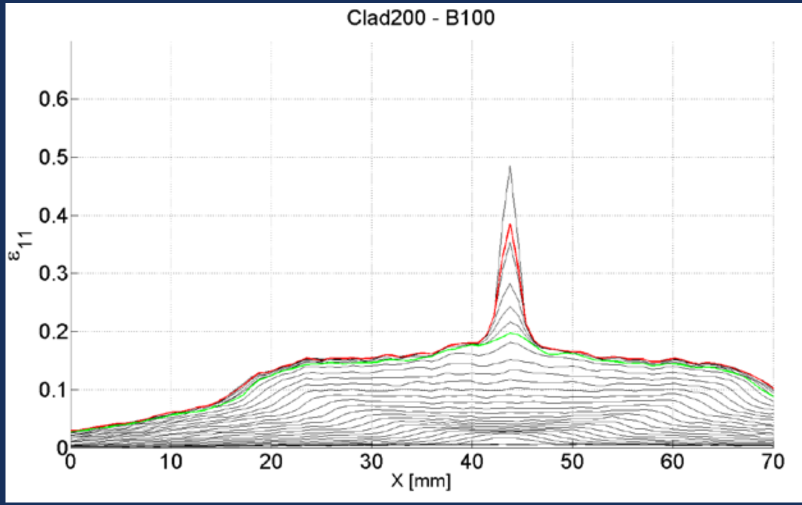

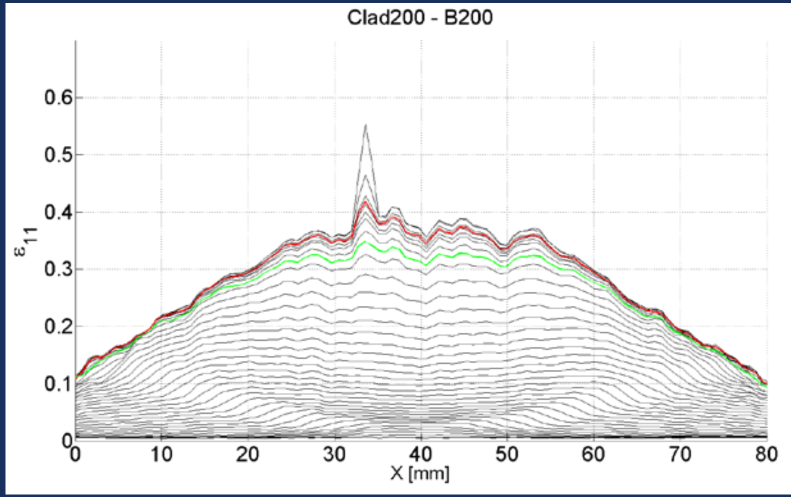

What is the appropriate localization level ?

What is the correct definition of the FLC values ?

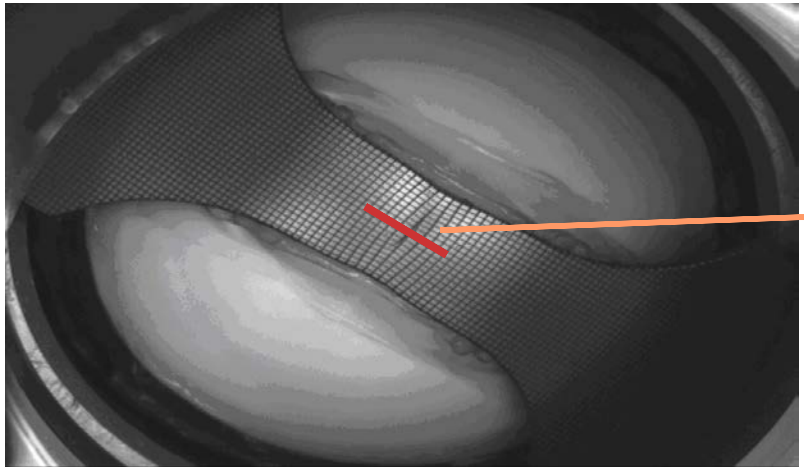

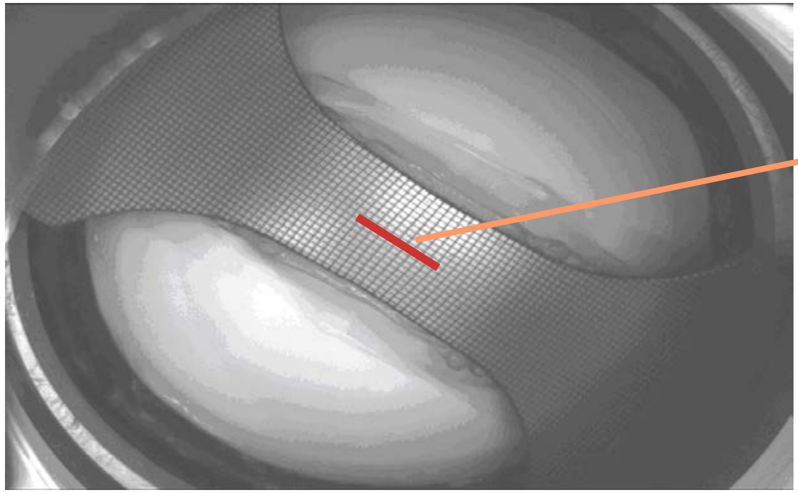

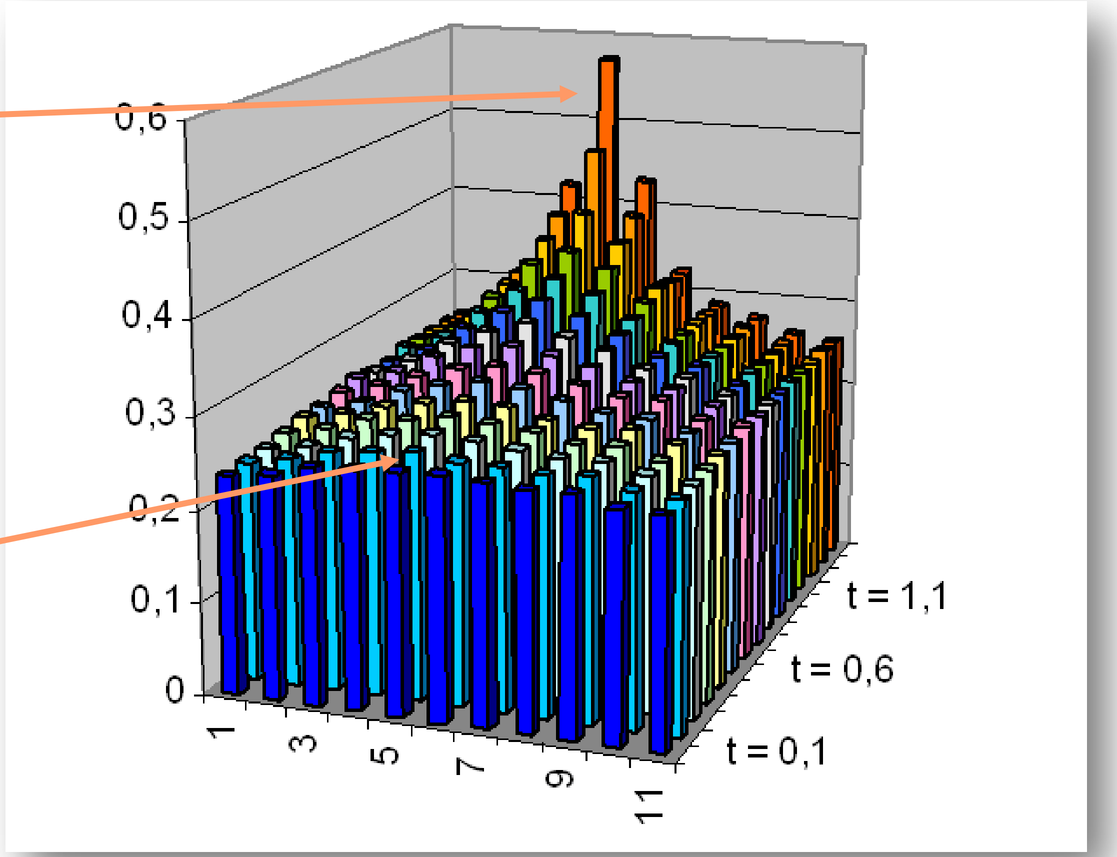

FLC evaluation methods

Test: Nakajima or Marciniak test
Evaluation: Cross-section or time dependant evaluation method

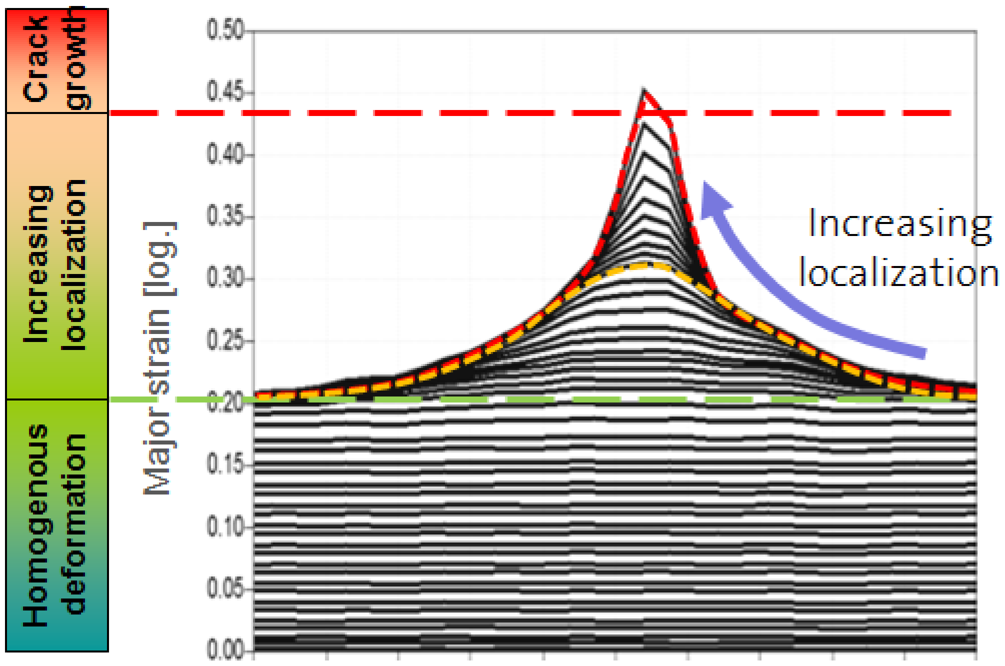

Continuous development of the localized necking zone

Cross section method

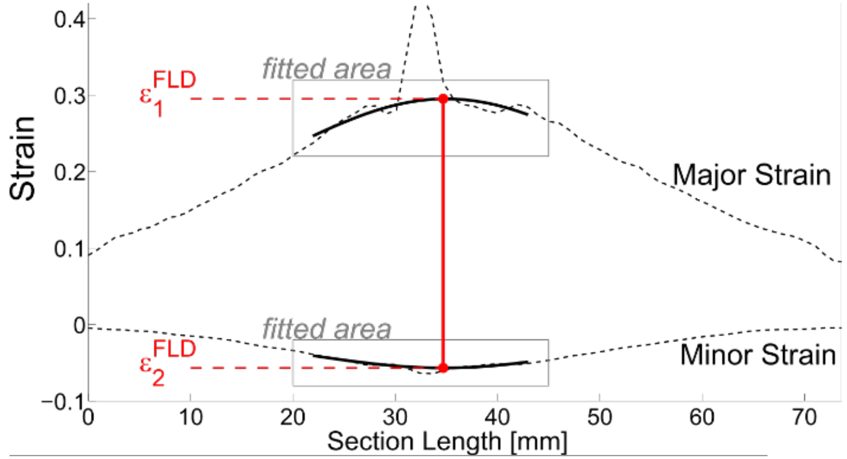

Time dependent method

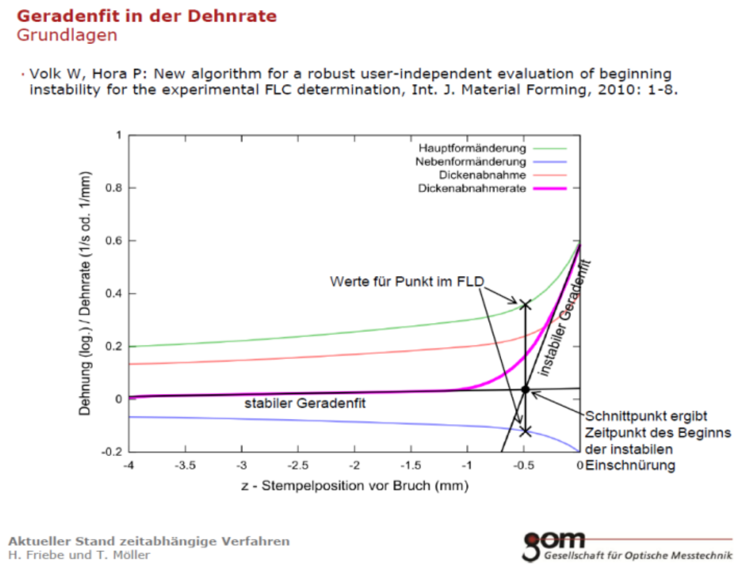

FLC does not describe the rupture

…. but only the start of the necking process under some loading conditions

Standard “misleading” FLC interpretation

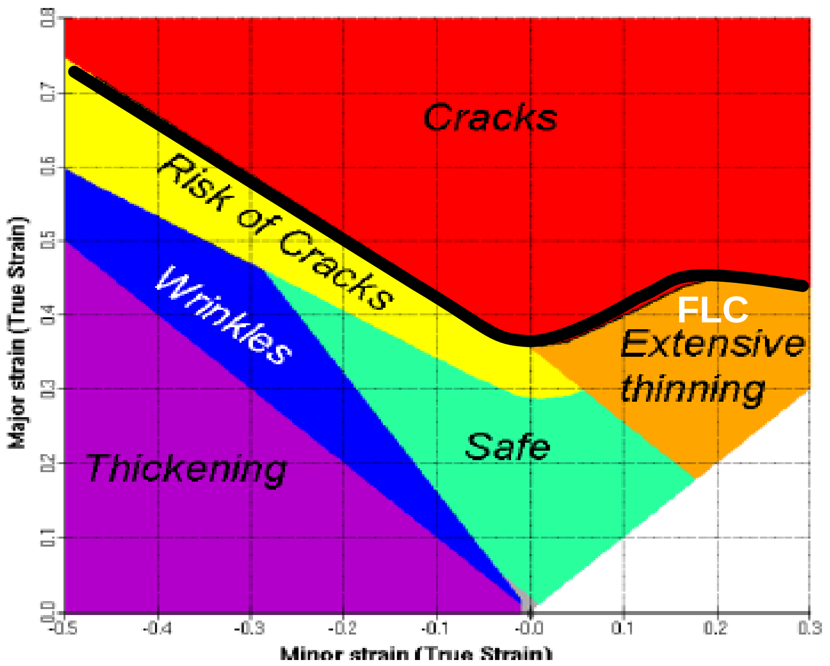

Conventional forming limit curve (FLC)

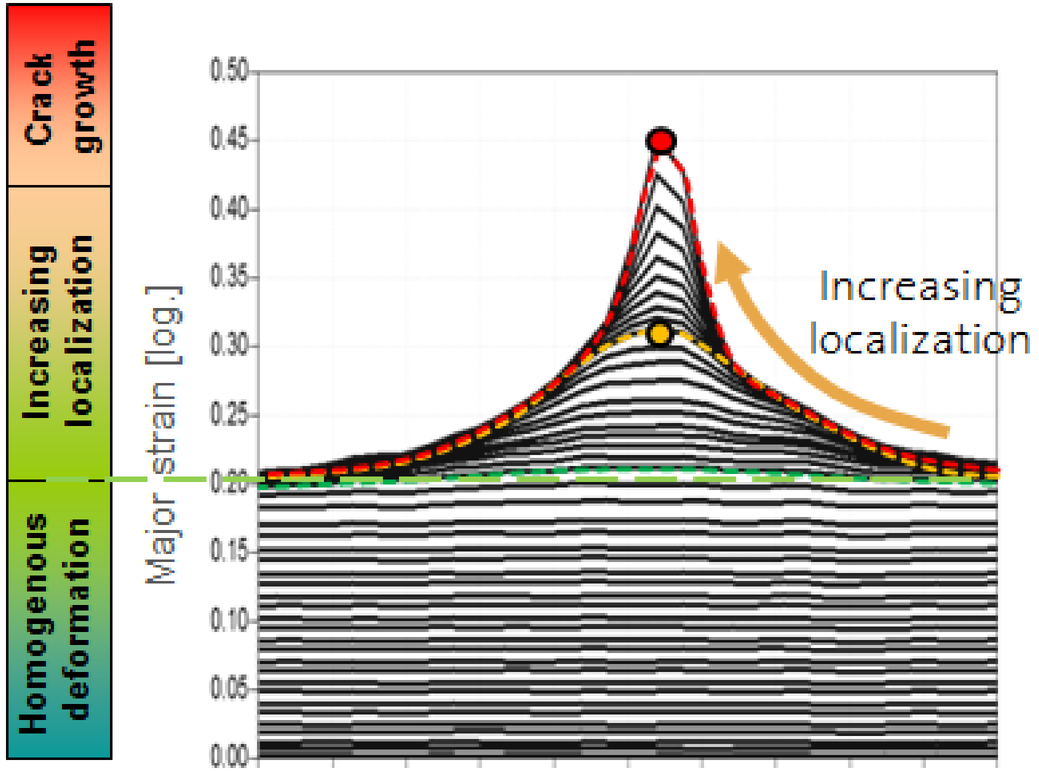

Continuous development of the localized necking zone

FLC does not describe the rupture

…. but only the start of the necking process under some loading conditions

For incremental forming processes the limits are above the FLC

…. also other processes like hemming are above the FLC

Forming in the conditional stable area

Source Company AMINO

Limitations in the FLC prediction

Crack strains in hemming

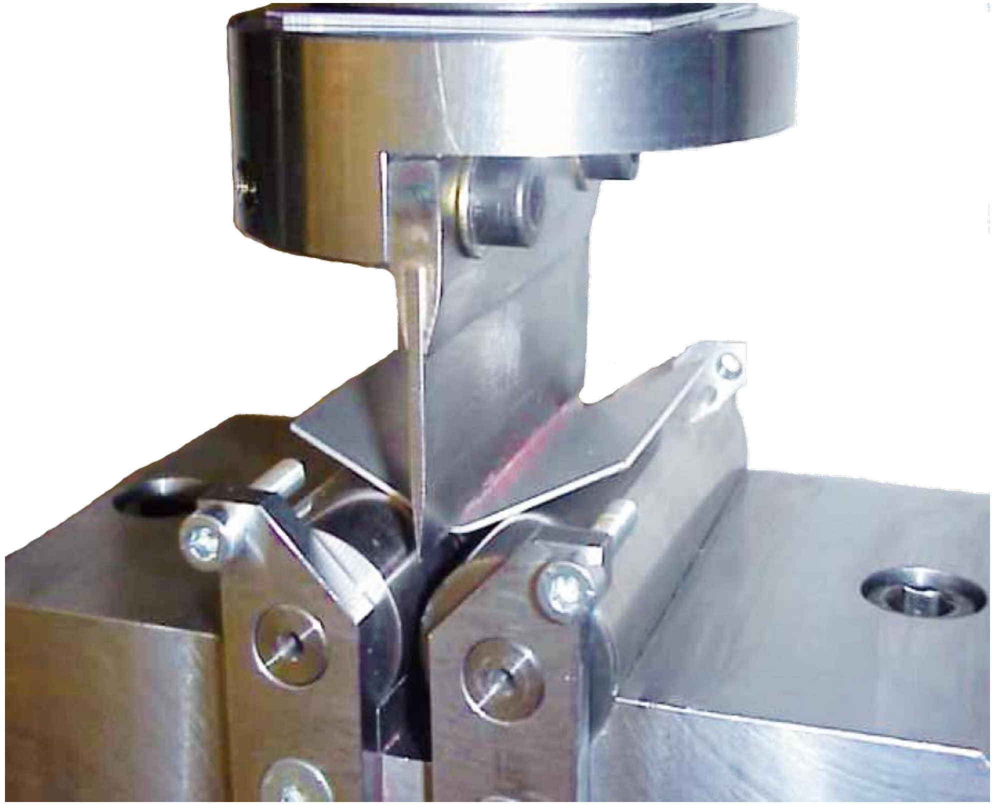

Hemming test – detection of crack strains

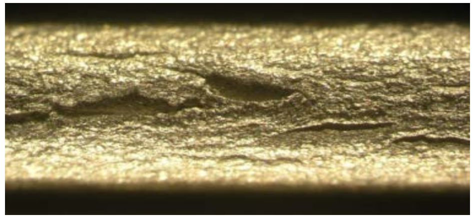

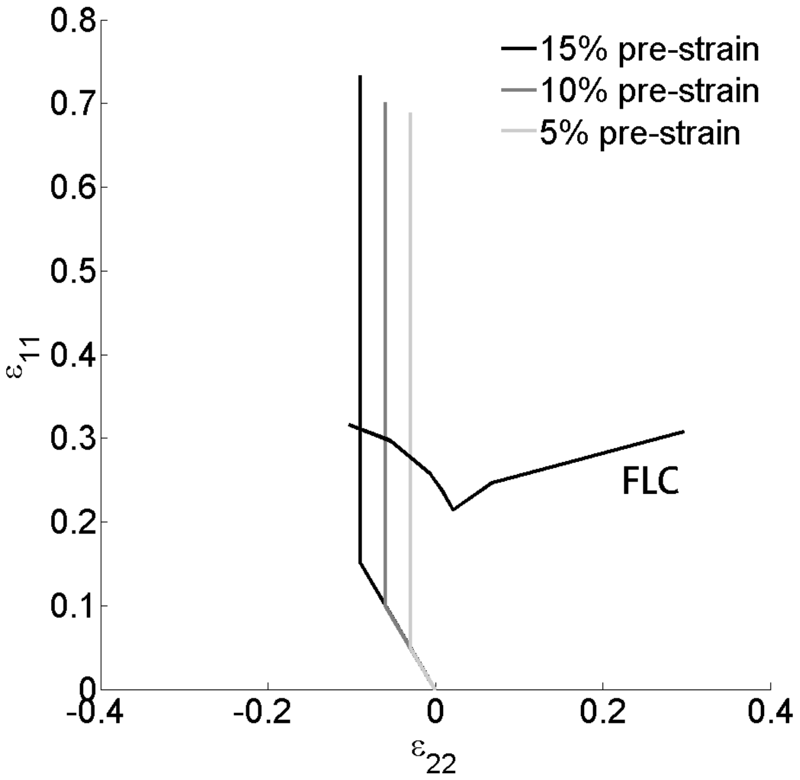

3-point Bending Experiment- AA6016

Source: M. Gorji. Diss. ETH 2016

Conditionally stable behavior in the range above the FLC

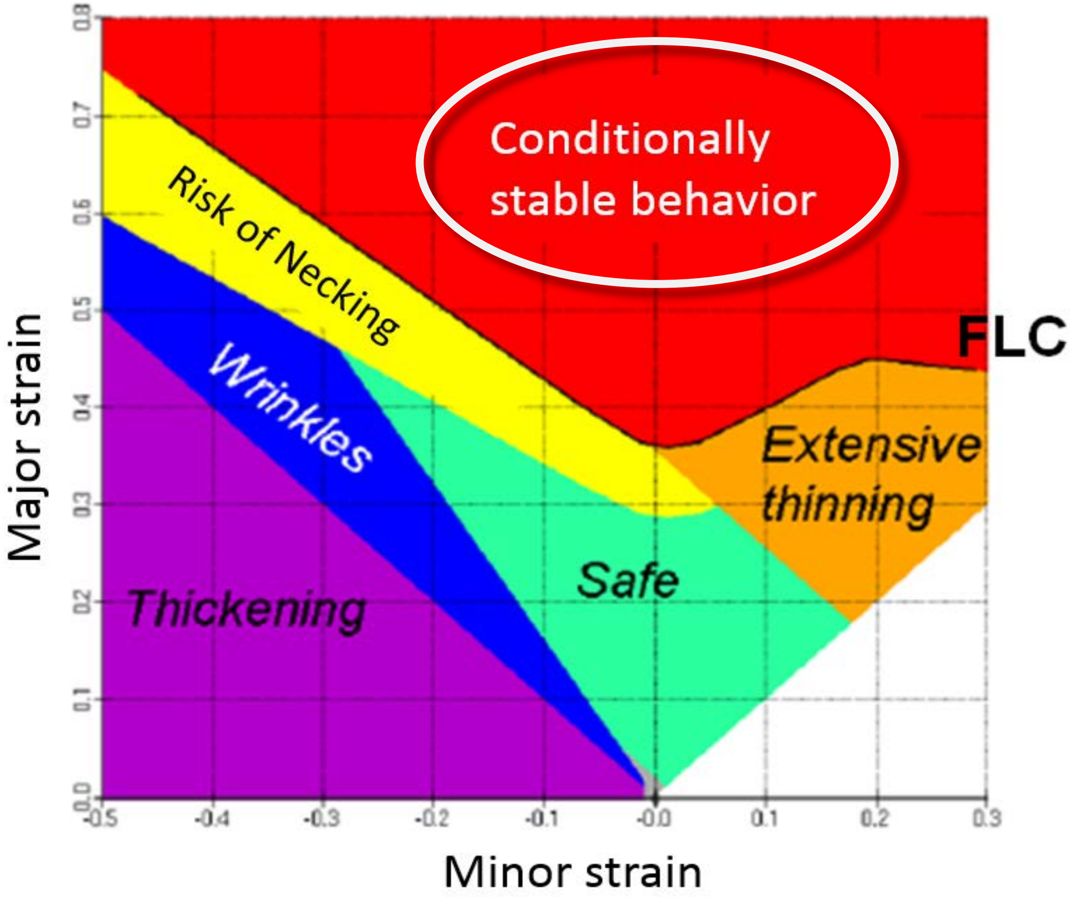

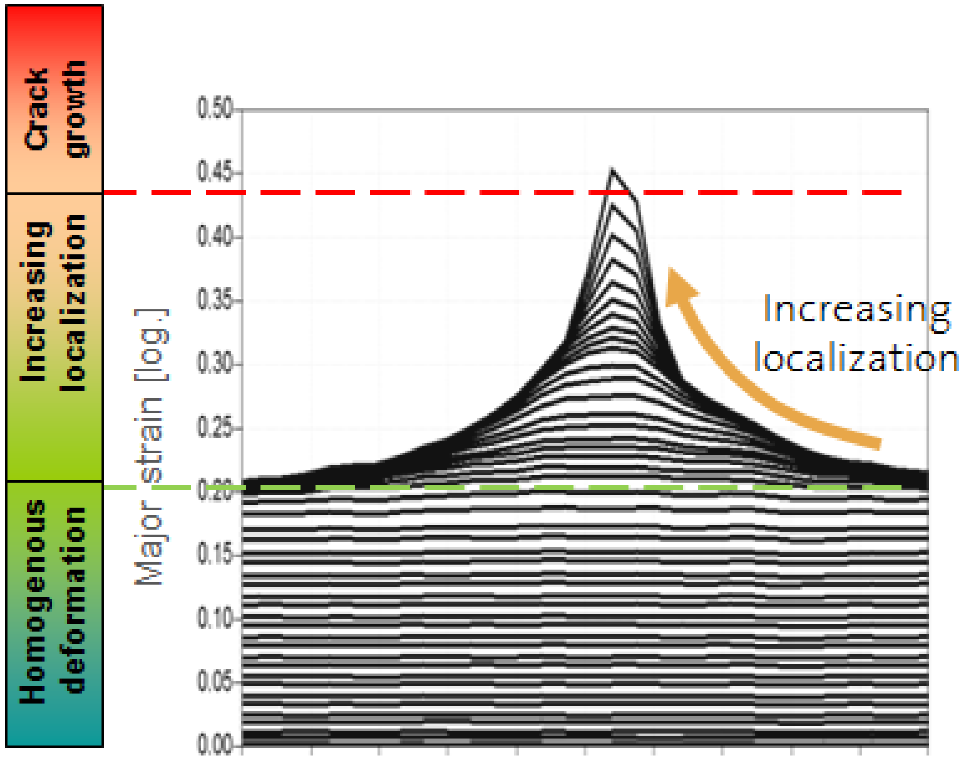

Continuous development of the localized necking zone

Content

… some Nakajima specimens may not cover correctly the deep drawing behavior

Validity of Nakajima tests

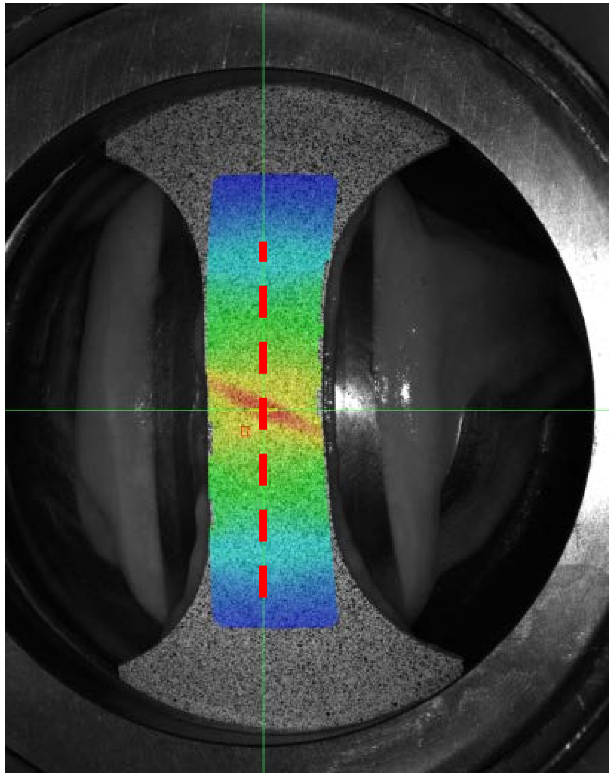

?

… does B20 correspond to the DD behavior on real parts?

… does B20 correspond to the DD behavior on real parts?

HC220YD, 0.8 mm

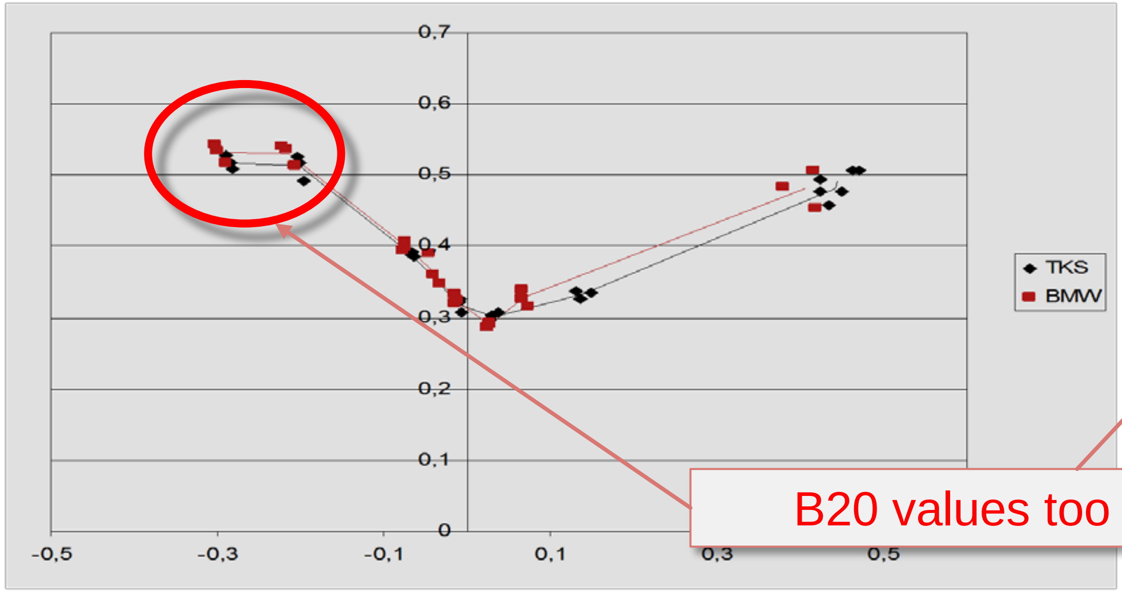

AA5182, 1.1 mm

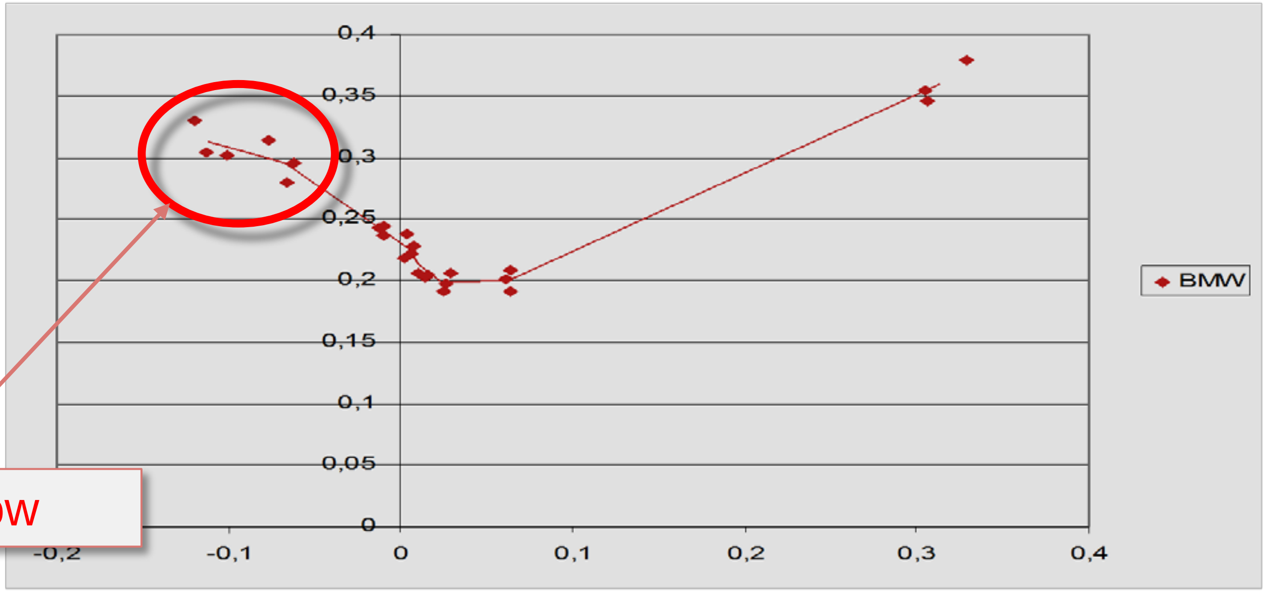

B20 values too low

The most left B20 specimen measurements deviates from the strain constrained conditions in the deep drawing case. For those reasons the so evaluated FLC shows a drop down of the FLC on the left hand side which cannot be observed under real deep drawing conditions.

FLC data: Numisheet BM 2008 - FLC-Benchmark

Based on the experimental FLC the simulation shows to conservative behavior

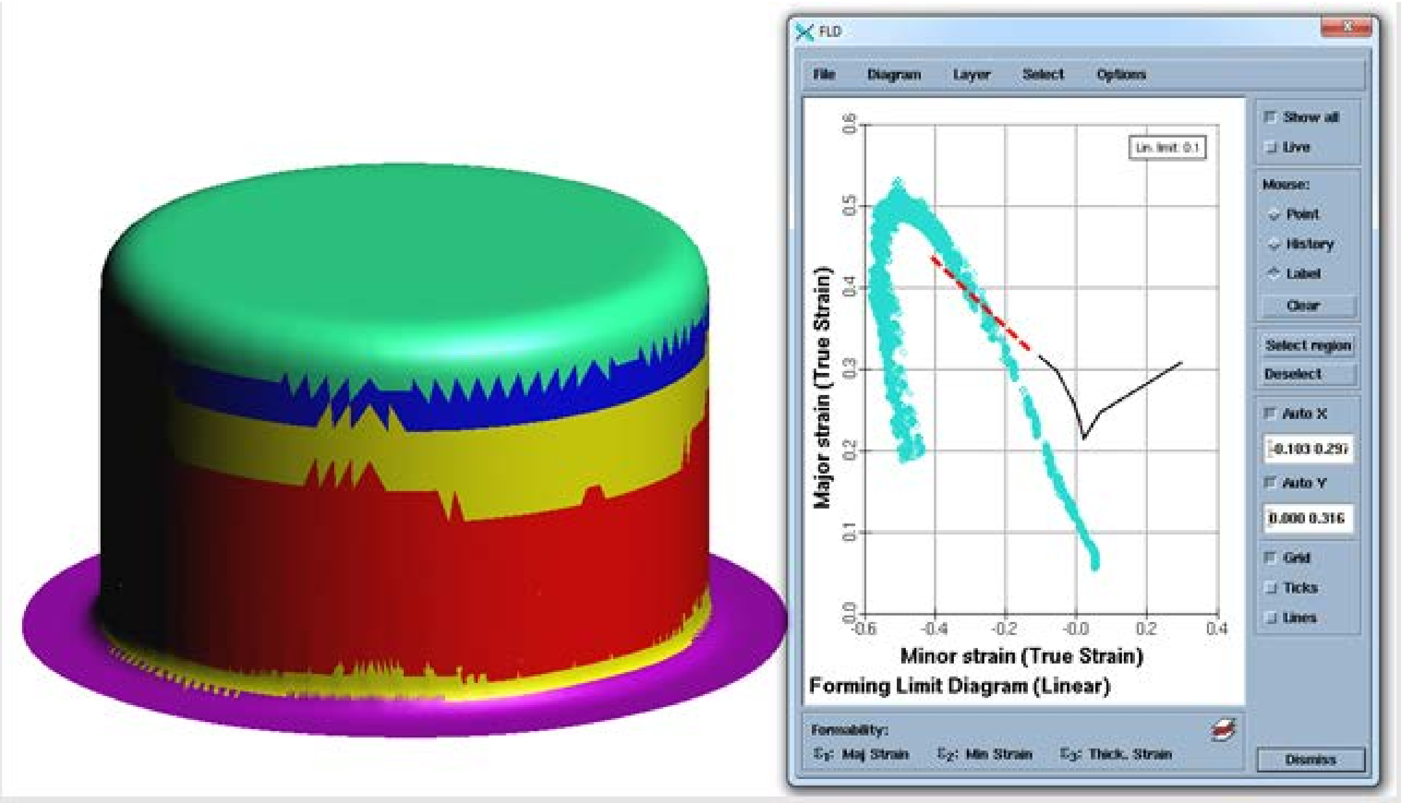

Differences between DD and B20 forming conditions

Stress driven BC

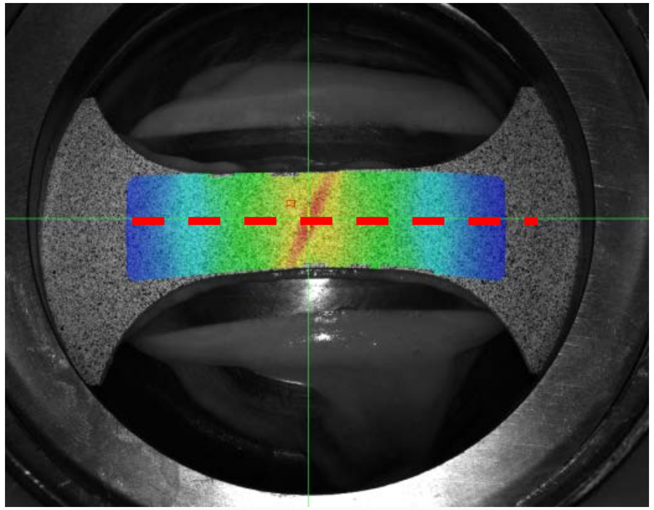

Strain driven BC

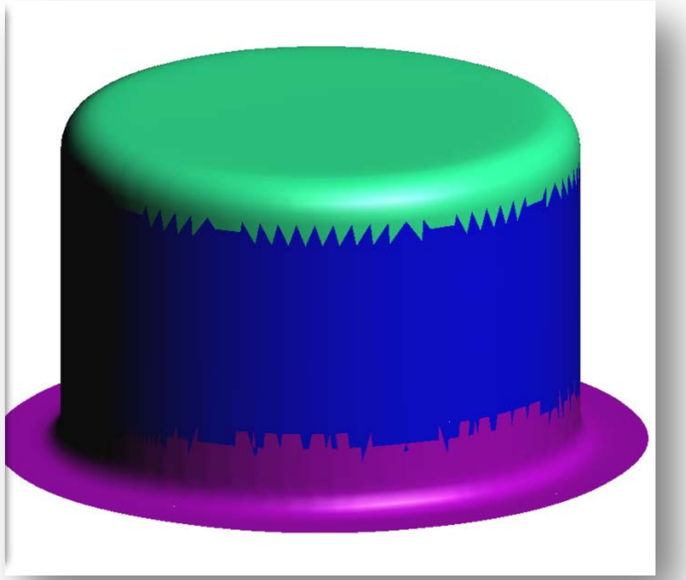

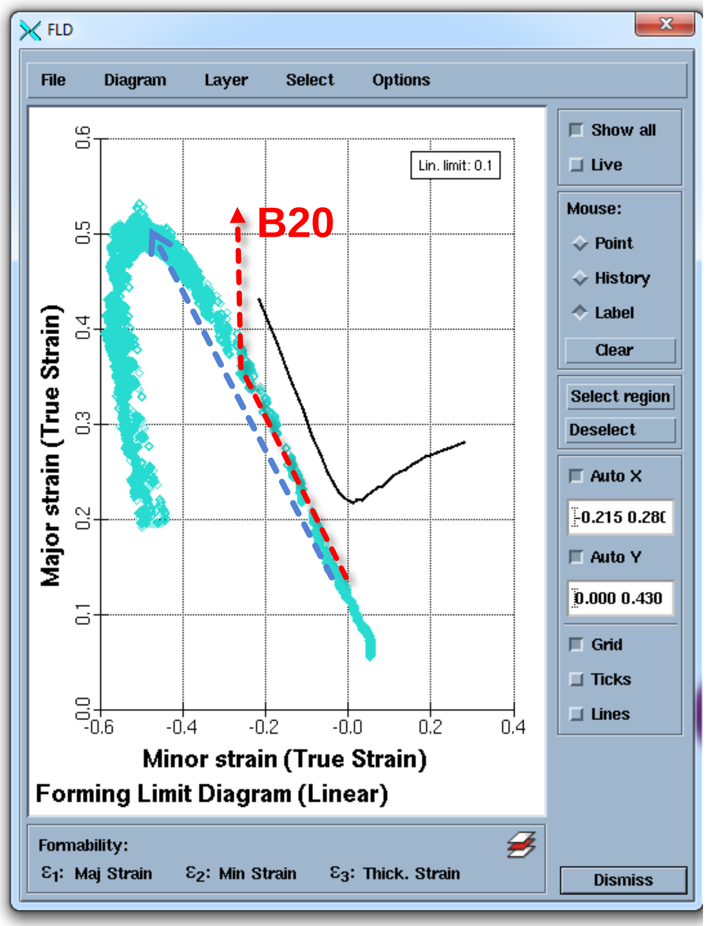

Stress BC

Tensile Test - Condition β=-0.5

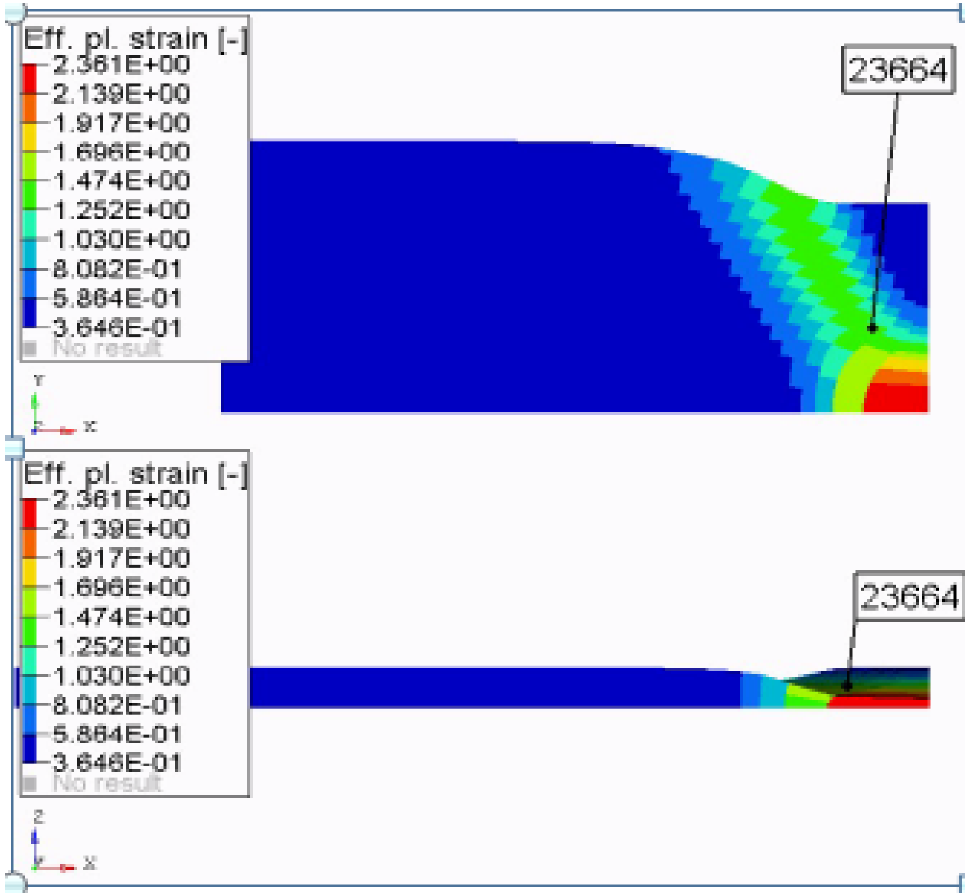

Strain BC

DD-case

Condition β=-0.499

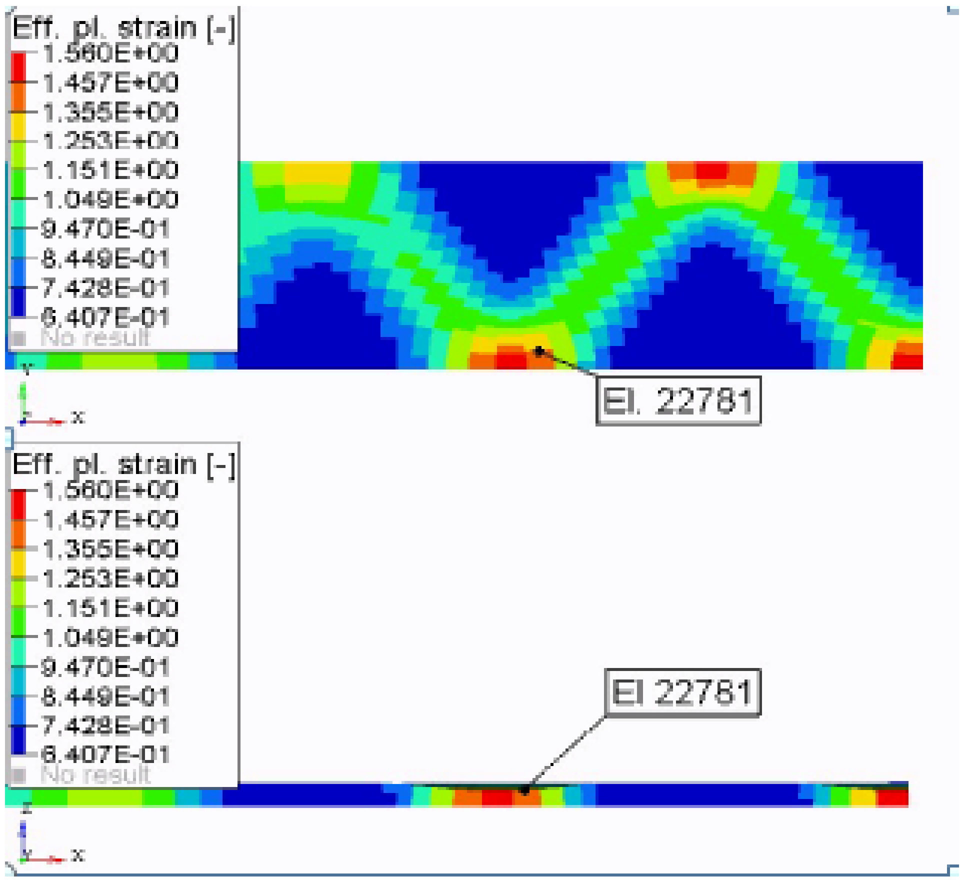

Material AA 6016

Differences between strain and stress BC

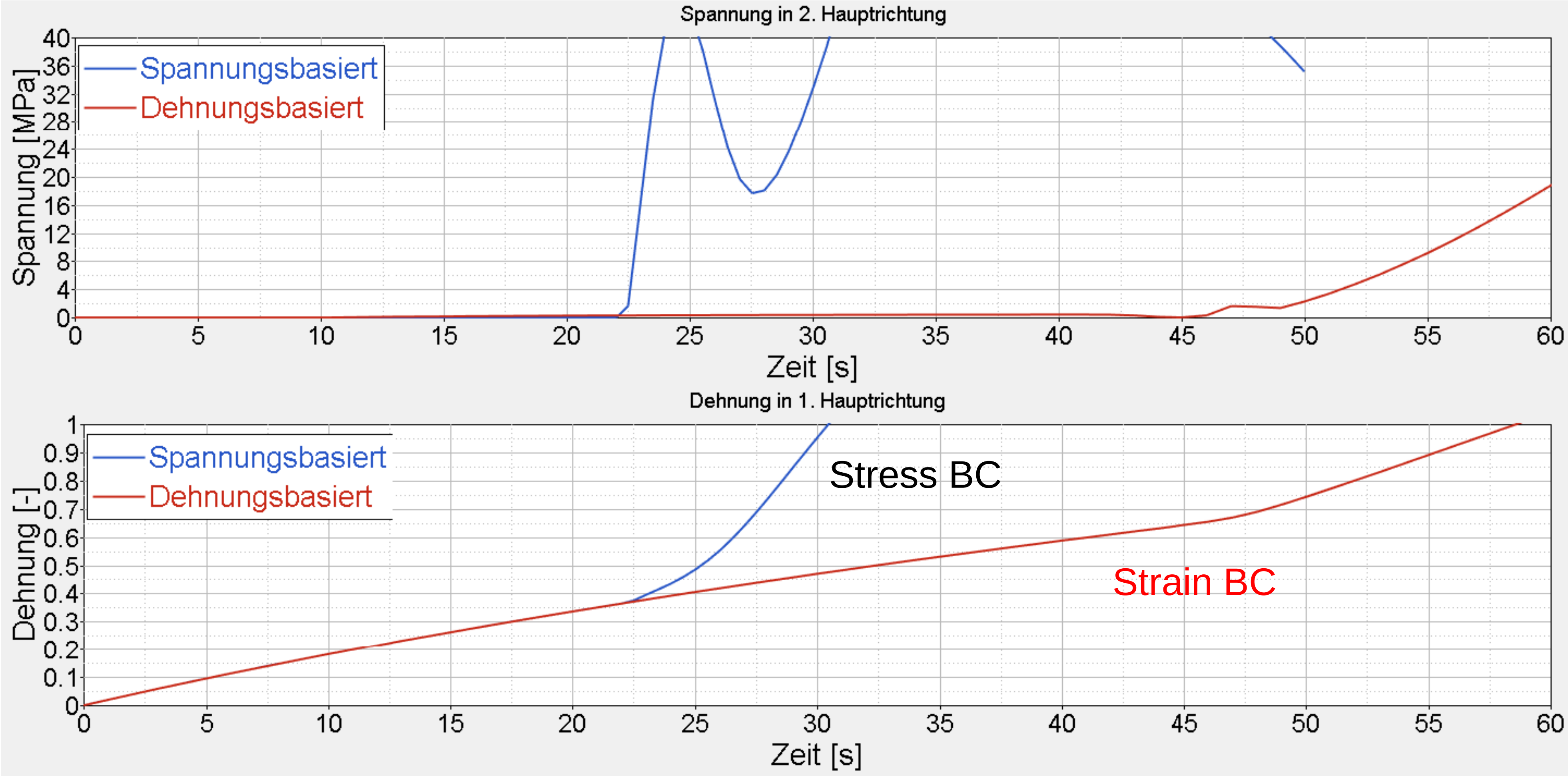

Stress-based:
Eps11=~0.4
Strain-based:
Eps11=~0.6
At localization

Impact of the BC on the necking behavior

Stress driven BC

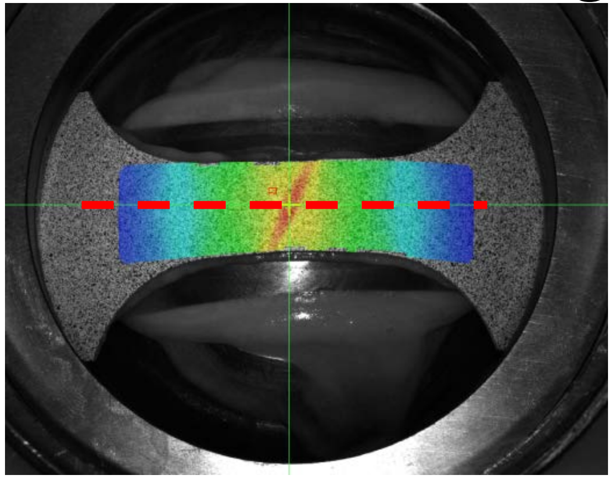

Strain driven BC

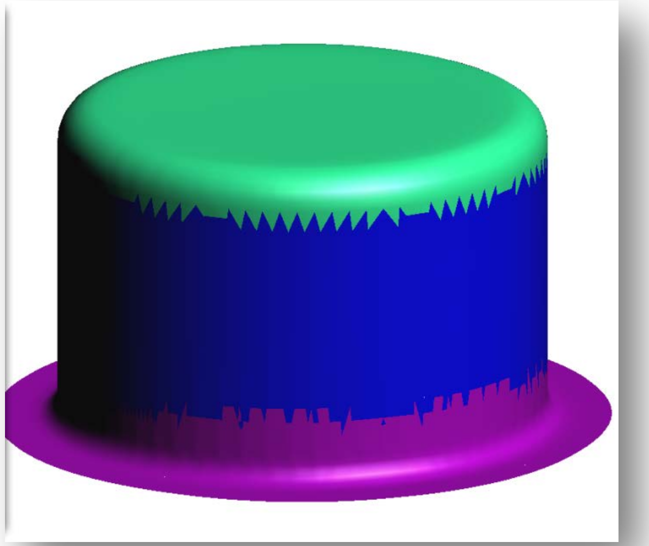

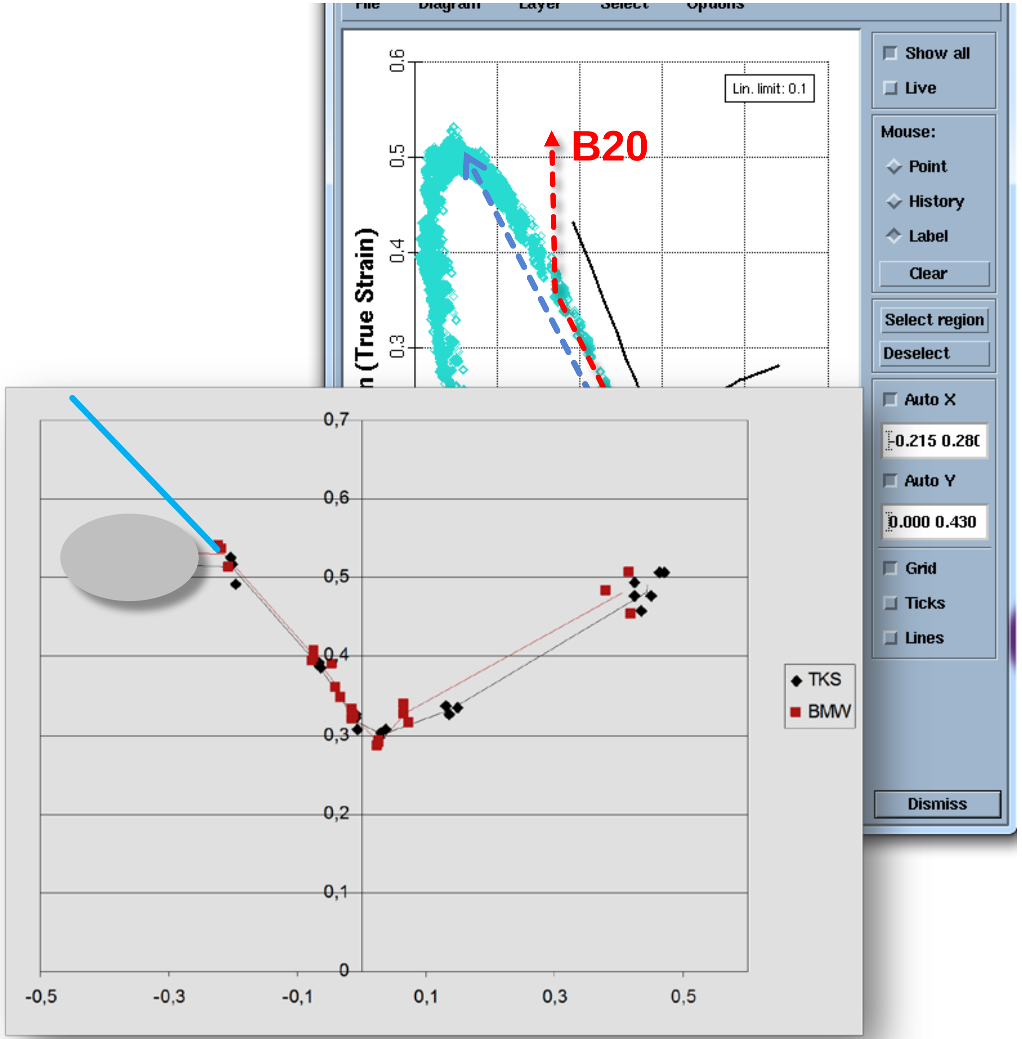


AC_10
D150
50KN

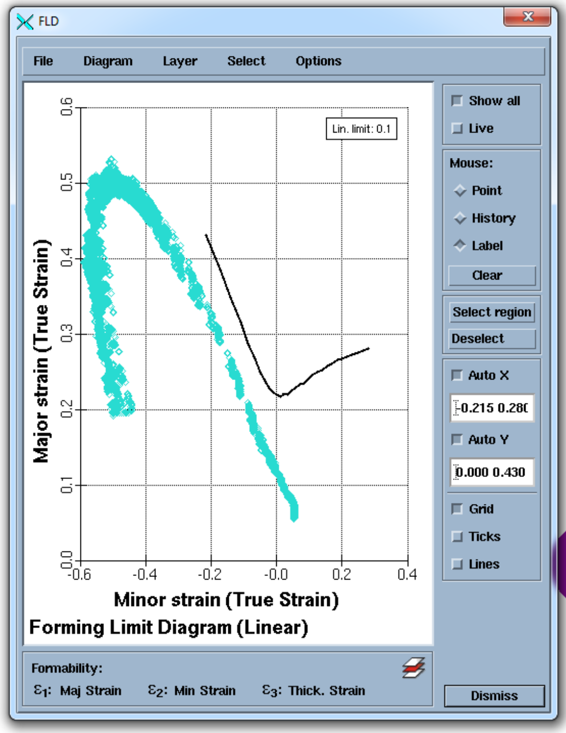
FLD
File
Diagram
Layer
Select
Options
Lin. limit: 0.1
Major strain (True Strain)
Minor strain (True Strain)
Forming Limit Diagram (Linear)
Show all
Live
Mouse:
Point
History
Label
Clear
Select region
Deselect
Auto X
-0.215 0.280
Auto Y
0.000 0.430
Grid
Ticks
Lines
Formability:
ε1: Maj Strain
ε2: Min Strain
ε3: Thick. Strain
Dismiss

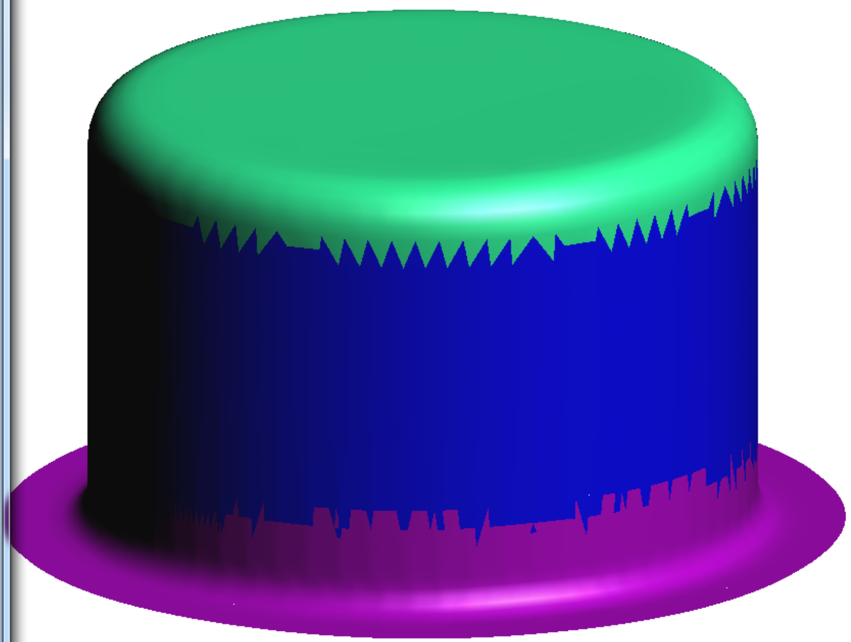

… different parameters like curvature may not be coverd correctly as well

Limitations in the FLC prediction

Influence of thickness

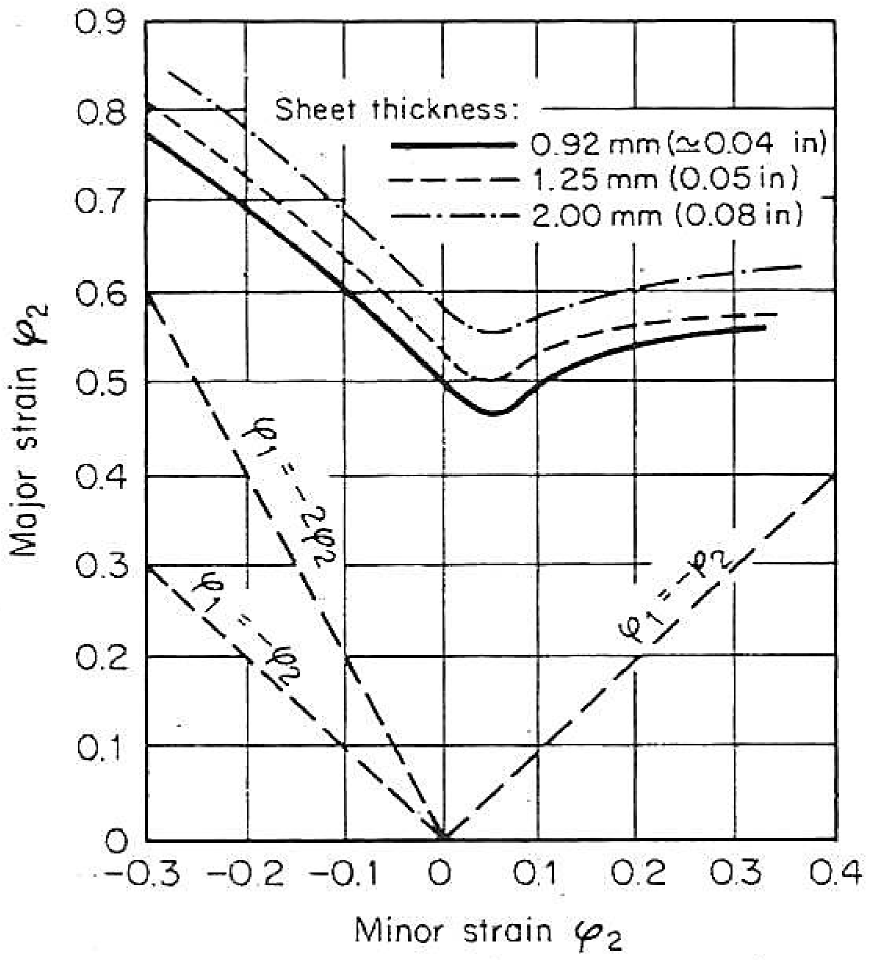

Material
RRSt 1403 (AISI 1006)

Source: Handbook of Metal Forming, Ed. McGraw –Hill Book Co. N.Y., 1985, p 18.13

Limitations in the FLC prediction

Influence of curvature

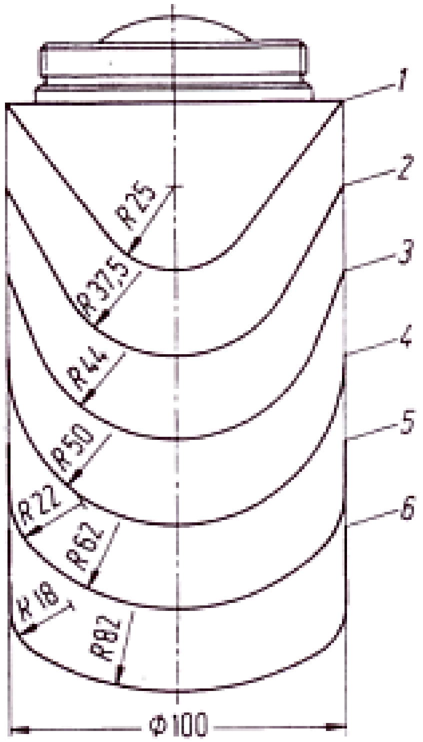

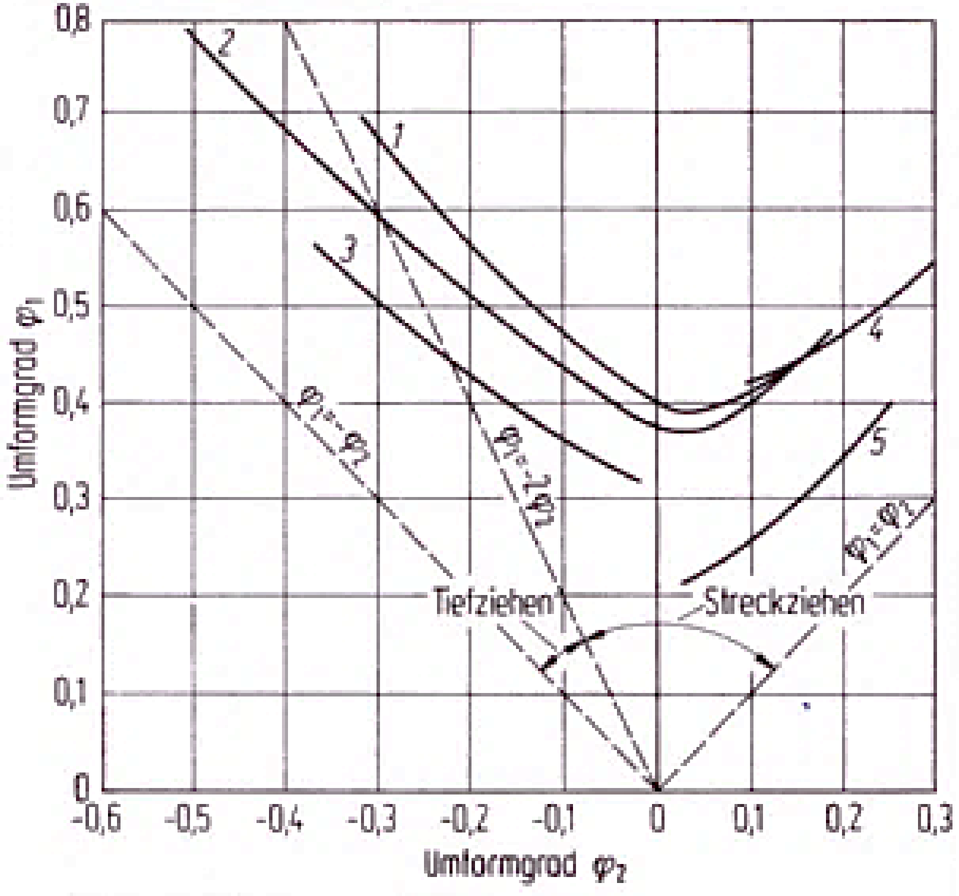

FLC evaluation with different punch geometries

Source: V.Hasek: Untersuchung und theoretische Beschreibung wichtiger Einflussgrössen auf das Grenzformänderungsschaubild. Blech-Rohre-Profile . 25(1978)213-220 or. Buch Lange Umfortmtechnik Bd. 3, p.51-57

Limitations in the FLC prediction

Influence of stretch bending in FLD0

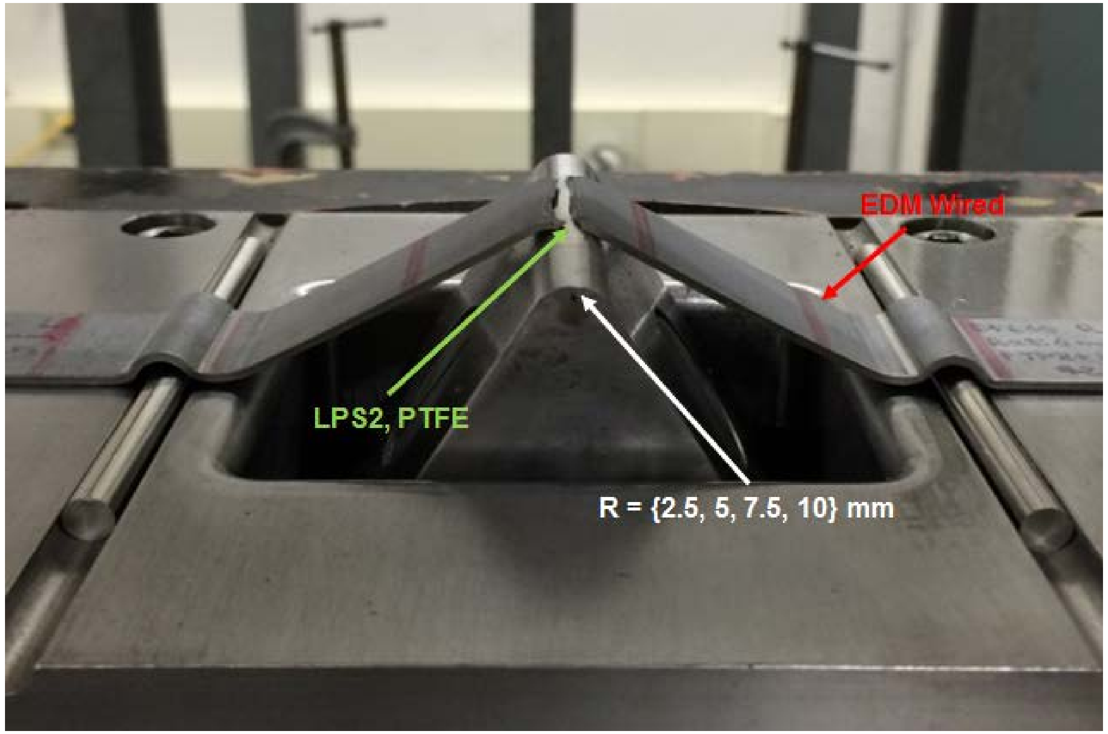

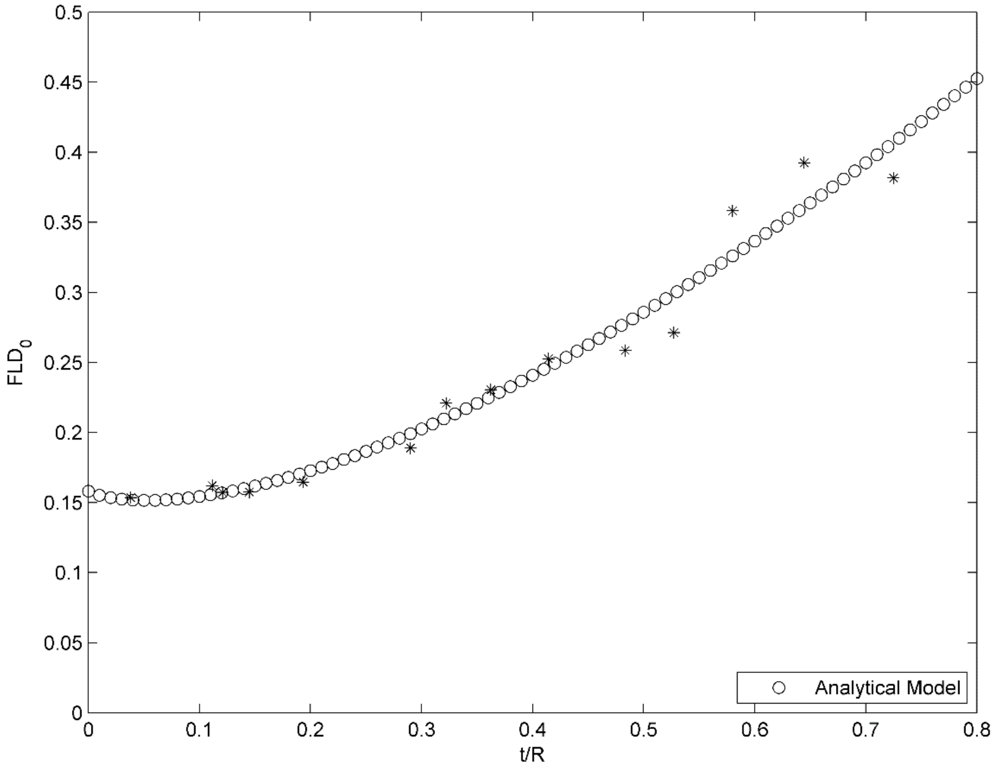

FLD0 – Values in a stretch-bending test

Source: F.M. Neuhauser[1,2], O.R. Terrazas[1], N. Manopulo[2], P. Hora[2] and C.J. Van Tyne
Stretch bending – the plane within the sheet where strains reach the forming limit curve. In Proceeding of IDDR2016

Limitations in the FLC prediction

Crack strains in hemming

Hemming test – detection of crack strains

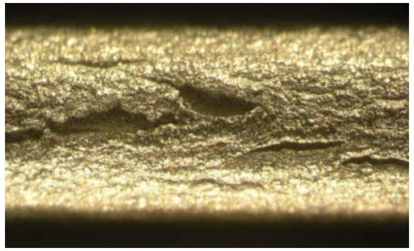

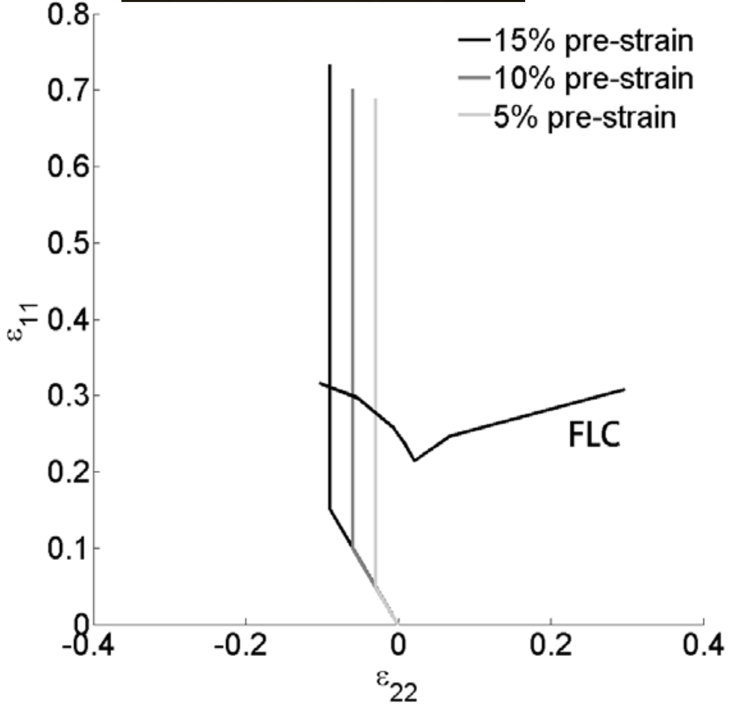

3-point Bending Experiment- AA6016

Source: M. Gorji. Diss. ETH 2016

… the strain path are even on simple parts not always linear

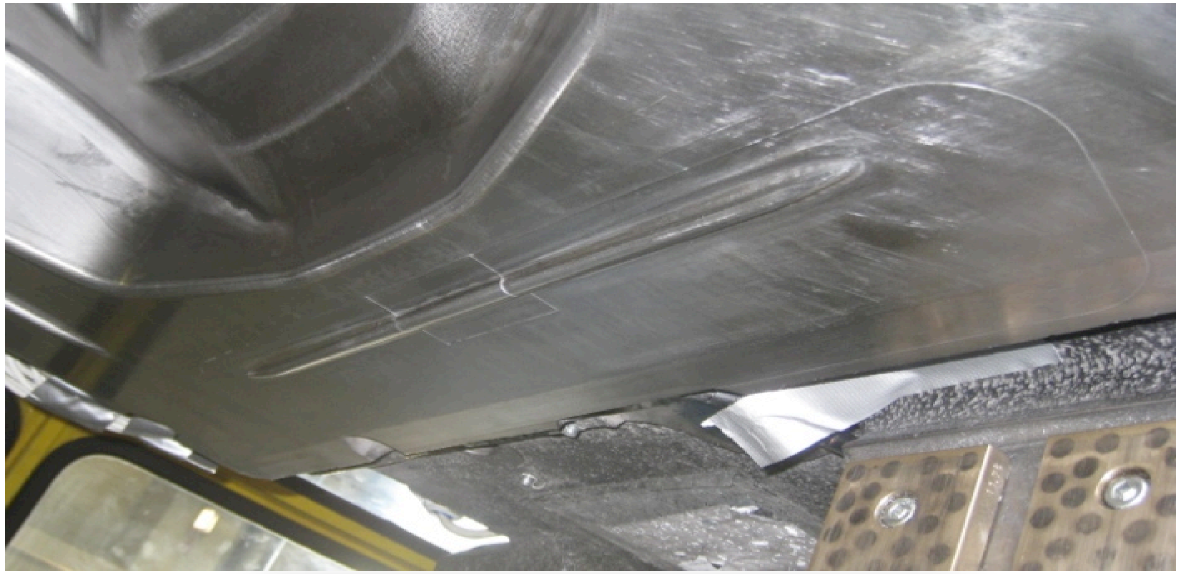

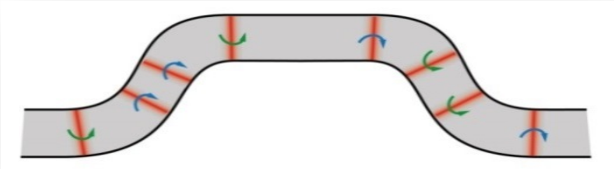

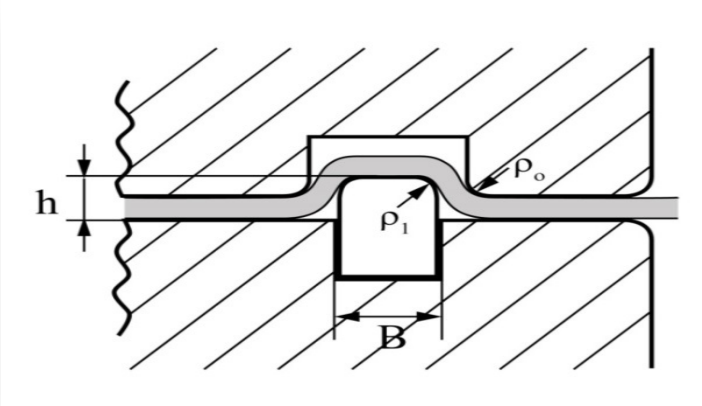

- When passing through a draw bead the sheet is bent up to 8 times.
- This results in a reversal load, which is not detected by the linear FLC
- Material specifically, this leads to an increase in the FLD_0 value [publications by T. Van den Boogaard (2008) or Neuhauser et.al (IDDRG 2016)]

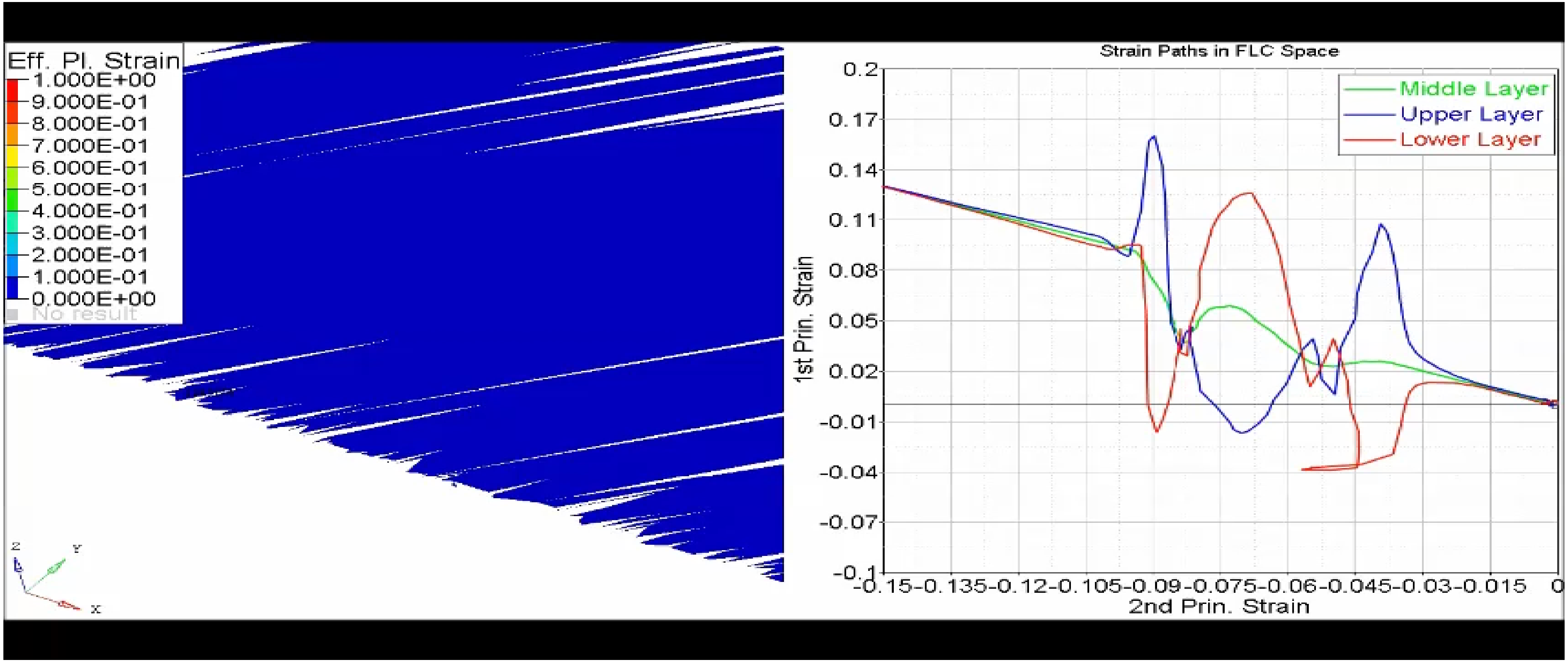
Eff. Pl. Strain
1.000E+00
9.000E-01
8.000E-01
7.000E-01
6.000E-01
5.000E-01
4.000E-01
3.000E-01
2.000E-01
1.000E-01
0.000E+00
No result
Strain Paths in FLC Space
Middle Layer
Upper Layer
Lower Layer
1st Prin. Strain
2nd Prin. Strain
0.2
0.17
0.14
0.11
0.08
0.05
0.02
-0.01
-0.04
-0.07
-0.1
-0.15
-0.135
-0.12
-0.105
-0.09
-0.075
-0.06
-0.045
-0.03
-0.015
0

Nonlinear Deformation Paths

Cross-Die

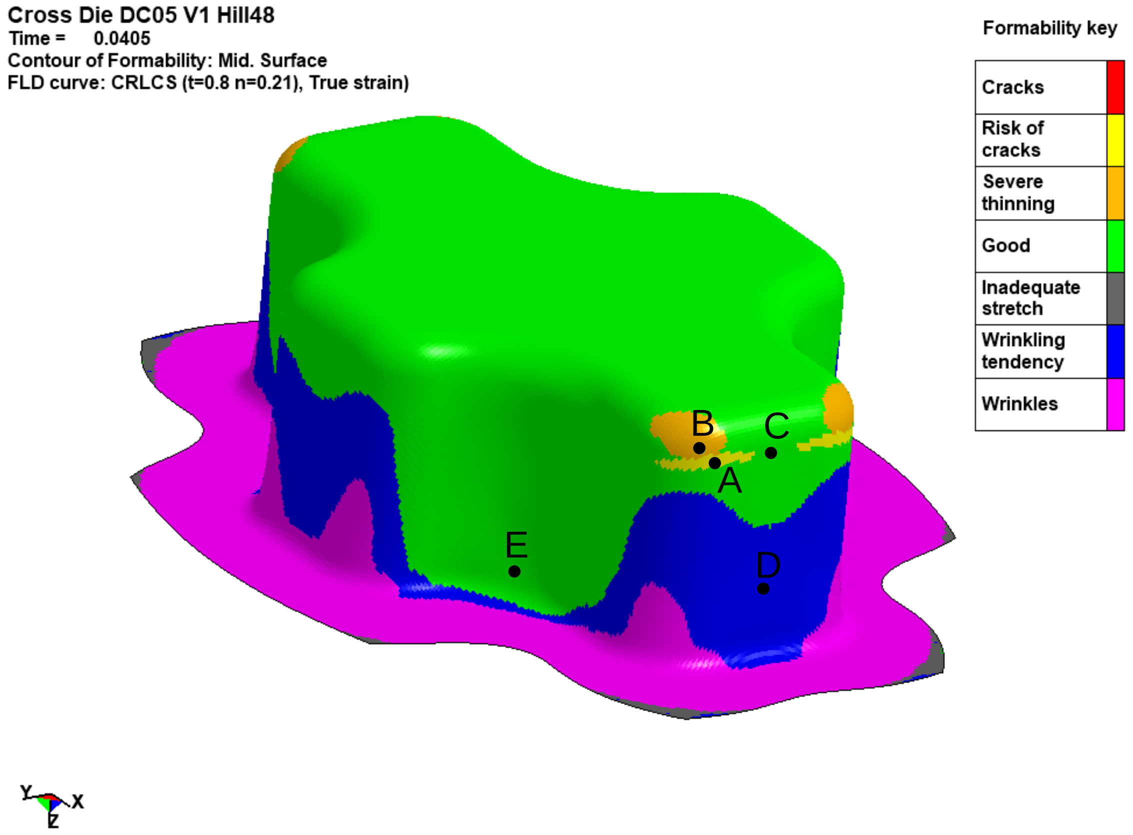

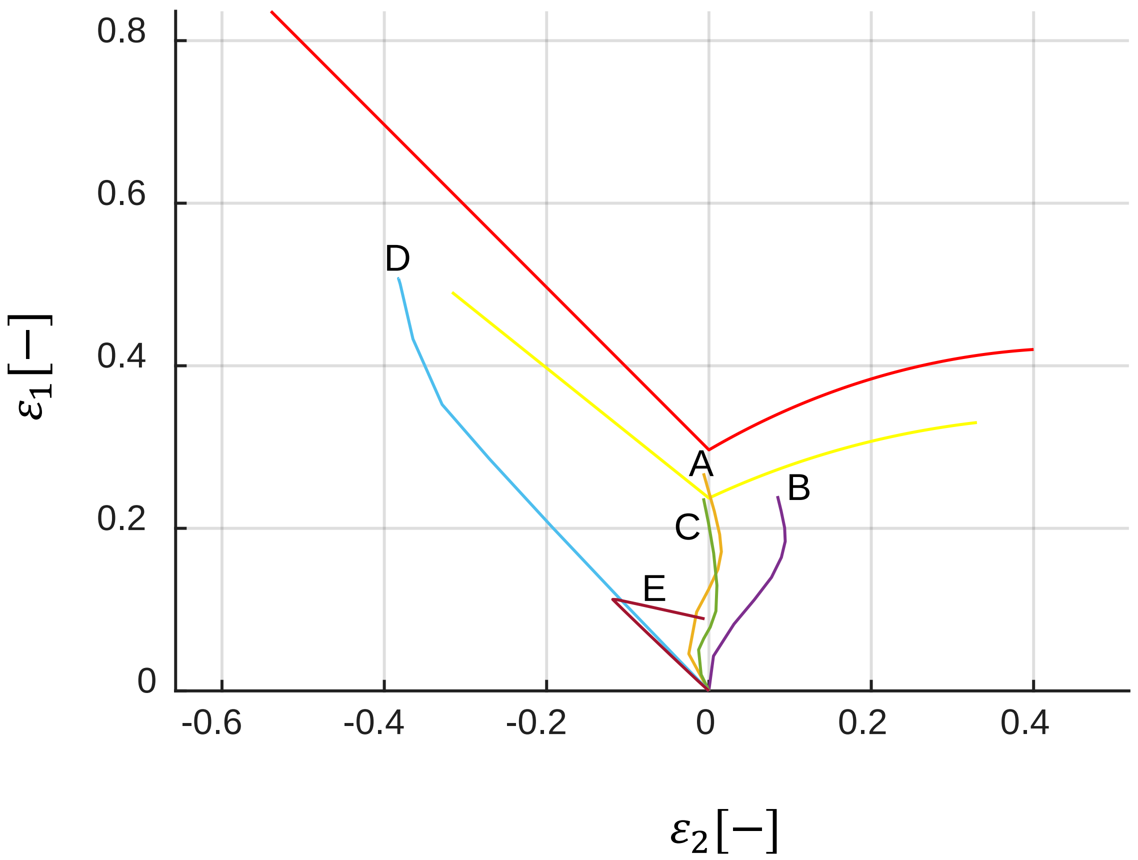

PREDICATBILITY OF NECKING LIMITS BASED ON NUMERICAL MODELS

Theoretical failure prediction

Virtual FLC Prediction

Theoretical models in failure predictions

- Marciniak
- Rice
- Hutchinson
- Ghosh
- Needleman
- Stören
- Keeler
- Miyauchi
- Budianski
- Kobayashi
- Koistinen

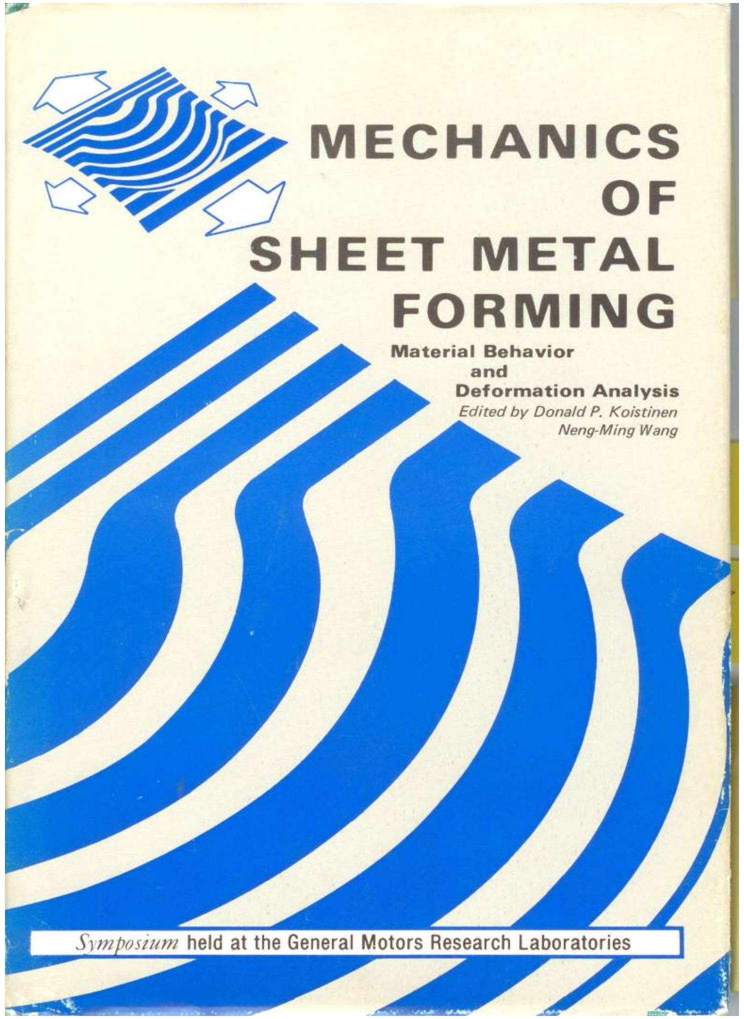

Applicability of numerical models

Effects	MK-Models	GTN Models	MMFC-Models	GFLC (Volk et.al)
Thickness	only t_A/t_B	(not explicitly)	Included as t/R ratio	(not explicitly)
Curvature	NO	(not explicitly)	Included as t/R ratio	(not explicitly)
Strain rate	YES	YES	YES	(not explicitly)
Non-linear path	YES	YES	YES	YES
Significant weaknesses	Inhomogeneity assumption	Unclear evolution of damage	Single point model	Based on experimental data

Content

MMFC

Localization condition with plane strain state

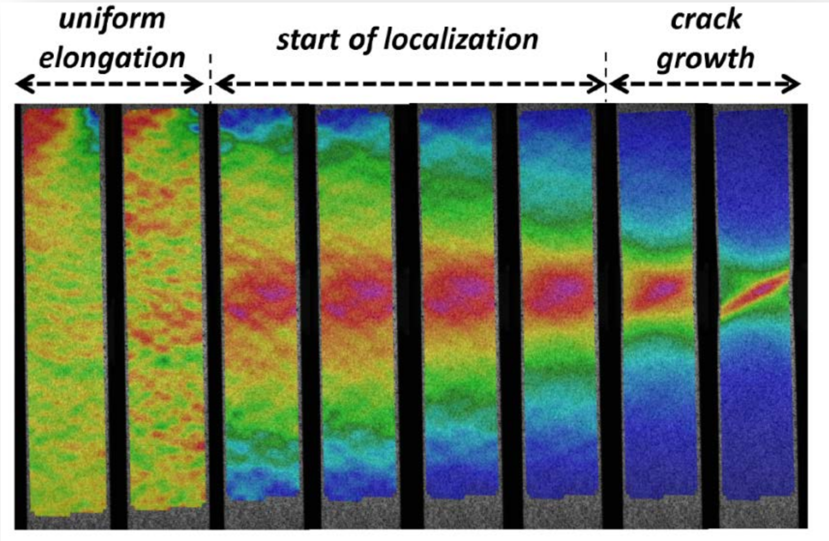

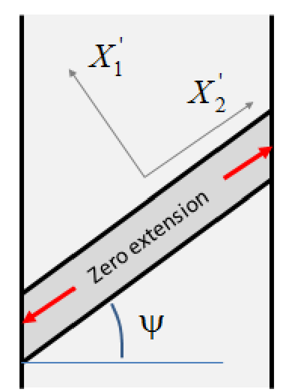

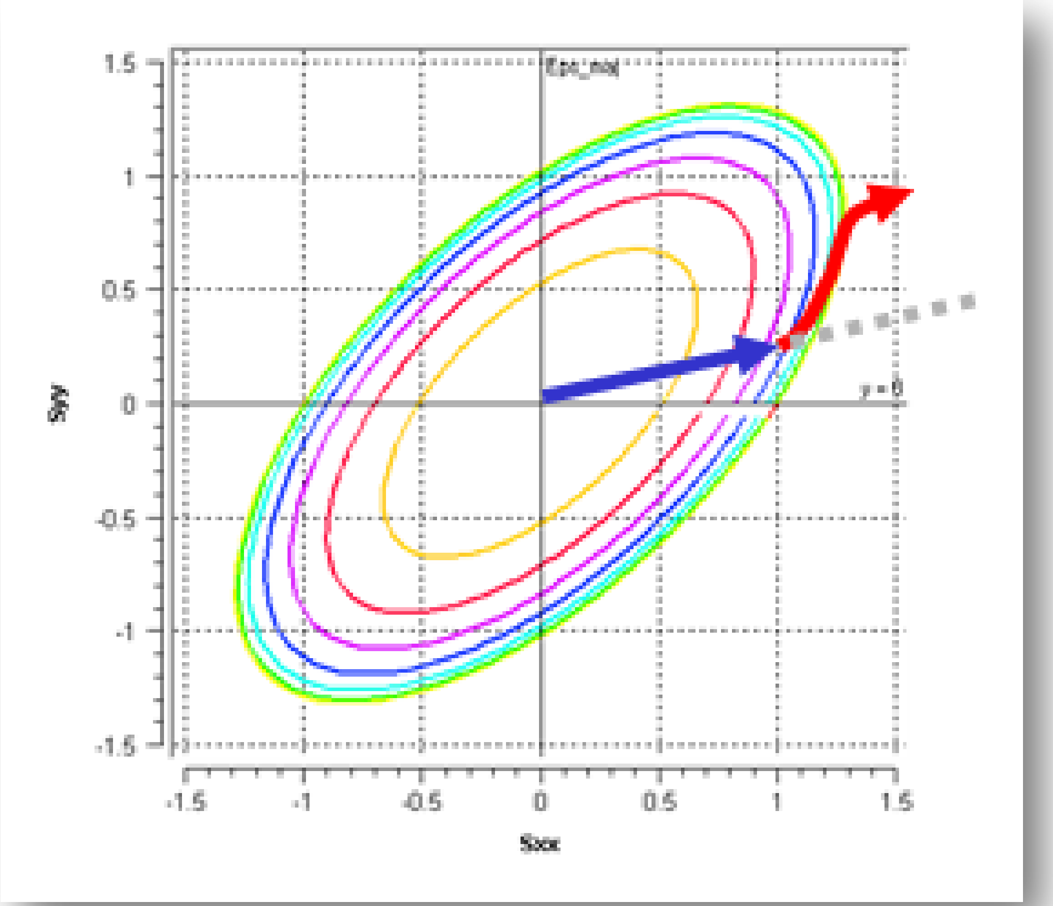

"M-K" FEM evaluation

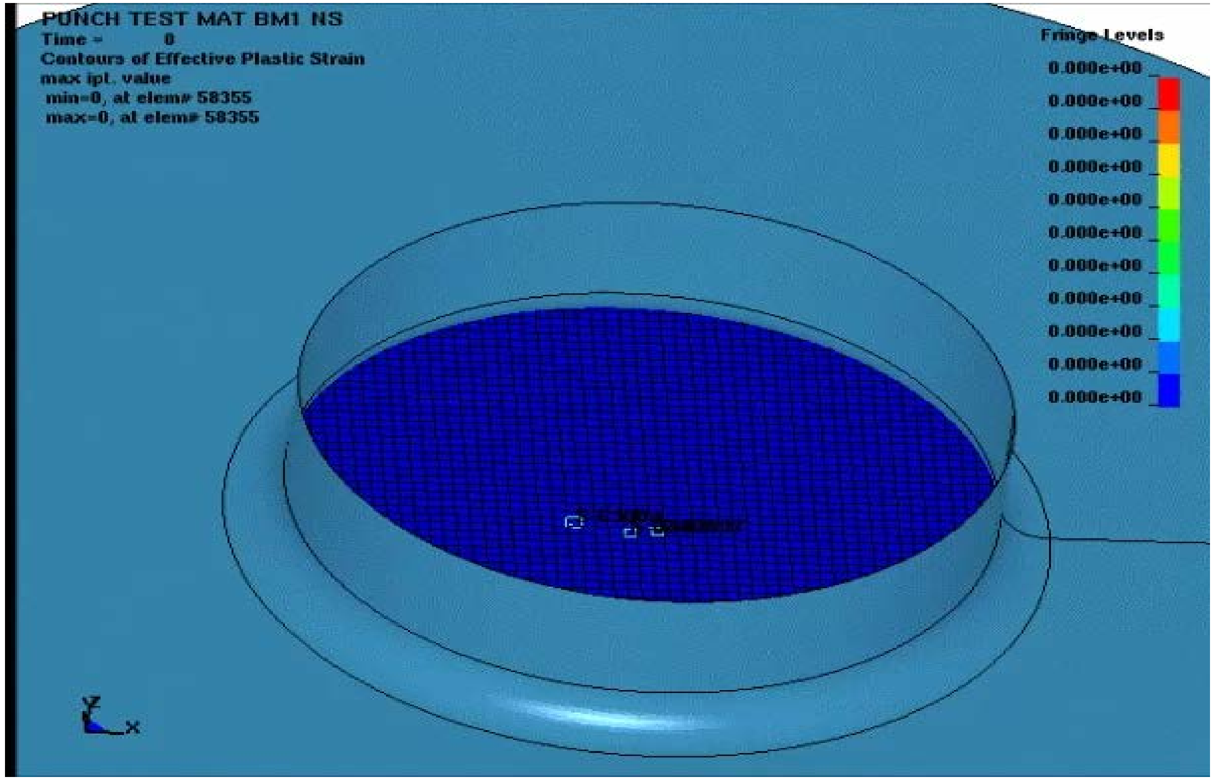

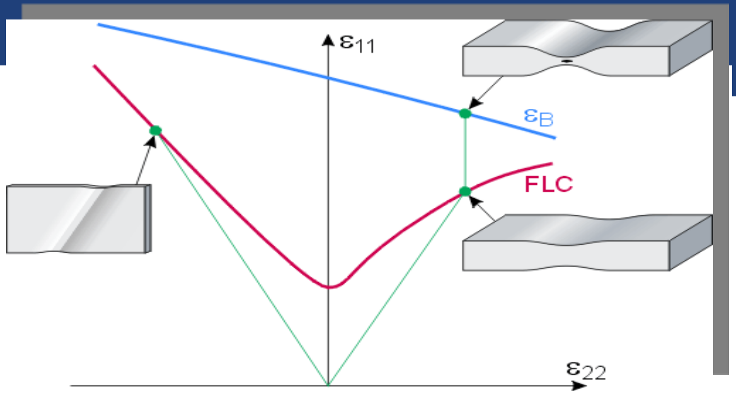

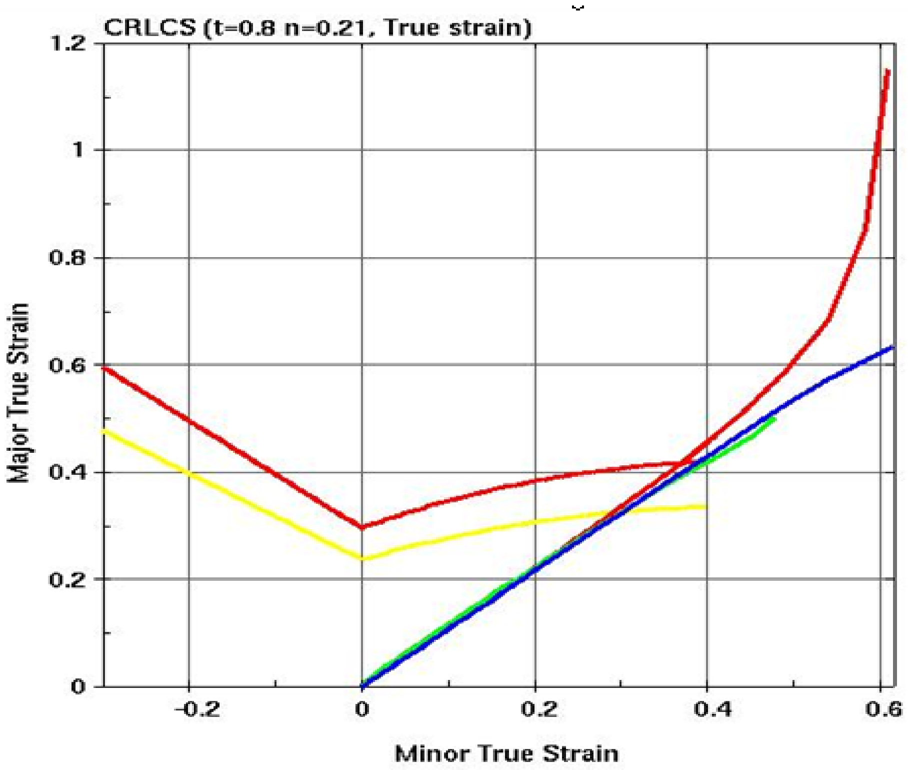

eMMFC with strain rate extension

Influence of bending

Influence of thickness

Influence of Strain rate

$$\frac{\partial \sigma_{11}}{\partial \varepsilon_{11}}\left[1+\frac{t}{2\rho}+E_o\left(\frac{t}{t_o}\right)^n\right]+\frac{\partial \sigma_{11}}{\partial \beta}\frac{\partial \beta}{\partial \varepsilon_{11}}+\frac{\partial \sigma_{11}}{\partial \dot{\varepsilon}}\frac{\partial \dot{\varepsilon}}{\partial \varepsilon_{11}} \geq \sigma_{11}$$

Influence of yield curve hardening by ß constant

Influence of yield locus hardening Induced by β-change

Description of the localization rate

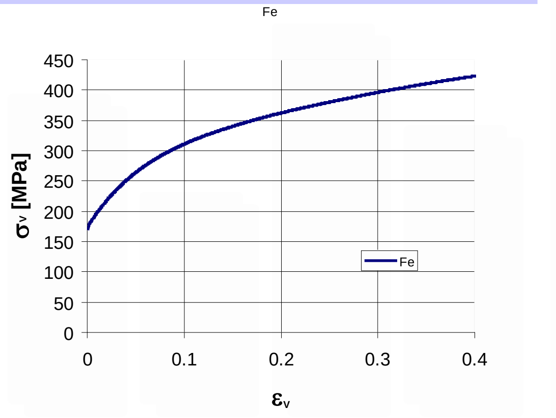

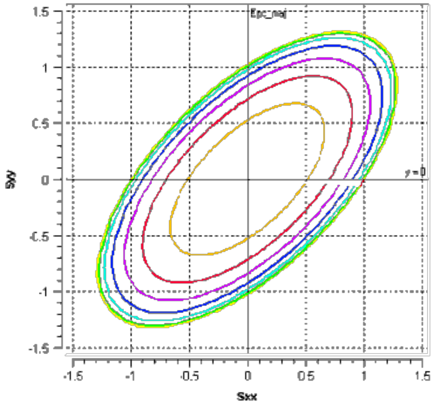

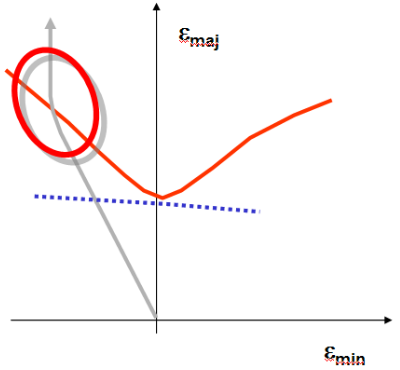

Institut für Virtuelle Produktion
Institute of Virtual Manufacturing

MMFC

Marciniak's remark GM symposium 1978

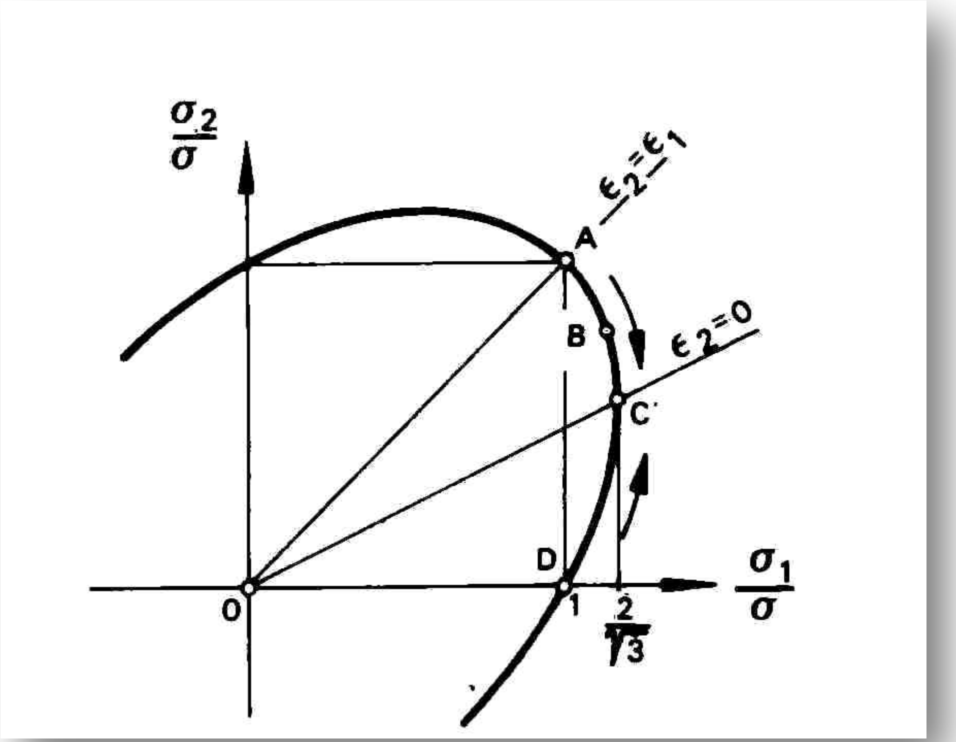

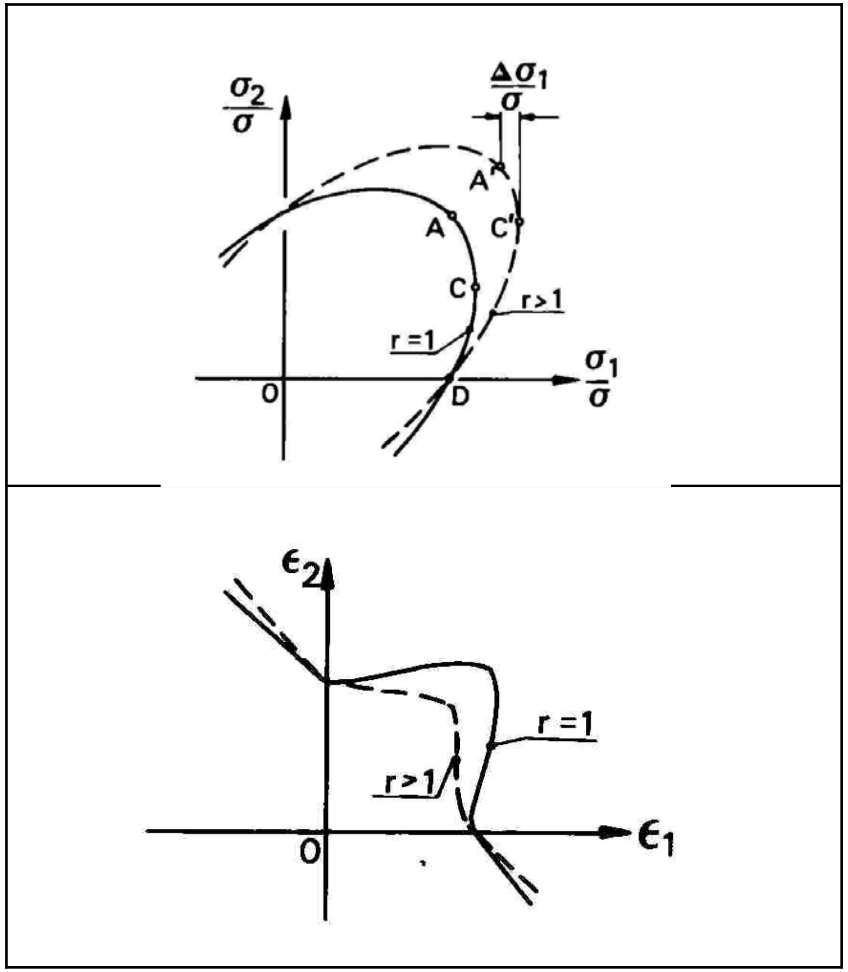

Reference:

Z. Marciniak: *Sheet metal forming limits.* In Koistinen D.P.; Wang N.M. (eds):Mechanics of Sheet Metal forming, New York/London Plenum Press 1978, pp. 215-235.

Ghosh's formulation (1974)

Under the assumption that the hardening is a function of

$$\bar{\sigma} = H(\bar{\varepsilon}, \dot{\bar{\varepsilon}}, \beta, T, \ldots)$$

Ghosh expressed the instability criterion in dependency of those parameters with

$$\left(\frac{\partial\sigma}{\partial\bar{\varepsilon}}\right)\frac{d\bar{\varepsilon}}{d\varepsilon_{11}} + \left(\frac{\partial\sigma}{\partial\dot{\bar{\varepsilon}}}\right)\frac{d\dot{\varepsilon}}{d\varepsilon_{11}} + \left(\frac{\partial\sigma}{\partial\beta}\right)\frac{d\beta}{d\varepsilon_{11}} + \left(\frac{\partial\sigma}{\partial T}\right)\frac{dT}{d\varepsilon_{11}} = \frac{\bar{\sigma}}{Z_d}$$

A.K. Ghosh: *Strain localization in the diffuse neck in the sheet metal*. Metalurgical Transaction, Vol. 5(1974), pp. 1607-1615

MMFC models

	Presented in	Type	MMFC-Version
MMFC_1993	TKS report 1993	Report	Theoretical basics
MMFC_1994	IDDRG'94	Paper	MMFC Temp. , Thickness/Curvature
MMFC_1996	Numisheet'96	Paper	MMFC n.-l. strain path
MMFC_2002	Numisheet'02	Paper	MMFC n.-l. strain path
MMFC_2003	Plasticity'03	Abstract	Enhanced MMFC / Thickness
MMFC_2006	Plasticity'06	Keynote	Enhanced MMFC / Thickness
MMFC_2007	IDDRG	Paper	eMMFC for FLC-T
MMFC_2007	Numiform'07	Paper	eMMFC for FLC-T Stainless steel
MMFC_2016	IDDRG	Paper	eMMFC-SR Strain rate dependency

See www.ivp.ethz.ch/docs/index

Theoretical prediction of FLC based on curvature and strain rate dependent MMFC criterions

P. Hora[1], L. Tong, N. Manopulo

[1] ETH Zurich, Institute of Virtual Manufacturing, Tannenstr. 3, 8092 Zurich, Switzerland

E-mail: hora@ivp.mavt.ethz.ch

Abstract. Formability predictions in industrial sheet metal forming applications still rely on the Forming Limit Diagrams (FLD). The FLD are commonly specified by the Nakajima tests and evaluated with the so called cross section method. For the theoretical prediction of FLC the well-known M-K criterion as well as the MMFC criterion can be used. The contribution discusses the applicability of an extended MMFC formulation under the consideration of bending as well as strain rate effects. The evaluation and comparison with the experimental FLD is given for the material HC220-YD.

1 Introduction

Nowadays forming limits in sheet forming processes are mostly predicted based on the necking initiation. This limit is usually evaluated with the Nakajima test. The FLC's are in this way only valid for linear strain paths and for negligible curvature radii. Typically, the so evaluated FLC will be used as reference for the forming limit prediction without further detailed consideration of superimposed bending. Figure 1 depicts the cracked Nakajima specimens (left) as well as the failure interpretation scheme according to the FLC (right).

IDDRG 2016

Theoretical background MMFC s.

IDDRG 2018

Software extension for non-linear strain path.

Skip basics MMFC

MMFC generalized equation

$$H'\left(1+\frac{t}{2\rho}+E_0*\left(\frac{t}{t_0}\right)^n\right)\leq\left(\frac{f(\alpha)+\frac{f'(\alpha)g(\beta)\beta}{\beta'(\alpha)\,\varepsilon}}{f(\alpha)g(\beta)}\right)*\mathrm{H}$$

Stress evaluation procedure:

$\sigma_i(\beta);\ \bar{\sigma}$: direct evaluation based on the yield locus function F

Topology:

t: Thickness
ρ: Die curvature

Material hardening function:

H: $Hardening\ curve\ H(\bar{\varepsilon},\dot{\varepsilon}\ ,\mathrm{T})$

Material model dependent functions:

$$\alpha=\frac{\sigma_2}{\sigma_1}\qquad f(\alpha)=\sigma_1(\beta)/\bar{\sigma}$$

$$g(\beta)=\bar{\varepsilon}/\varepsilon_1=\mathrm{f}(\alpha)(1+\alpha*\beta)$$

$$\beta=\frac{\frac{dF}{d\sigma_2}}{\frac{dF}{d\sigma_1}}=\frac{\Delta\varepsilon_2}{\Delta\varepsilon_1}$$

Skip theory

Theoretical prediction of FLC based on curvature and strain rate dependent MMFC criterions

P. Hora[1], L. Tong, N. Manopulo

[1] ETH Zurich, Institute of Virtual Manufacturing, Tannenstr. 3, 8092 Zurich, Switzerland

E-mail: hora@ivp.mavt.ethz.ch

Abstract. Formability predictions in industrial sheet metal forming applications still rely on the Forming Limit Diagrams (FLD). The FLD are commonly specified by the Nakajima tests and evaluated with the so called cross section method. For the theoretical prediction of FLC the well-known M-K criterion as well as the MMFC criterion can be used. The contribution discusses the applicability of an extended MMFC formulation under the consideration of bending as well as strain rate effects. The evaluation and comparison with the experimental FLD is given for the material HC220-YD.

1 Introduction

Nowadays forming limits in sheet forming processes are mostly predicted based on the necking initiation. This limit is usually evaluated with the Nakajima test. The FLC's are in this way only valid for linear strain paths and for negligible curvature radii. Typically, the so evaluated FLC will be used as reference for the forming limit prediction without further detailed consideration of superimposed bending. Figure 1 depicts the cracked Nakajima specimens (left) as well as the failure interpretation scheme according to the FLC (right).

IDDRG 2016

Theoretical background MMFC s.

IDDRG 2018

Software extension for non-linear strain path.

Skip theory

Numerical evaluation of the Yield locus specific functions

- $f(\alpha) = \frac{\sigma_1(\beta)}{\bar{\sigma}} = Yield\ Locus\ (\ Hill48, Hill79, Hill90, Barlat2000, \ldots\ldots)$

- $\beta(\alpha) = \frac{\frac{dF}{d\sigma_2}}{\frac{dF}{d\sigma_1}} = \frac{\Delta\varepsilon_2}{\Delta\varepsilon_1}$ → $\frac{dF}{d\sigma_1}; \frac{dF}{d\sigma_2}$ analytical derivates

- $f'(\alpha)\ and\ \beta'(\alpha)$ → Numerical evaluation by $\Delta\alpha$ difference

Evaluation based on plastic work equivalence $\Delta W = \Delta\varepsilon_1 * \sigma_1 + \Delta\varepsilon_2 * \sigma_2 = \Delta\bar{\varepsilon} * H$ leads to:

- $g(\beta) = \frac{\bar{\varepsilon}}{\varepsilon_1} = f(\alpha)(1 + \alpha * \beta)$

Specification for Hill'79 (1)

Funktion $f(\alpha)$

Yield function

$$2(R+1)\sigma_v^m = (2R+1)|\sigma_{11}-\sigma_{22}|^m + |\sigma_{11}+\sigma_{22}|^m$$

Expressed with tress ratio α

$$\sigma_v = \left[\frac{2R+1}{2(R+1)}|1-\alpha|^m + \frac{|1+\alpha|^m}{2(R+1)}\right]^{1/m} \sigma_1$$

Function $\mathrm{f}(\alpha)$

$$f(\alpha) = \left[\frac{2R+1}{2(R+1)}|1-\alpha|^m + \frac{|1+\alpha|^m}{2(R+1)}\right]^{-1/m}$$

Derivates $\mathrm{f}'(\alpha)$

$$f'(\alpha) = \left[\frac{2R+1}{2(R+1)}|1-\alpha|^m + \frac{|1+\alpha|^m}{2(R+1)}\right]^{-\frac{m+1}{m}} \left[\frac{2R+1}{2(R+1)}|1-\alpha|^{m-1} - \frac{|1+\alpha|^{m-1}}{2(R+1)}\right]$$

Specification for Hill'79 (2)

Funktion $g(\beta)$

Equivalent strain increment

$$\Delta\varepsilon_v = \frac{[2(R+1)]^{\frac{1}{m}}}{2}\left\{\frac{1}{(1+2R)^{\frac{1}{m-1}}}|\Delta\varepsilon_1 - \Delta\varepsilon_2|^{\frac{m}{m-1}} + |\Delta\varepsilon_1 + \Delta\varepsilon_2|^{\frac{m}{m-1}}\right\}^{\frac{m-1}{m}}$$

Expressed in function of β

$$\Delta\varepsilon_v = \frac{[2(R+1)]^{\frac{1}{m}}}{2}\left\{\frac{1}{(1+2R)^{\frac{1}{m-1}}}|1-\beta|^{\frac{m}{m-1}} + |1+\beta|^{\frac{m}{m-1}}\right\}^{\frac{m-1}{m}}\Delta\varepsilon_1$$

Function $g(\beta)$

$$g(\beta) = \frac{[2(R+1)]^{\frac{1}{m}}}{2}\left\{\frac{1}{(1+2R)^{\frac{1}{m-1}}}|1-\beta|^{\frac{m}{m-1}} + |1+\beta|^{\frac{m}{m-1}}\right\}^{\frac{m-1}{m}}$$

Specification for Hill'79 (3)

Funktion $\boldsymbol{\beta}(\boldsymbol{\alpha})$

$$\beta(\alpha) = \frac{-(2R+1)|\sigma_{11}-\sigma_{22}|^{m-1} + |\sigma_{11}+\sigma_{22}|^{m-1}}{(2R+1)|\sigma_{11}-\sigma_{22}|^{m-1} + |\sigma_{11}+\sigma_{22}|^{m-1}} = \frac{-(2R+1)|1-\alpha|^{m-1} + |1+\alpha|^{m-1}}{(2R+1)|1-\alpha|^{m-1} + |1+\alpha|^{m-1}}$$

Derivates $\beta'(\alpha)$: $u'v + uv'$

$$\beta'^{(\alpha)} = \frac{(m-1)[(2R+1)|1-\alpha|^{m-2} + |1+\alpha|^{m-2}]}{(2R+1)|1-\alpha|^{m-1} + |1+\alpha|^{m-1}} +$$

$$[-(2R+1)|1-\alpha|^{m-1} + |1+\alpha|^{m-1}] \frac{(m-1)[(2R+1)|1-\alpha|^{m-2} + |1+\alpha|^{m-2}]}{[(2R+1)|1-\alpha|^{m-1} + |1+\alpha|^{m-1}]^2}$$

Numerical evaluation for YLD2000

- $f(\alpha) = \frac{\sigma_1(\beta)}{\bar{\sigma}}$ = Yield Locus (Hill48, Hill'79, Barlat'89, Barlat2000,......)

  Set in an initiation procedure (initial_Falpha_YLD2000)

- $\beta(\alpha) = -\frac{\frac{dF}{d\sigma_2}}{\frac{dF}{d\sigma_1}} = \frac{\Delta\varepsilon_2}{\Delta\varepsilon_1}$ → analytical derivates $\frac{dF}{d\sigma_1}$; $\frac{dF}{d\sigma_2}$

  Numericaly evaluated in an initiation procedure (initial_BetaAlpha_YLD2000)

- $f'(\alpha)$ and $\beta'(\alpha)$ → Numerical evaluation by $\Delta\alpha$ difference

Evaluation based on plastic work equivalence $\Delta W = \Delta\varepsilon_1 * \sigma_1 + \Delta\varepsilon_2 * \sigma_2 = \Delta\bar{\varepsilon} * H$ leads to:

- $$g(\beta) = \frac{\bar{\varepsilon}}{\varepsilon_1} = f(\alpha)(1 + \alpha * \beta)$$

YLD2000 (skip theory) ▷

MMFC modelling of the strain rate influence

MMFC is a single point evaluation method

The increase of strain rates due to localization can be mapped only by an additional function

Strain rate influence

Influence of bending

Influence of thickness

Influence of Strain rate

$$\frac{\partial \sigma_{11}}{\partial \varepsilon_{11}}\left[1+\frac{t}{2\rho}+E_o\left(\frac{t}{t_o}\right)^n\right]+\frac{\partial \sigma_{11}}{\partial \beta}\frac{\partial \beta}{\partial \varepsilon_{11}}+\frac{\partial \sigma_{11}}{\partial \dot{\varepsilon}}\frac{\partial \dot{\varepsilon}}{\partial \varepsilon_{11}}\geq \sigma_{11}$$

Influence of yield curve hardening by ß constant

Influence of yield locus hardening Induced by β-change

Description of the localization rate

Influence of strain rate

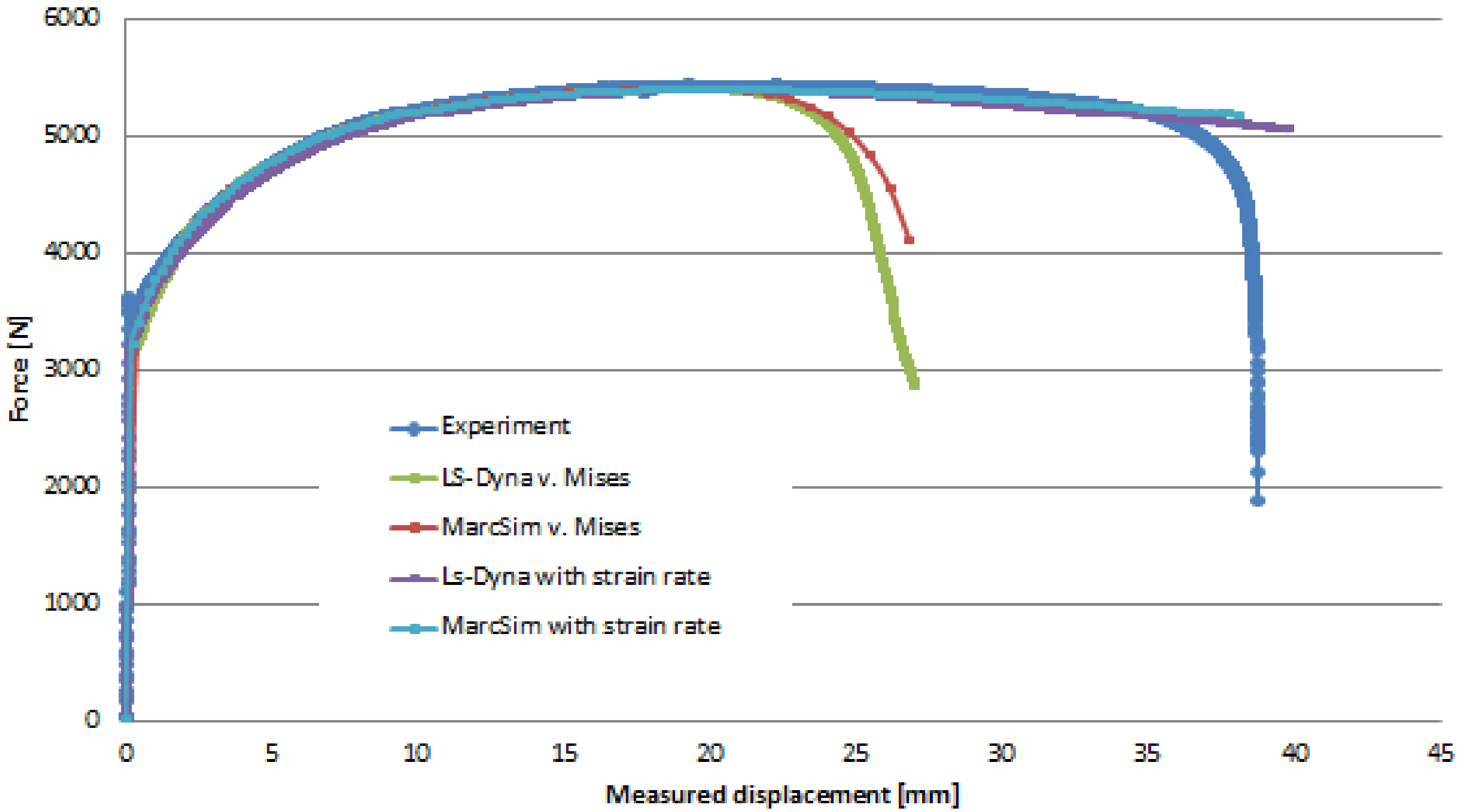

FEM simulation of a tensile test for a DC05 material

Strain rate dependency

$$\dot{\varepsilon}_{11}(\varepsilon_{11}, \beta)$$

FEM Implementation
linear interpolation of A(β)

Beta	$A_{(k)}$
-0.5	2.1
0.0	40.6
1.0	220.1
p	2.0

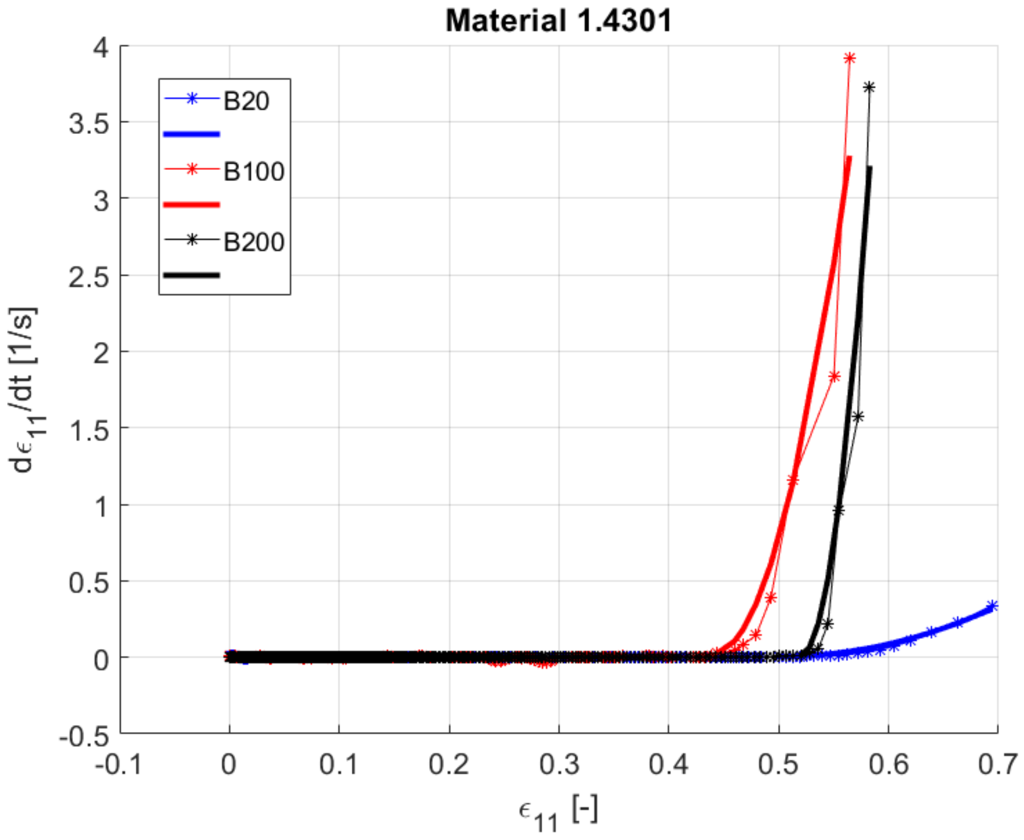

$$\dot{\varepsilon}_{11} = \dot{\varepsilon}_{11}^{\mathrm{hom}} + A(\beta) * [\left(\varepsilon_{11} - \varepsilon_{11}^{uni}\right) / \varepsilon_{11}^{uni}]^{p}$$

Validation linear FLC

Validation examples

- Validation linear FLC
- Influence curvature

MMFC VALIDATION ON AUTOFORM MATERIAL CARDS

DX53D

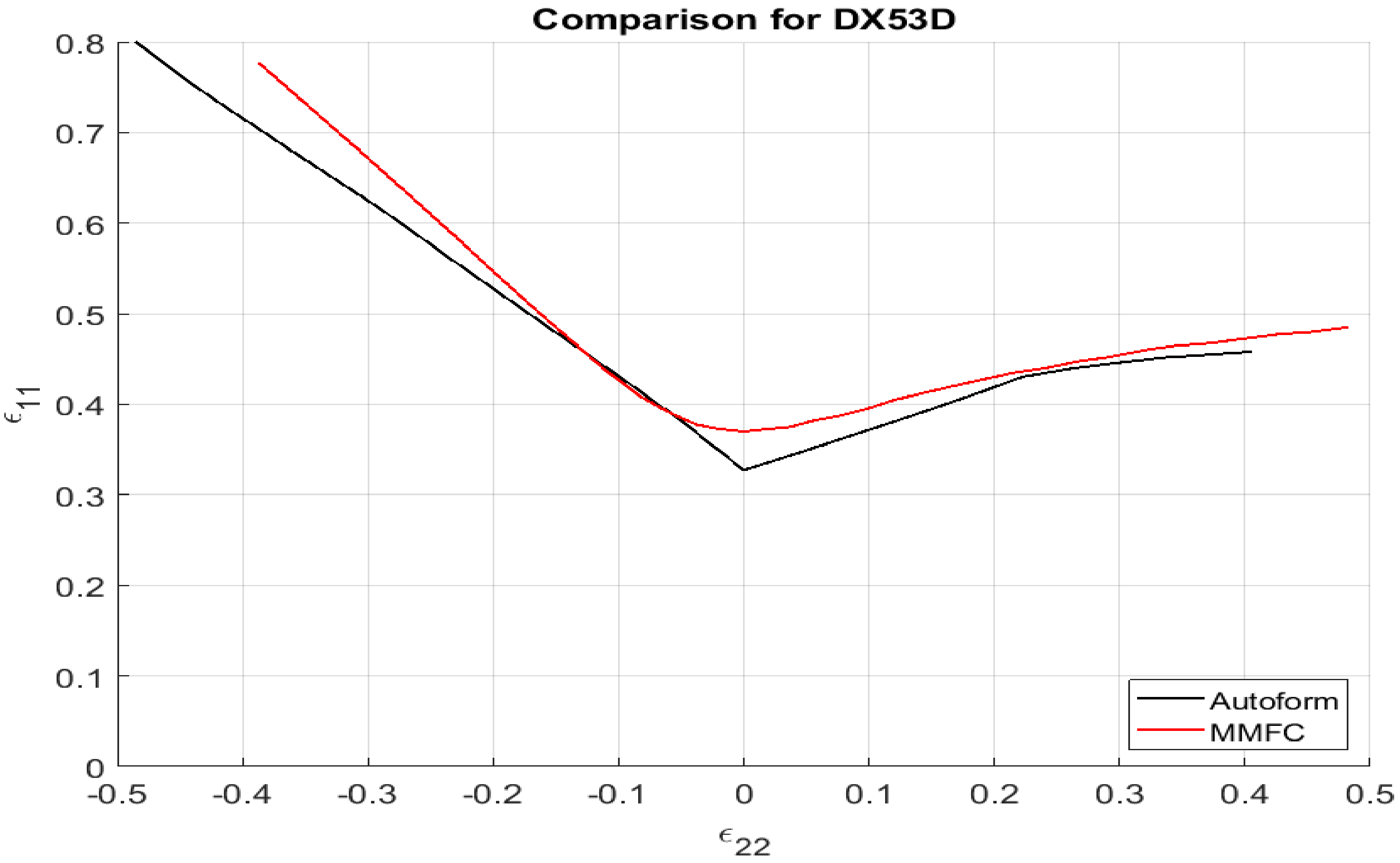

Comparison for DX53D
0.8
0.7
0.6
0.5
0.4
0.3
0.2
0.1
0
-0.5
-0.4
-0.3
-0.2
-0.1
0
0.1
0.2
0.3
0.4
0.5
ϵ_{11}
ϵ_{22}
Autoform
MMFC

HX260BD

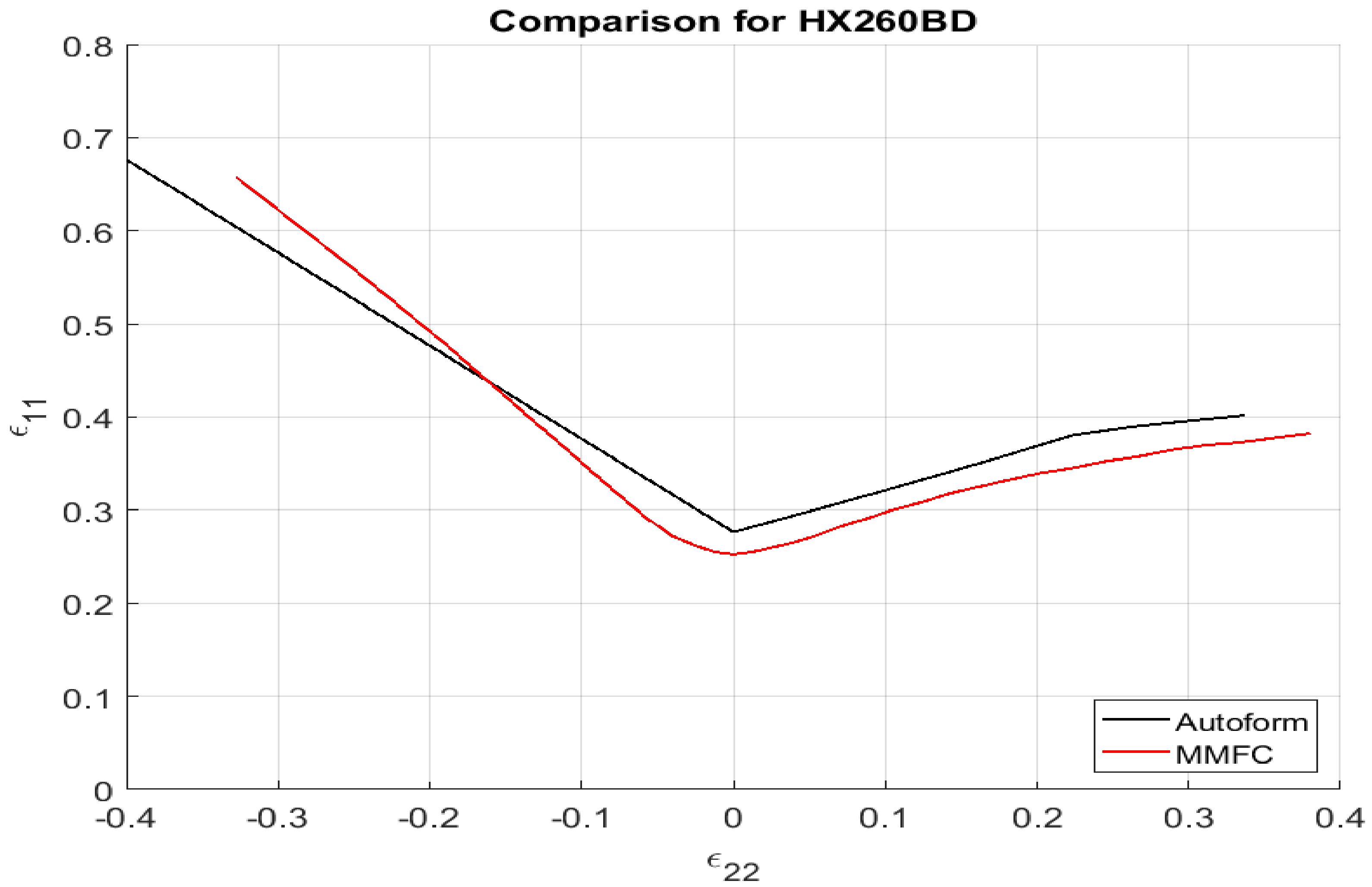
Comparison for HX260BD
0.8
0.7
0.6
0.5
0.4
0.3
0.2
0.1
0
ϵ11
-0.4
-0.3
-0.2
-0.1
0
0.1
0.2
0.3
0.4
ϵ22
Autoform
MMFC

VALIDATION LINEAR FLC

Validation examples

- Validation linear FLC
- Influence curvature

MMFC

Influence of curvature

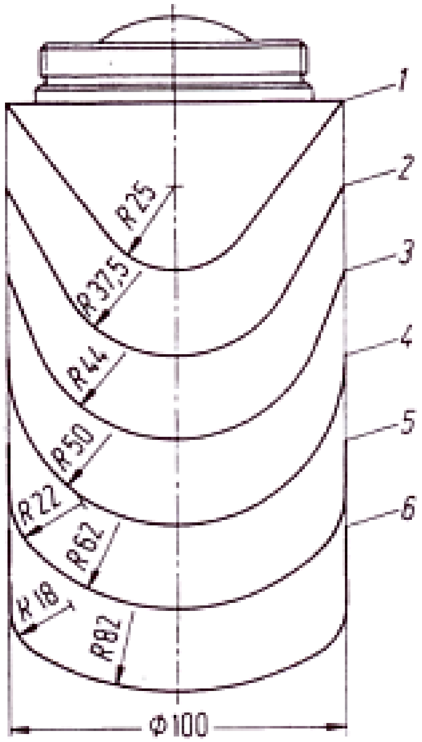

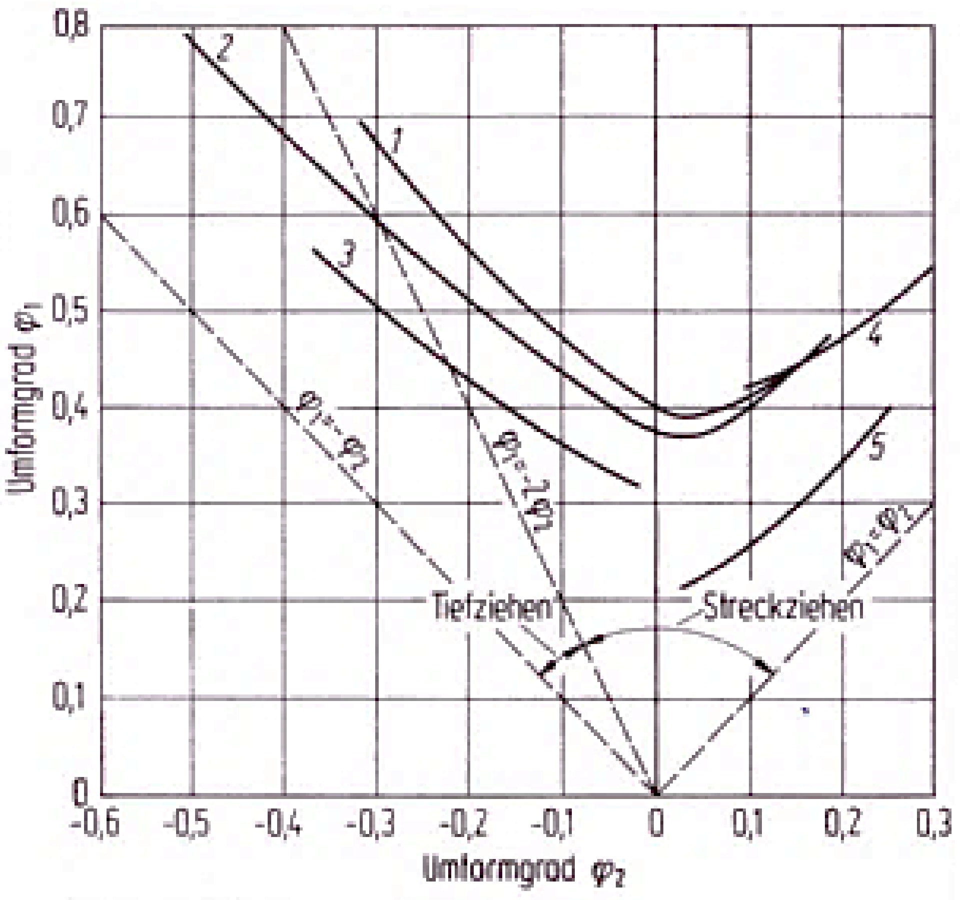

eMMFC allows the FLC evaluation under consideration of additional effects

Additional influences on FLC	Parameters
Curvature	Tool Radius R
Thickness	Relative sheet thickness t/R
Temperature	T
Phase transformation effects	TRIP
Non-linear load history	Multi-step forming
Reverse bending	Draw beads, …
Incremental forming	Stabilizing effects

eMMFC criterion

$$H'\left(1+\frac{t}{2\rho}+E_0*\left(\frac{t}{t_0}\right)^n\right)\leq\left(\frac{f(\alpha)+\frac{f'(\alpha)g(\beta)\beta}{\beta'(\alpha)\,\varepsilon}}{f(\alpha)g(\beta)}\right)*\mathrm{H}$$

$\frac{t}{\rho}$: thicknes/curvature ratio

$$H=H(\varepsilon_{eq},\dot{\varepsilon},T,V_M,\ldots)$$

Prediction of extended FLC based on MMFC

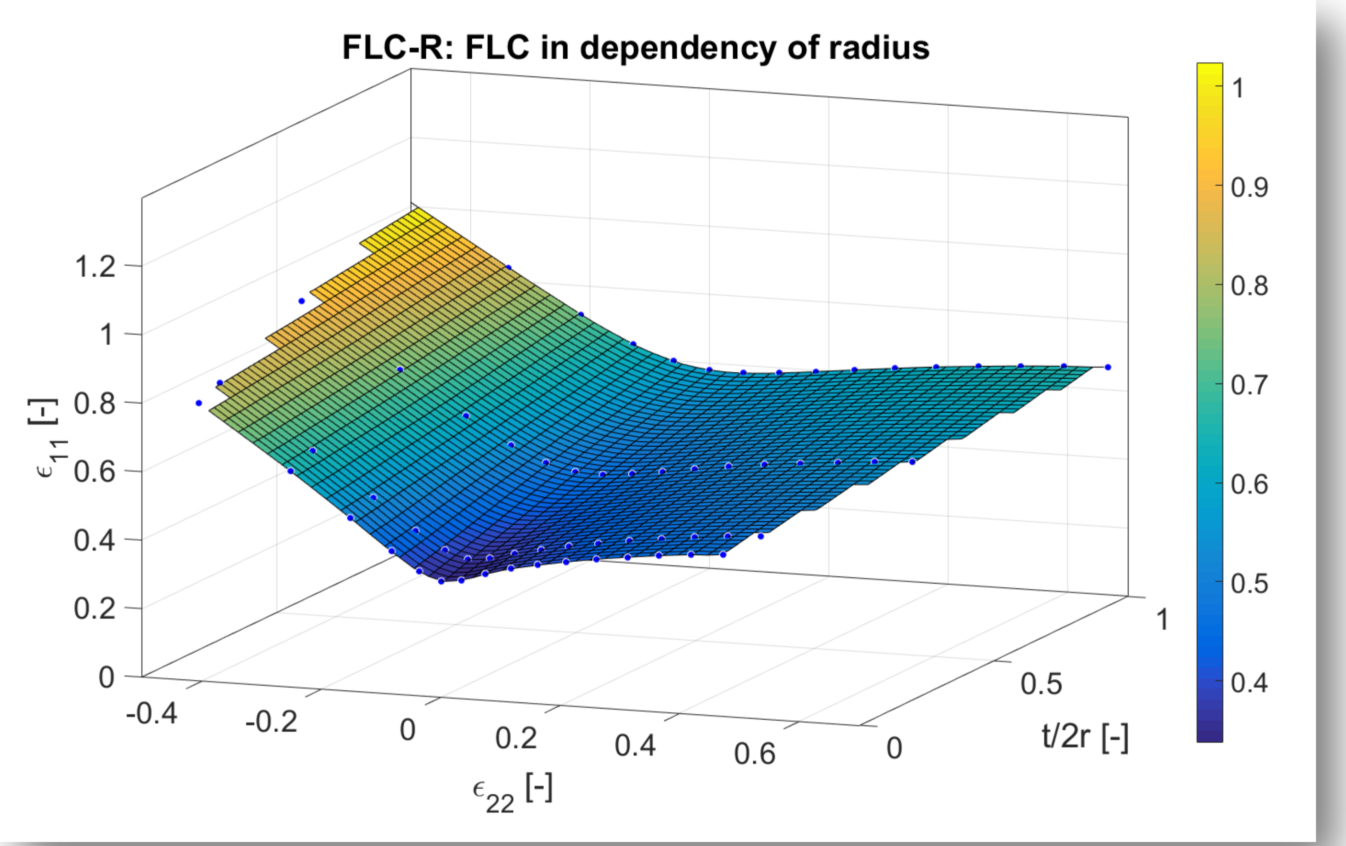

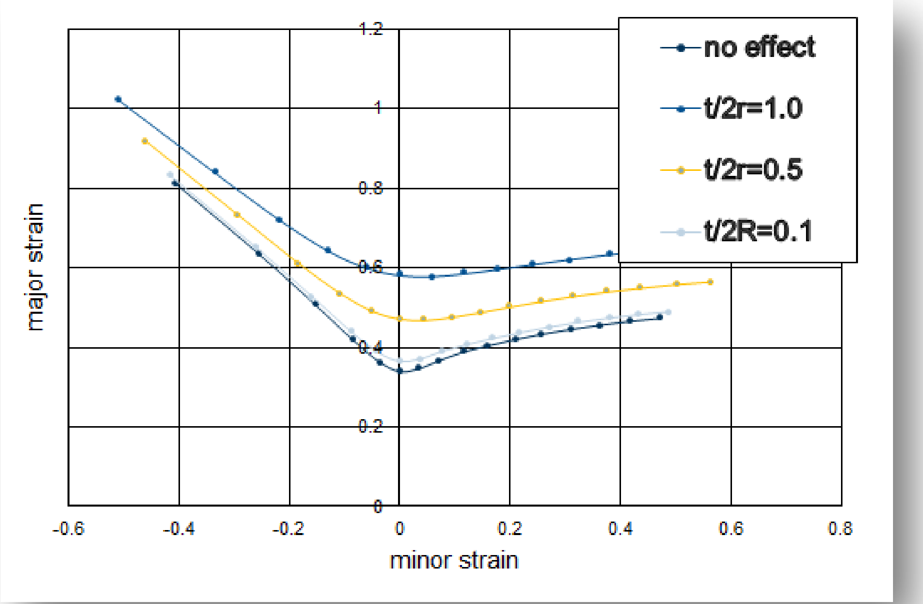

$$a_{FLC}(\rho) = \frac{\varepsilon_{FLC}(\rho)}{\varepsilon_{FLC}(\rho_{\infty})}$$

$$k_{FLC} = \frac{1}{a}\frac{\varepsilon_{maj}(\rho)}{\varepsilon_{FLC}(\rho)}$$

Limitations in the FLC prediction

Influence of stretch bending in FLD0

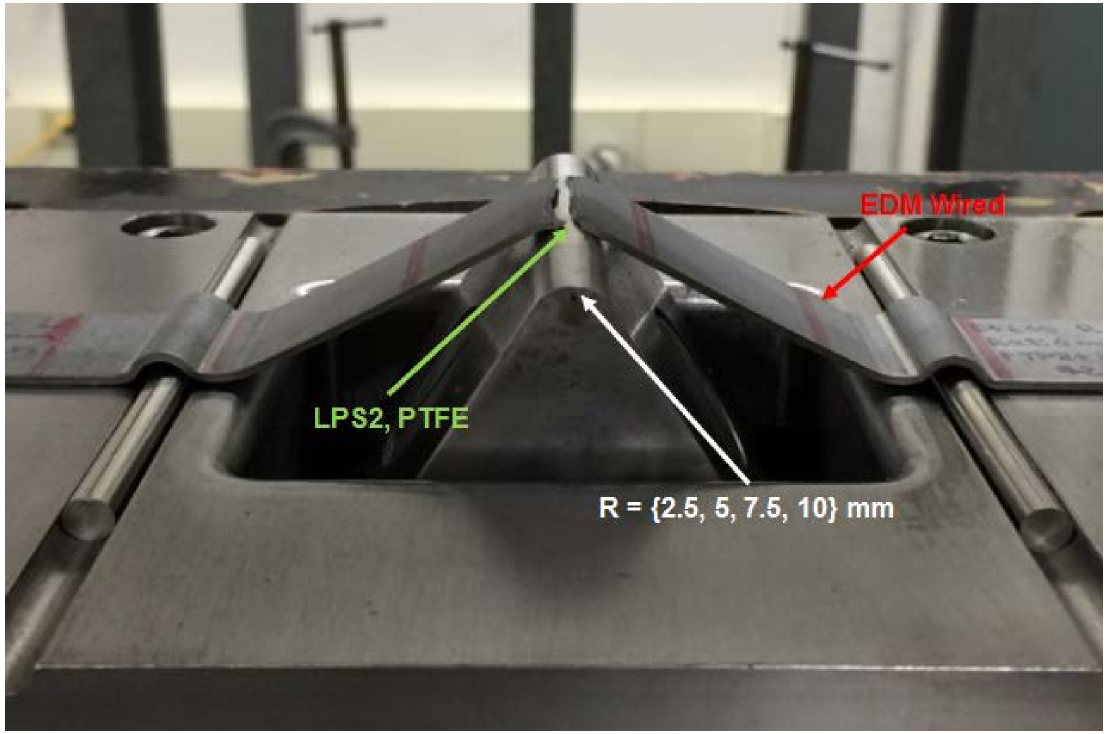

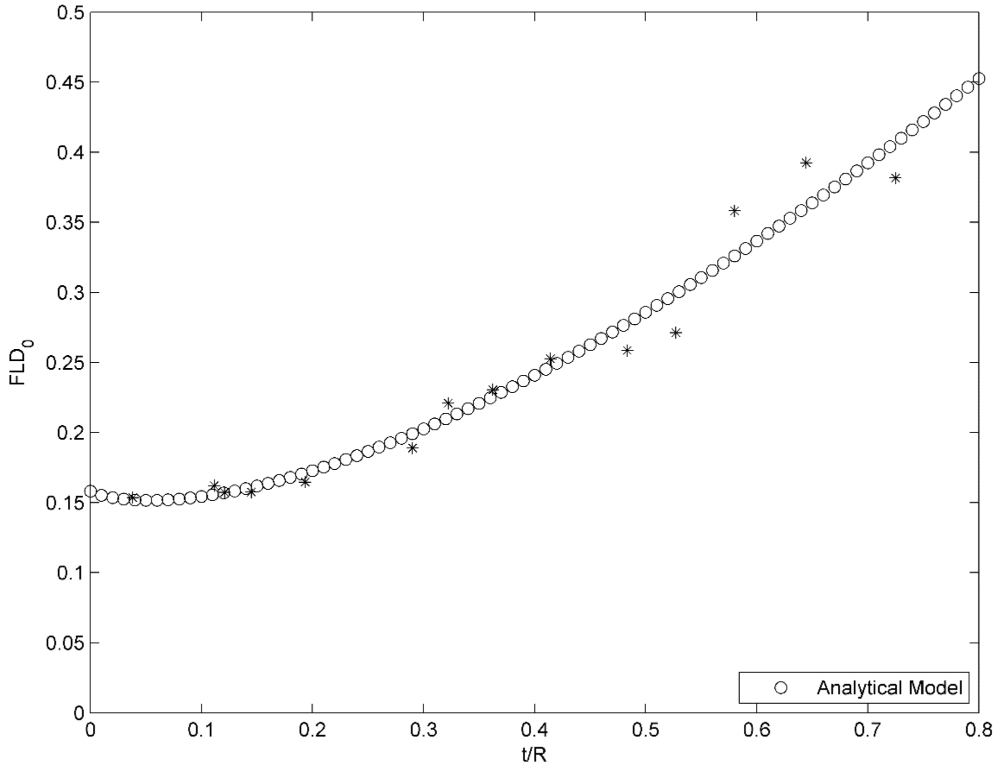

FLD0 – Values in a stretch-bending test

Source: F.M. Neuhauser[1,2], O.R. Terrazas[1], N. Manopulo[2],P. Hora[2] and C.J. Van Tyne
Stretch bending – the plane within the sheet where strains reach the forming limit curve. In Proceeding of IDDR2016

Content

MMFC

Non-linear FLC

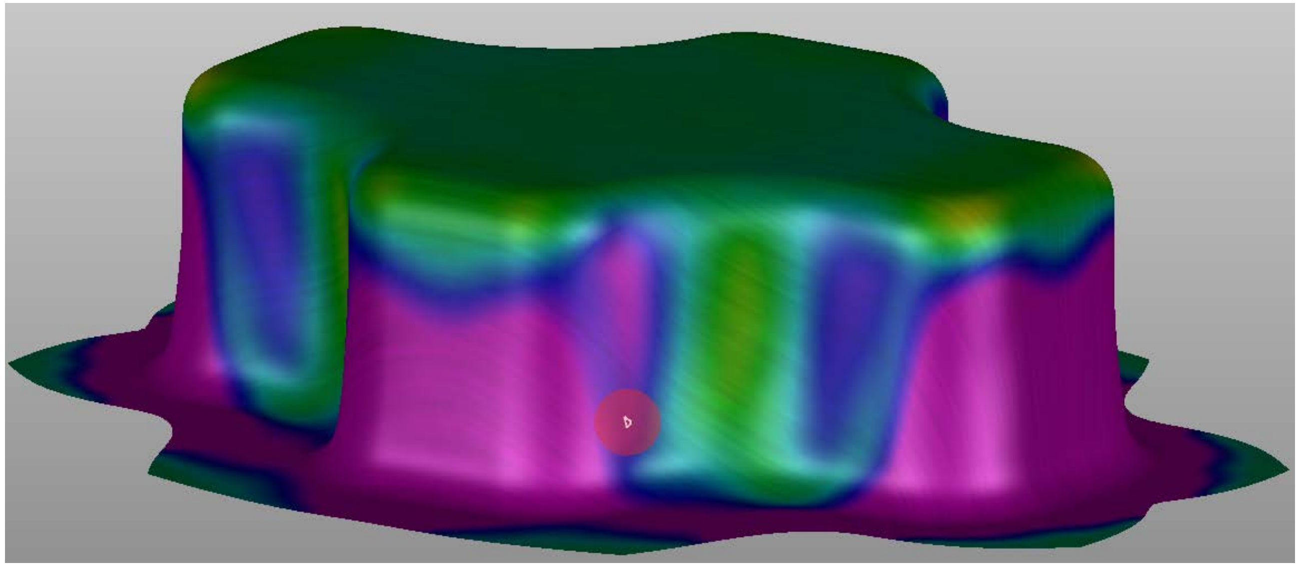

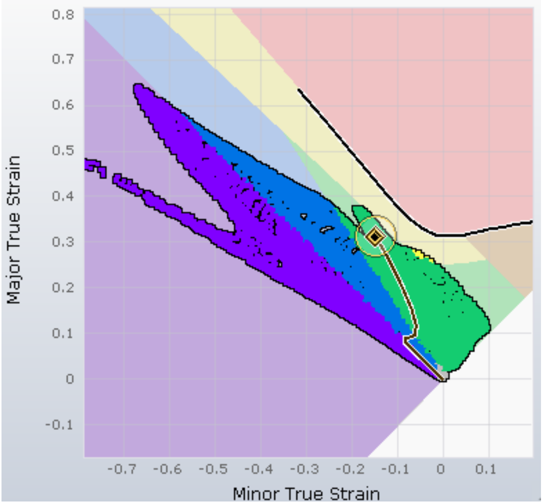

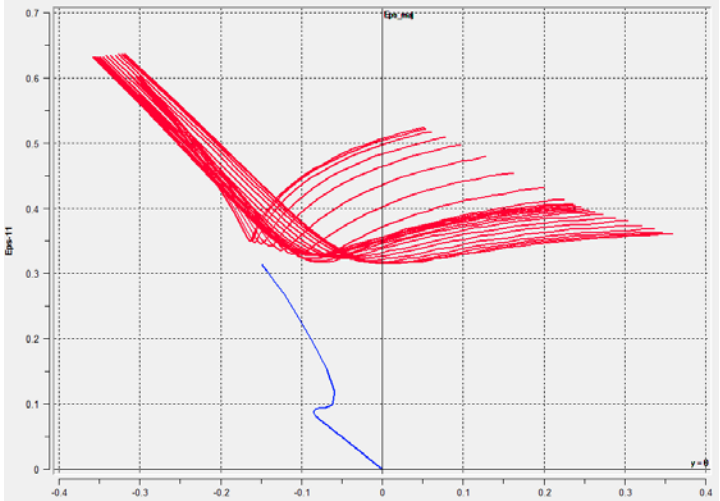

Nonlinear Deformation Paths

Cross-Die

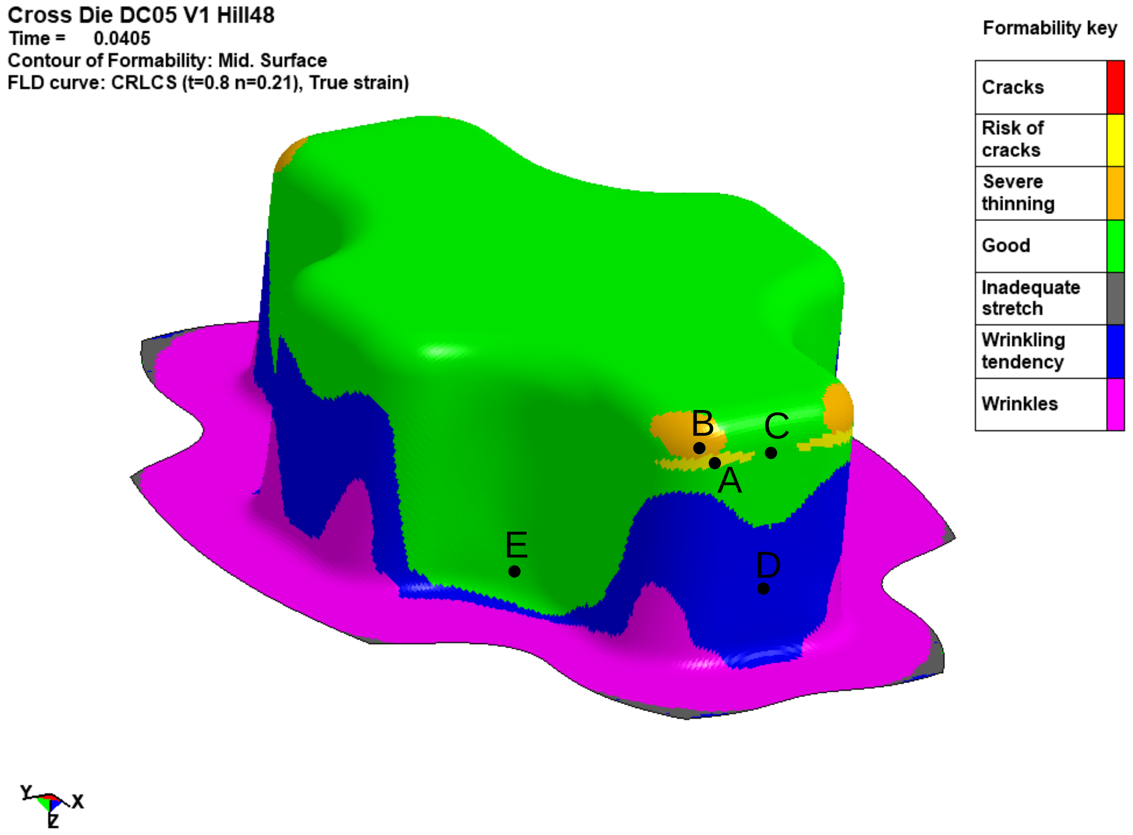

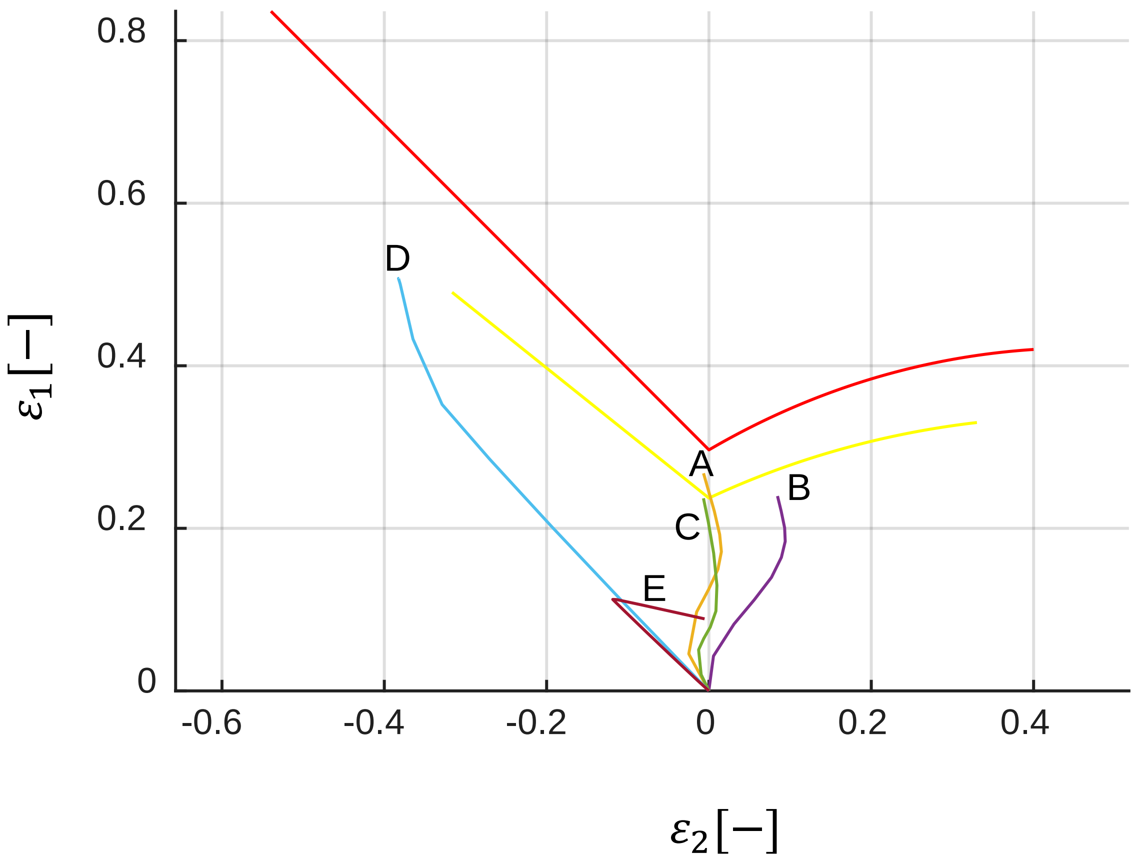

MMFC

Non-linear FLC

The evaluation bases on an incremental evaluation of the condition

$$H'\left(1+\frac{t}{2\rho}+E_0*\left(\frac{t}{t_0}\right)^n\right)\leq\left(\frac{f(\alpha)+\frac{f'(\alpha)g(\beta)\beta}{\beta'(\alpha)\,\varepsilon}}{f(\alpha)g(\beta)}\right)*\mathrm{H}$$

β can follow a path

Step 1: classical strain field evaluation procedure

Step 2: detection of non linear path nodes

Step 3: evaluation with ***nl-eMMFC***

NON-LINEAR FLC

Validation examples

- Validation - Simple tensile test Material HC340LA
- Case study - Different non-linear loading cases – material DC04
- Application Cross die – Evaluation based on FEM predicted strain paths

Influence of slight β>0 prestreching of Nakajima tests

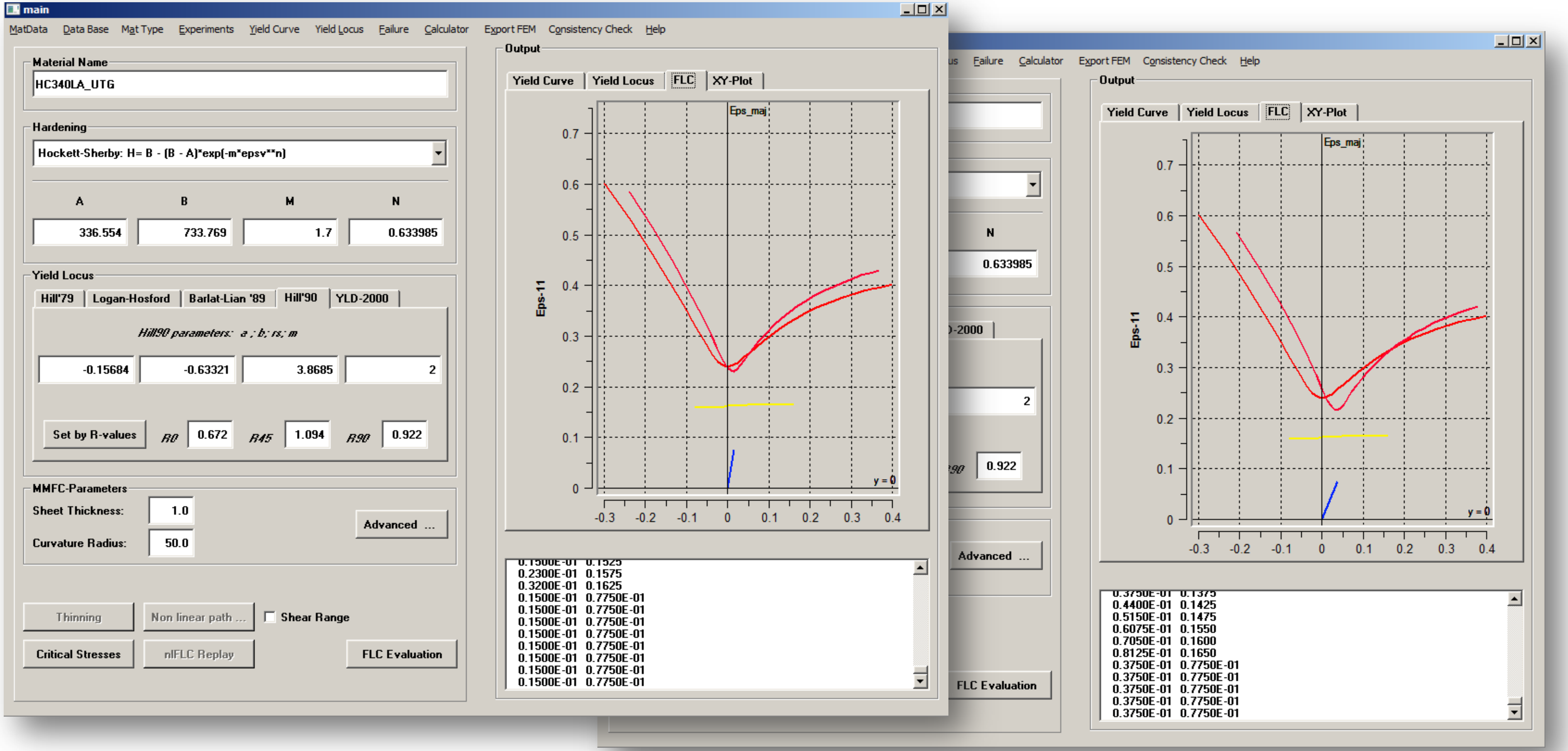

HC340 LA

Case 1

Prestrained under **plane strain** condition β= 0.0

Preformed

ε_{maj}: 0.10 ; 0.15 ; 0.20

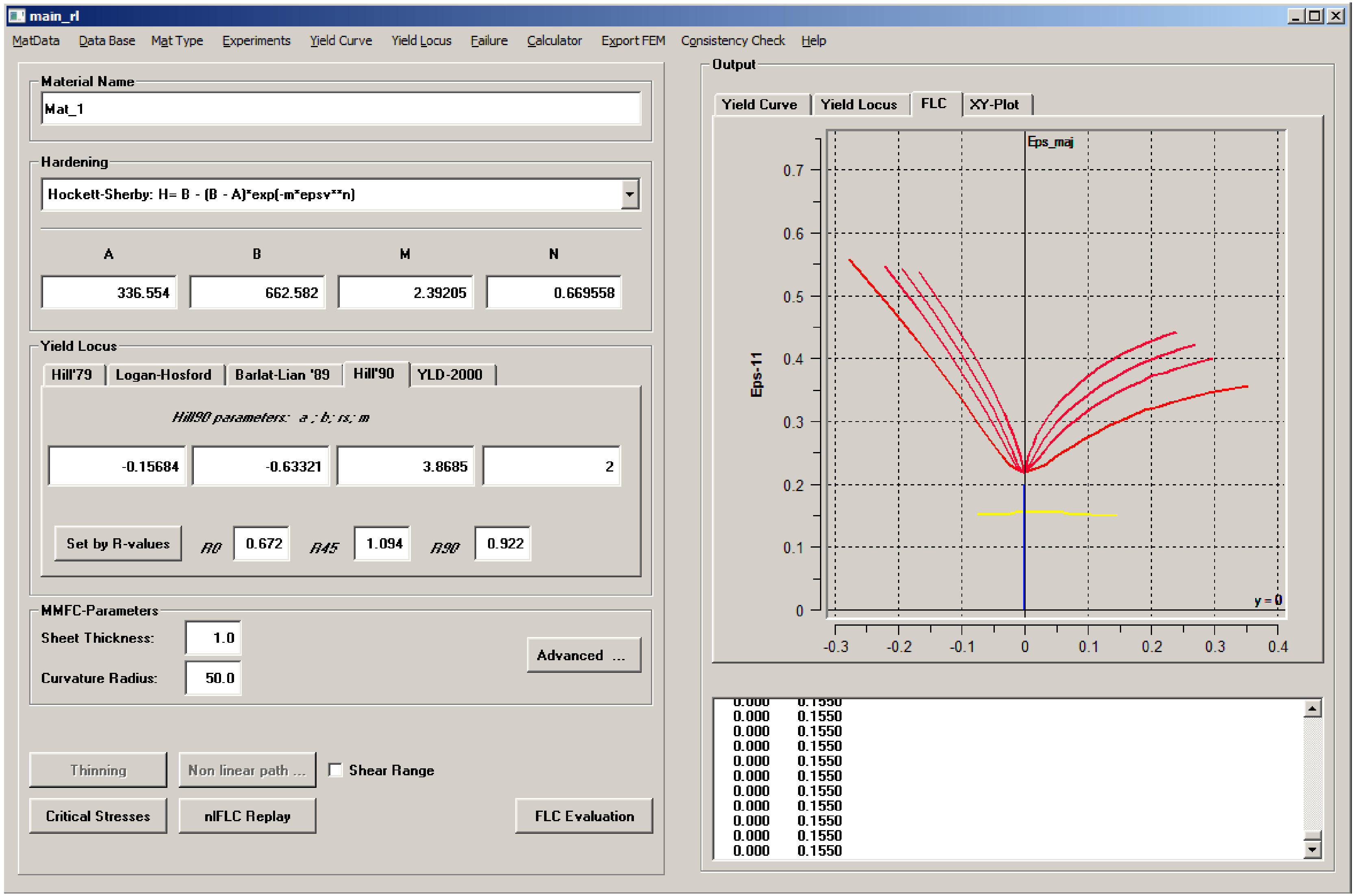

HC340 LA

Preformed
β = 0.0
ε_{maj}: 0.10 ; 0.15 ; 0.20

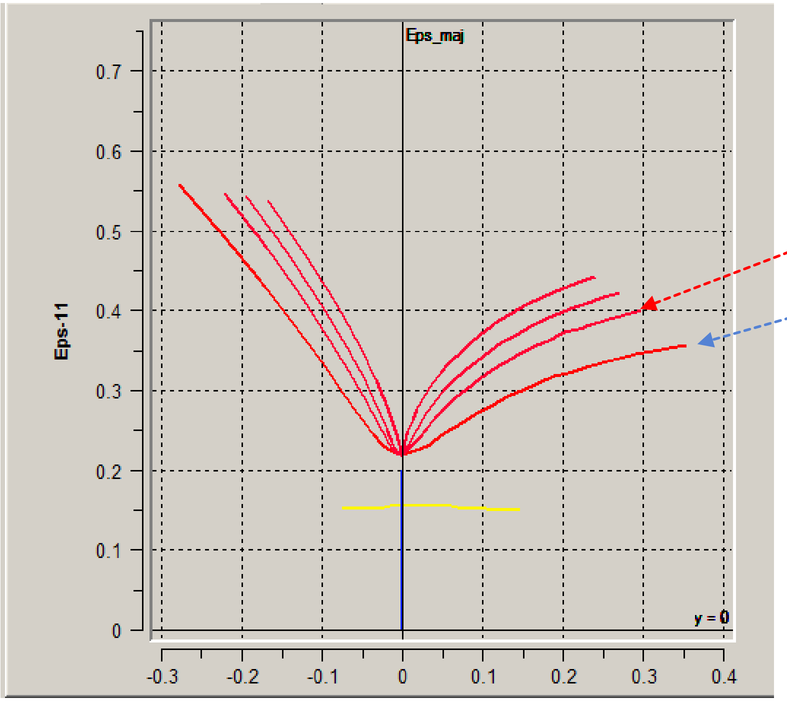

Experimentally evaluated nl FLC

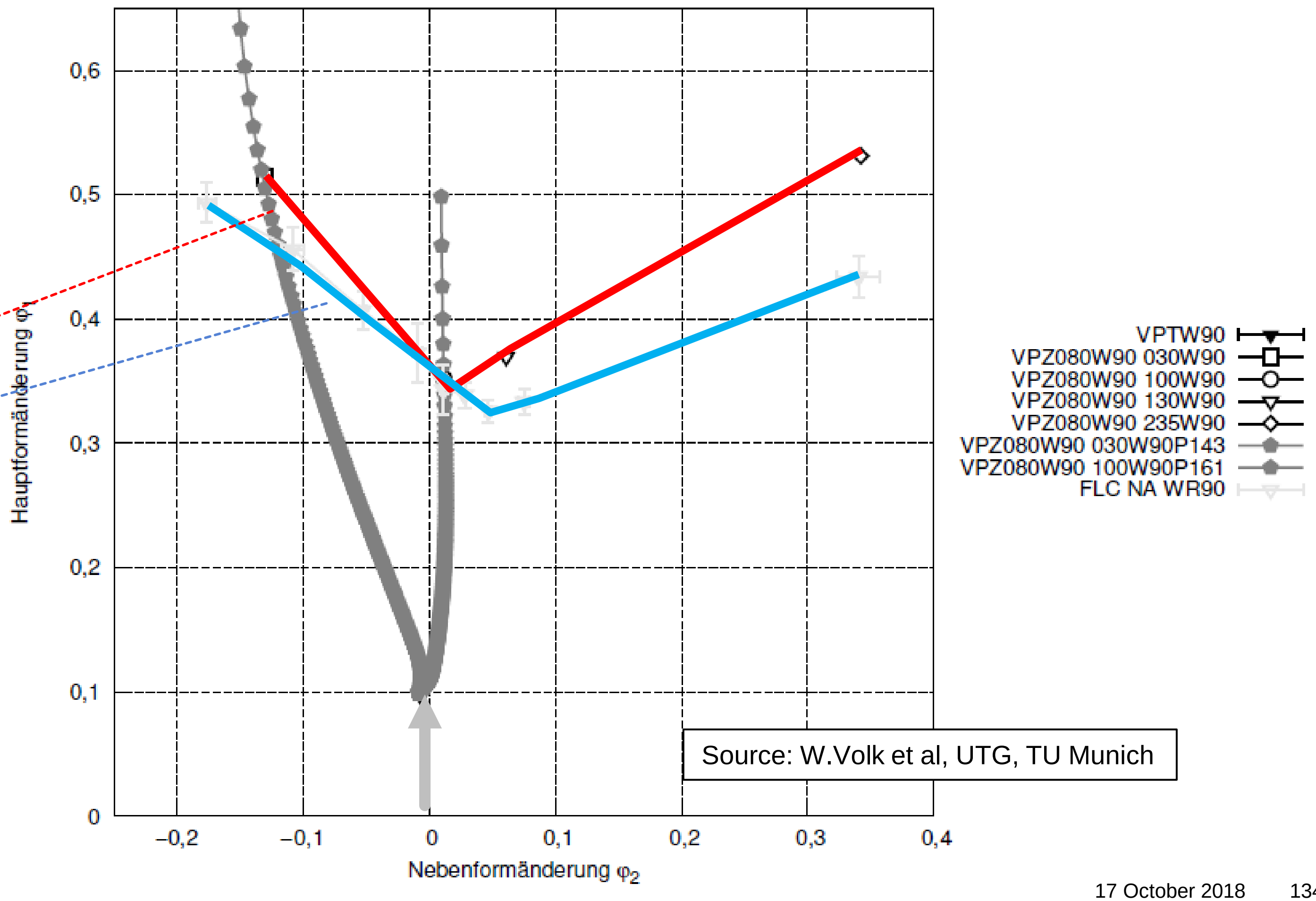

HC340 LA

Preformed
β = 0.0

ε_{maj}: 0.10 ; 0.15 ; 0.20

Experimentally evaluated nl FLC

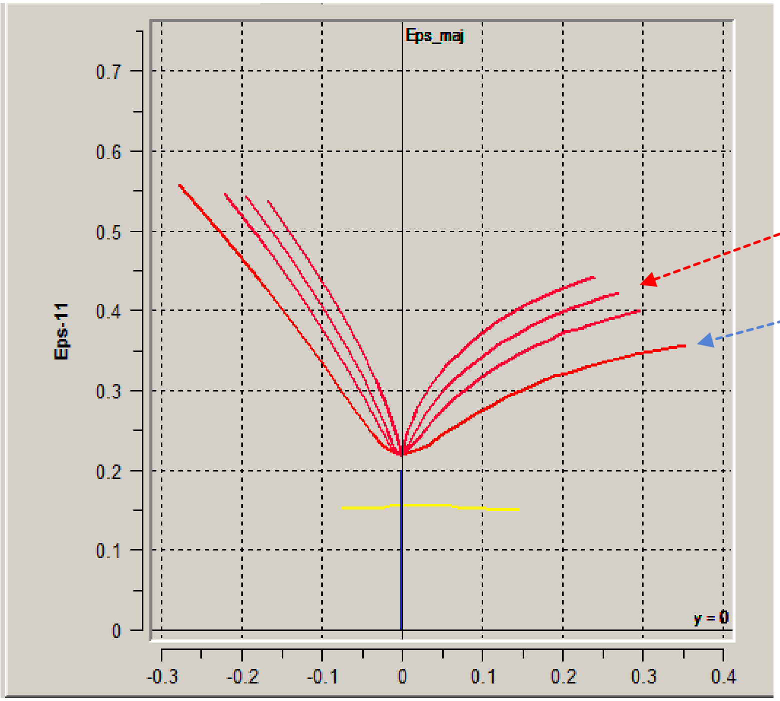

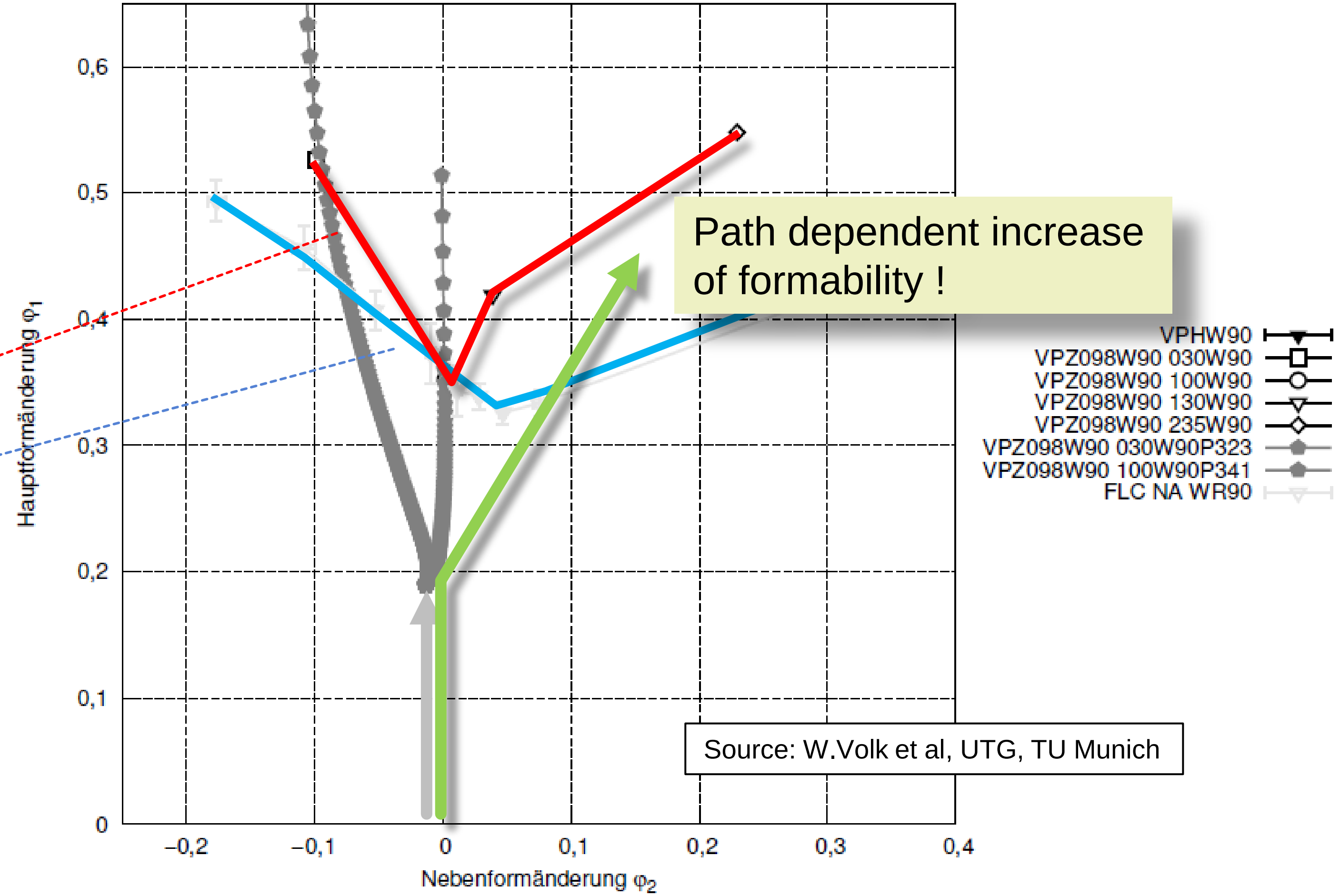

HC340 LA

Case 2

Prestrained under **tensile** conditions

Preformed
β = -0.5 (= tensile test)
ε_{maj}: 0.10 ; 0.20 ; 0.30

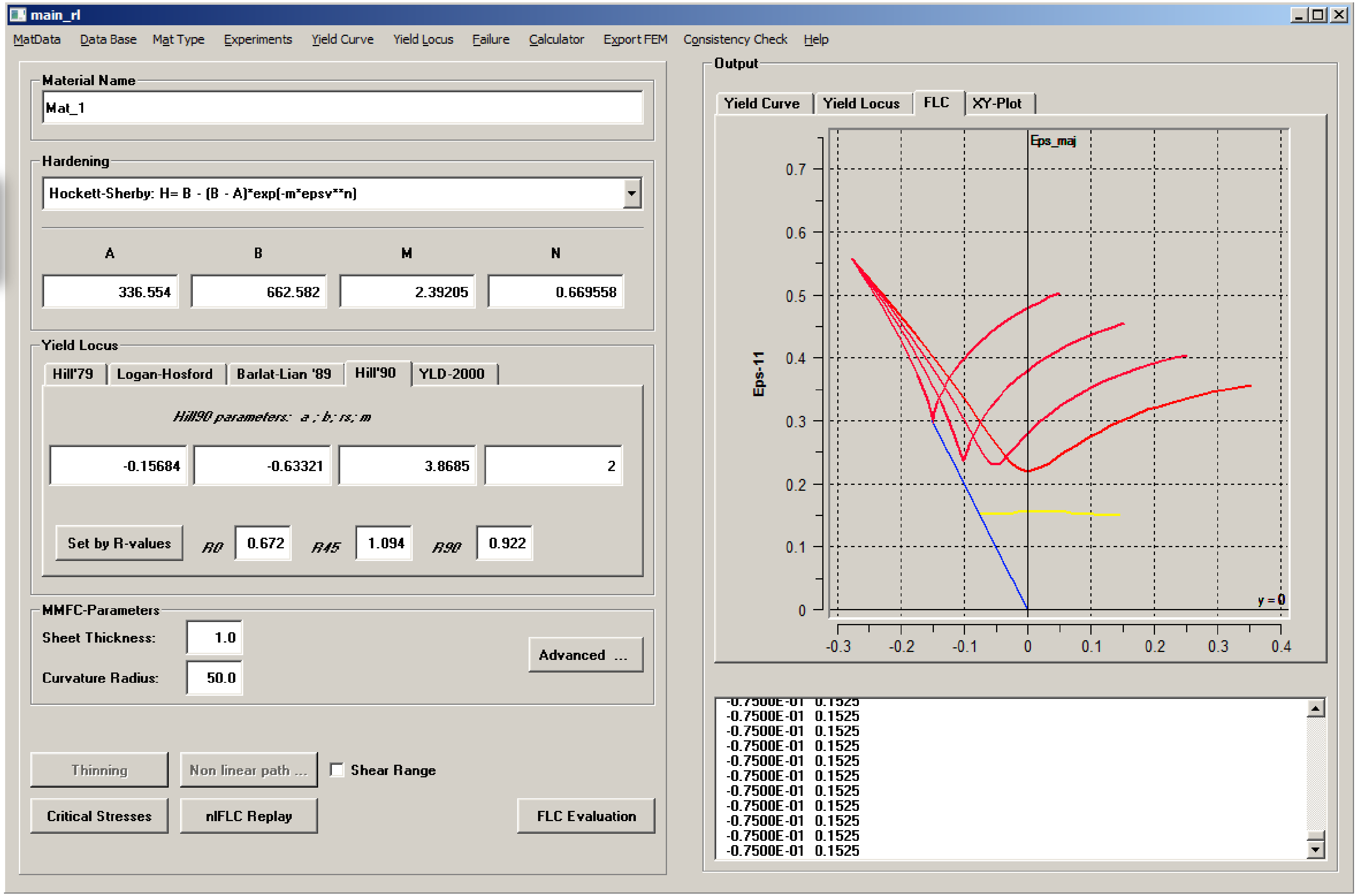

HC340 LA

Preformed

β = -0.5 , ε_{maj}: 0.10 ;

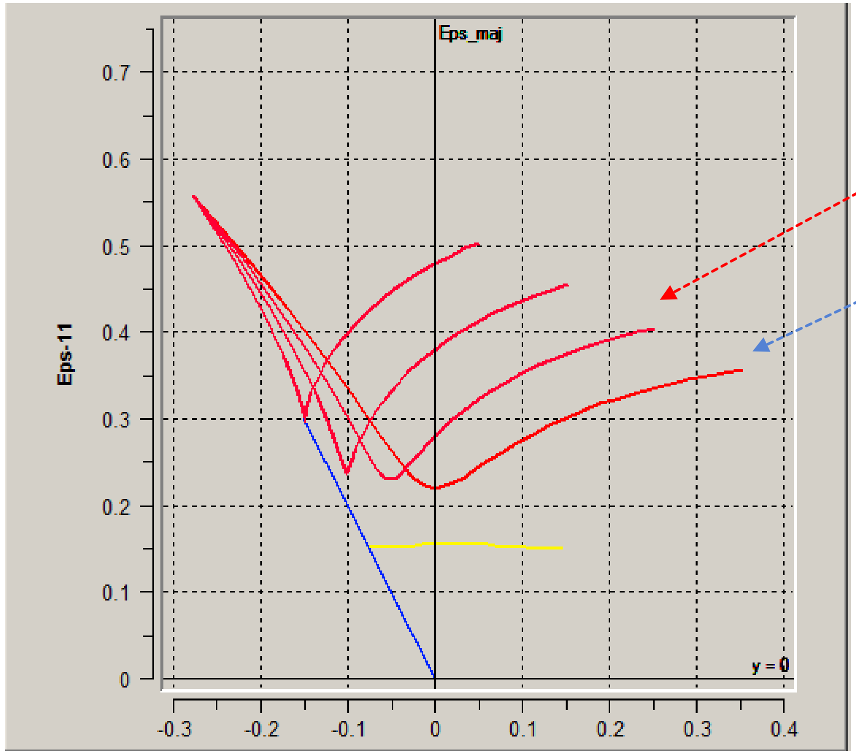

Experimentally evaluated nl FLC

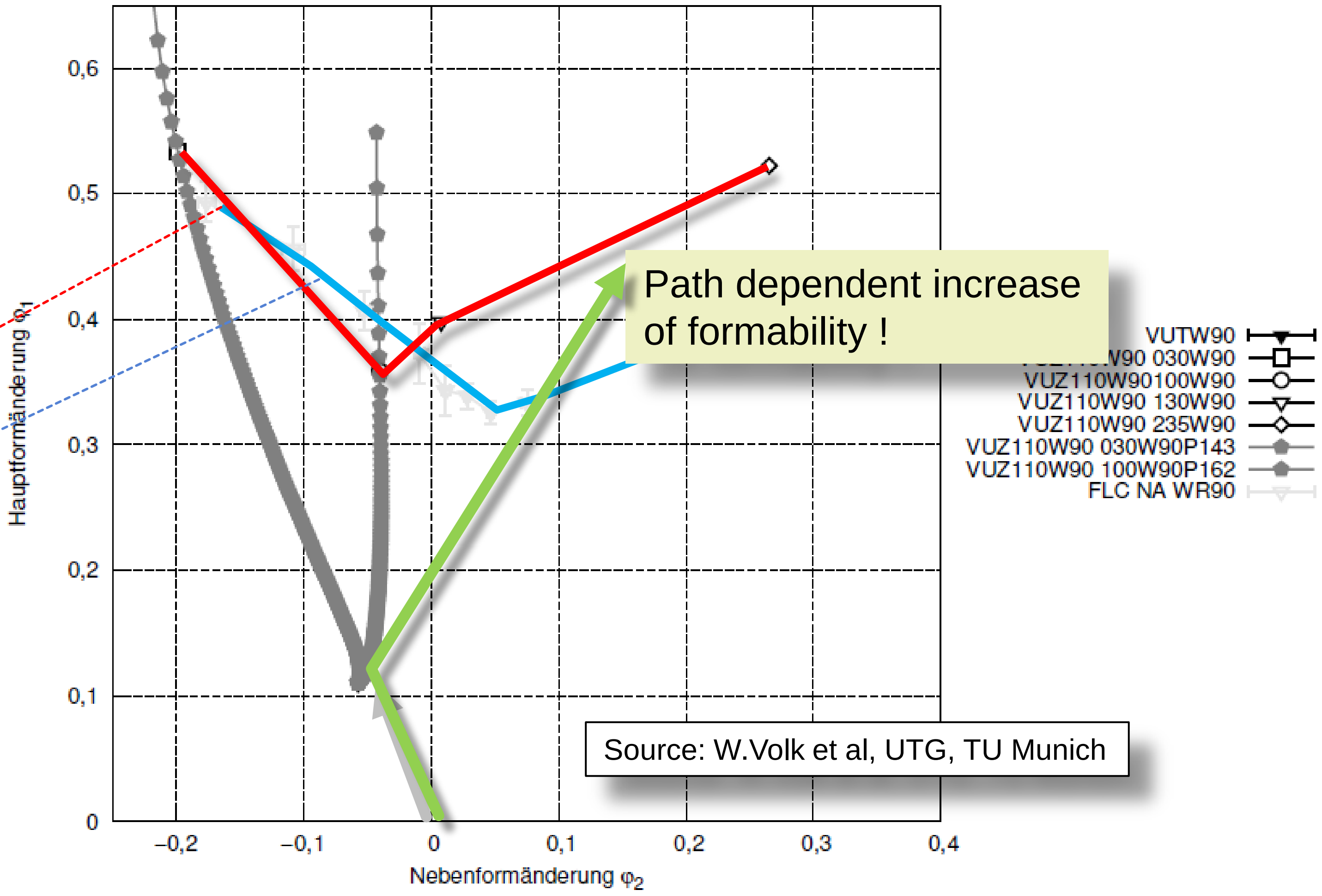

HC340 LA

Preformed

β = -0.5 ; ε_{maj}: 0.30

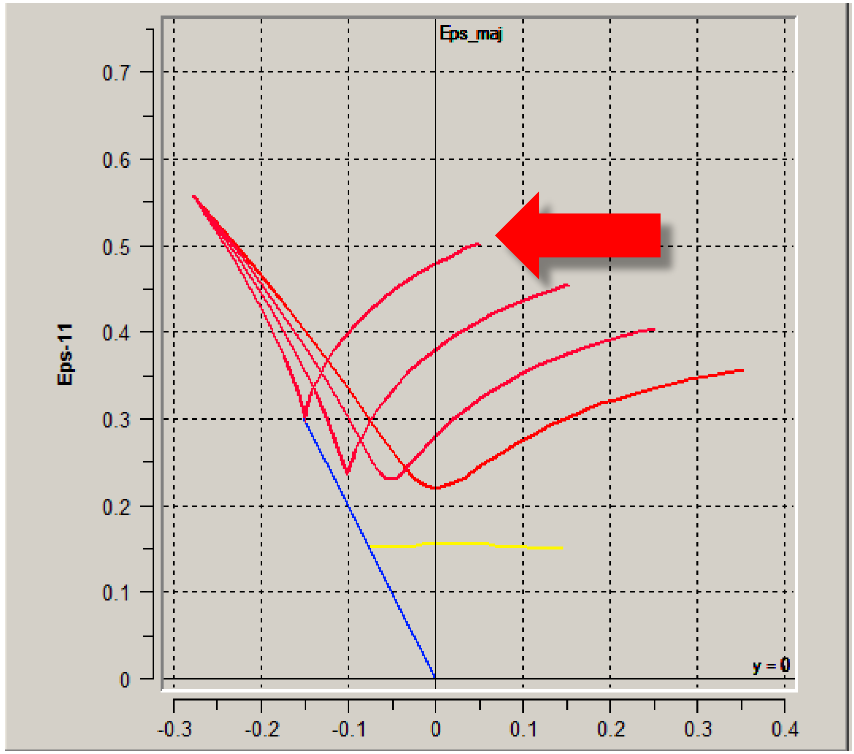

Experimentally evaluated nl FLC

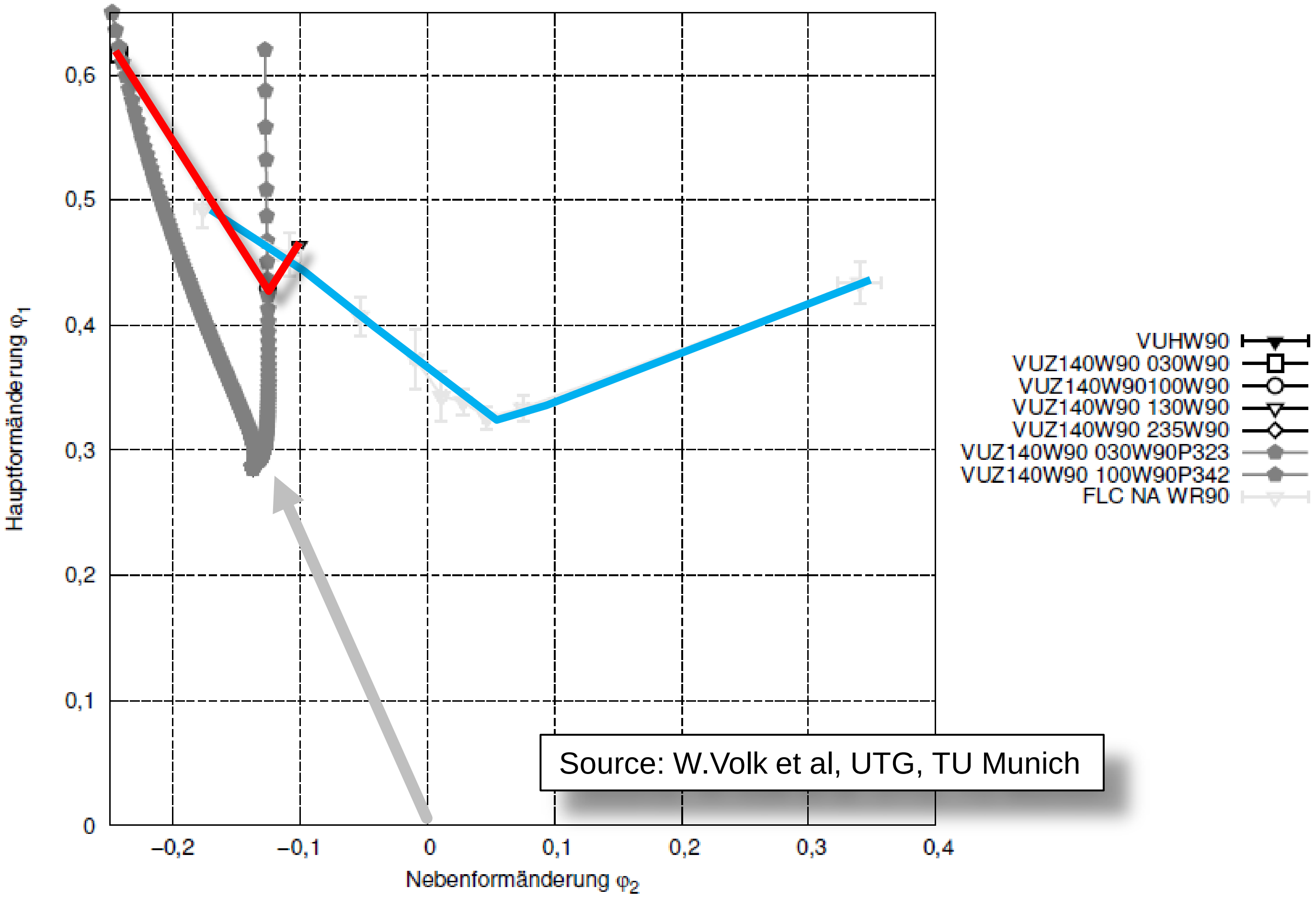

PART II

NON-LINEAR FLC

Validation examples

- Validation - Simple tensile test Material HC340LA
- Case study - Different non-linear loading cases – material DC04
- Application Cross die – Evaluation based on FEM predicted strain paths

MMFC

Non-linear FLC

Examples

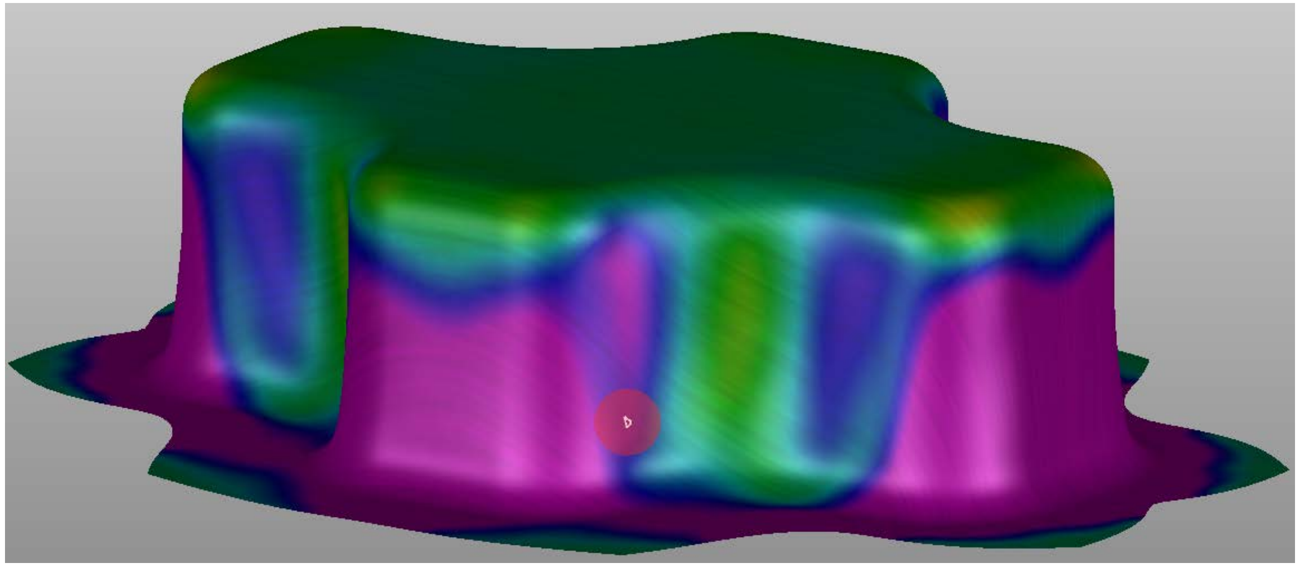

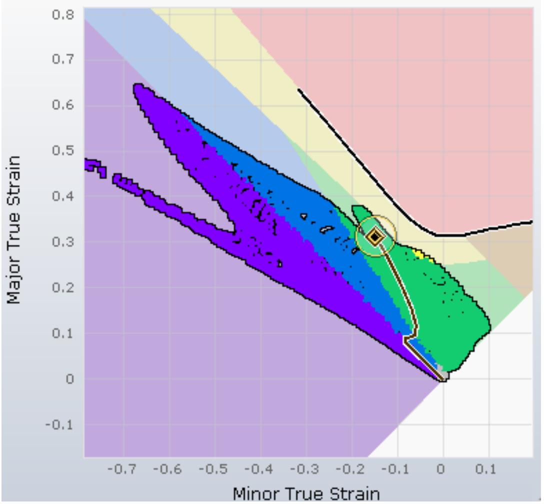

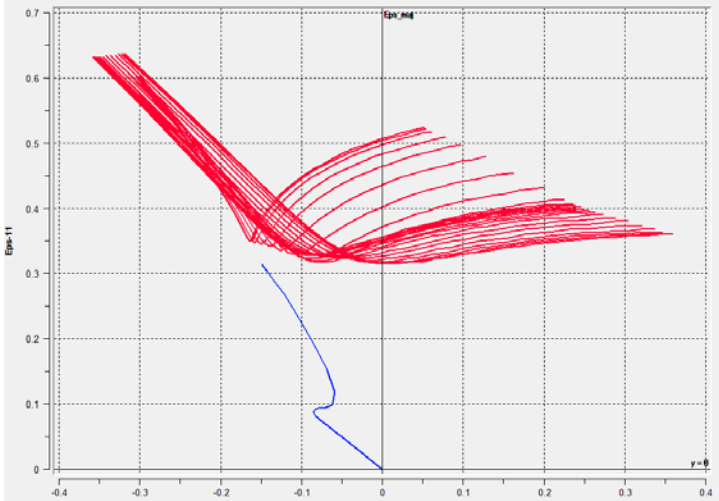

Examples from the Cross Die and Lackfrosch

- Material: DC04
- Yield Curve: Hockett-Sherby
- Yield Locus: Hill ‘79
- Failure: eMMFC-Fe

M	B	m	n
154.41	611.36	1.568	0.563

R	m	σ_b/σ_0
1.87	2.0	1.568

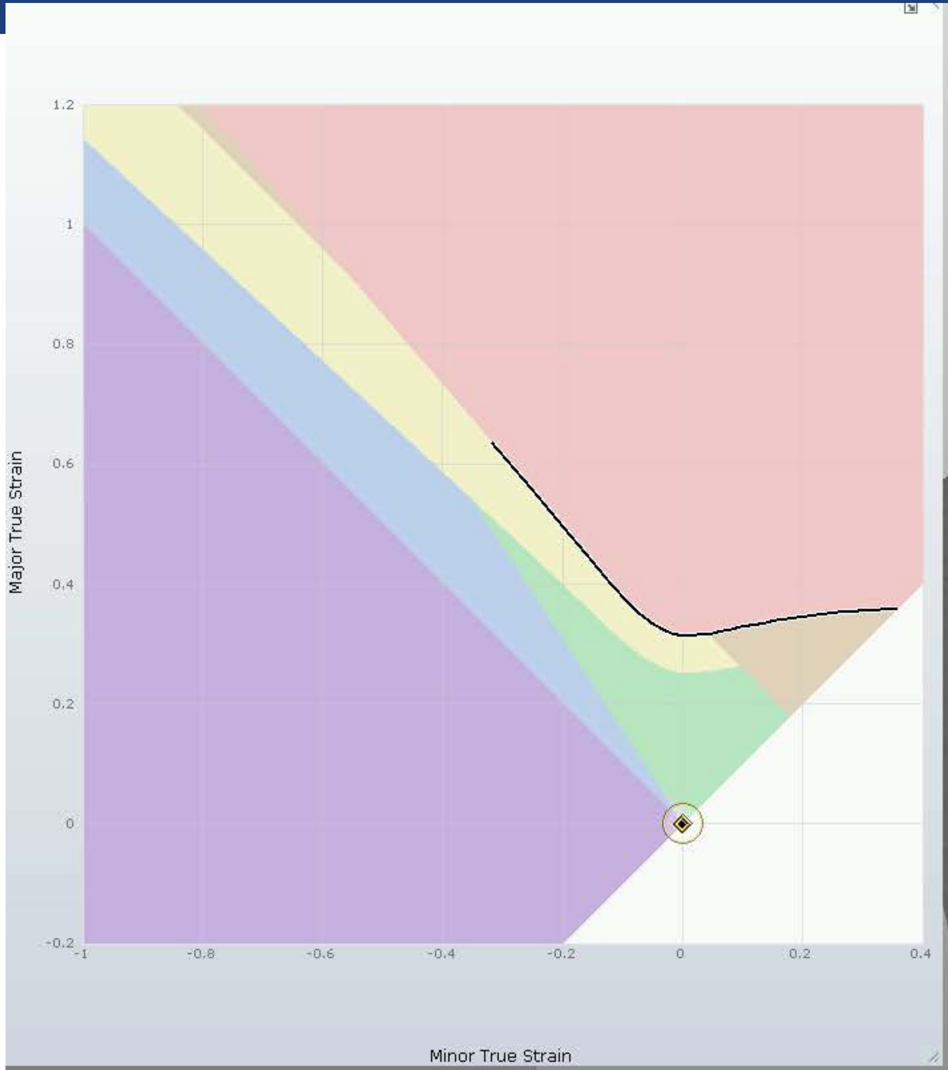
1.2
1
0.8
0.6
0.4
0.2
0
-0.2
-1
-0.8
-0.6
-0.4
-0.2
0
0.2
0.4
Major True Strain
Minor True Strain

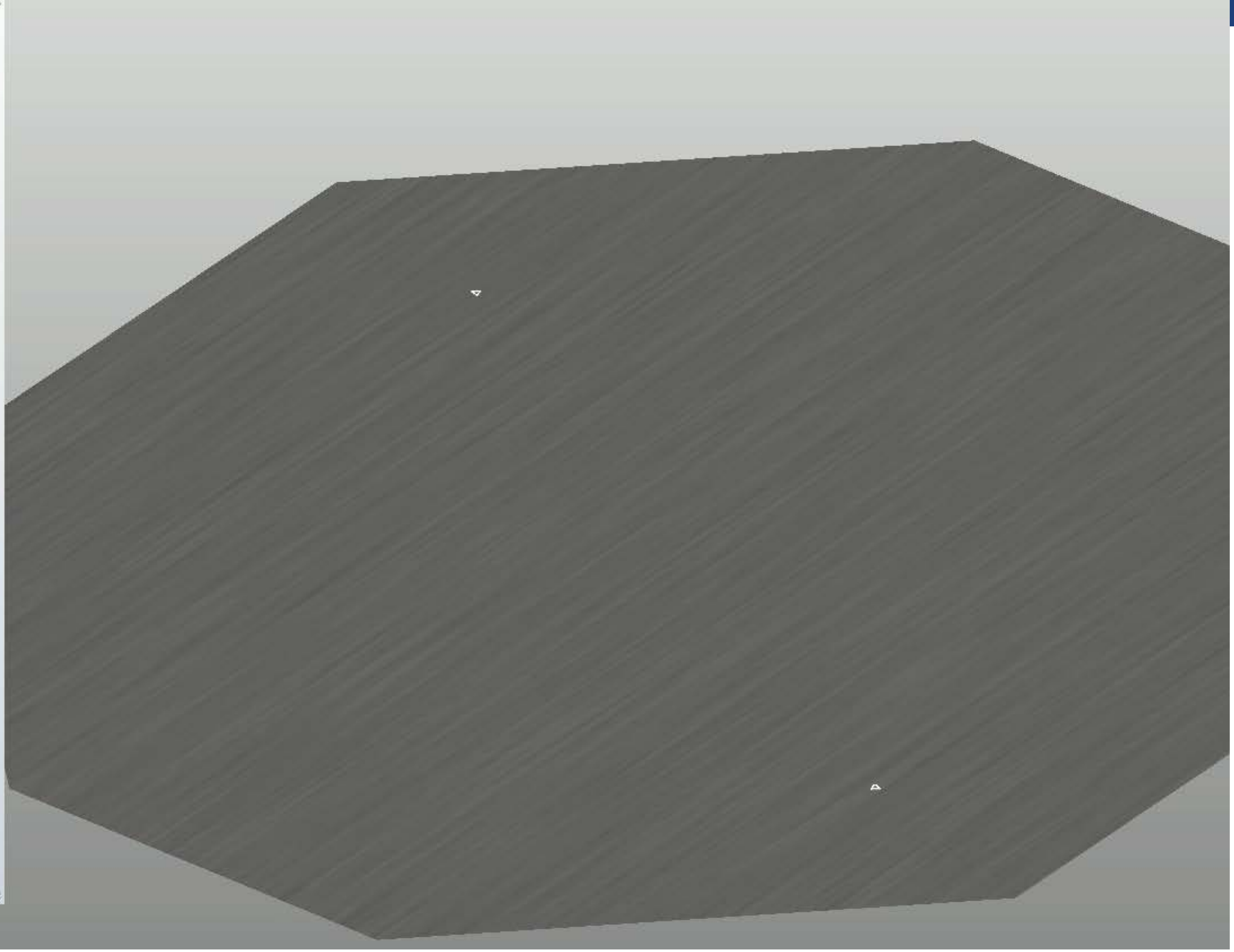

Example 1

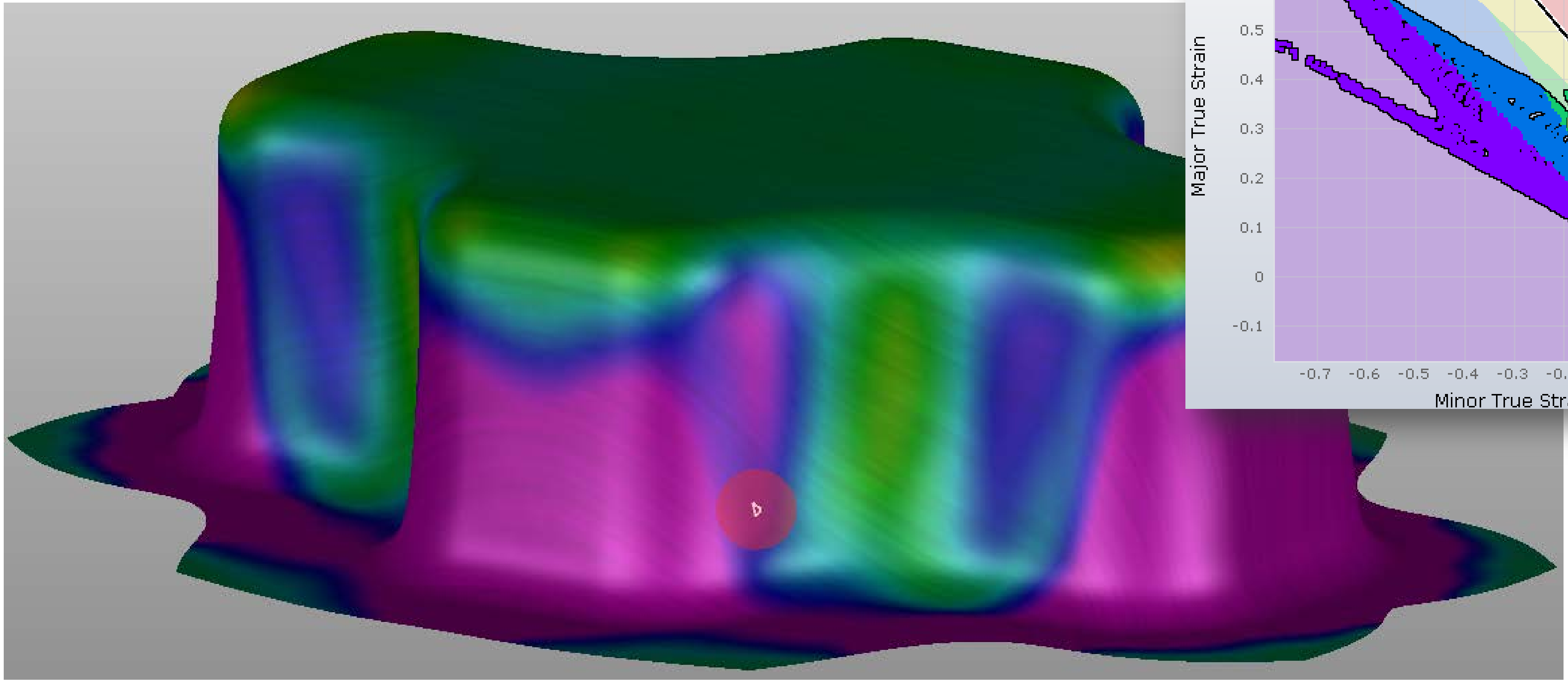

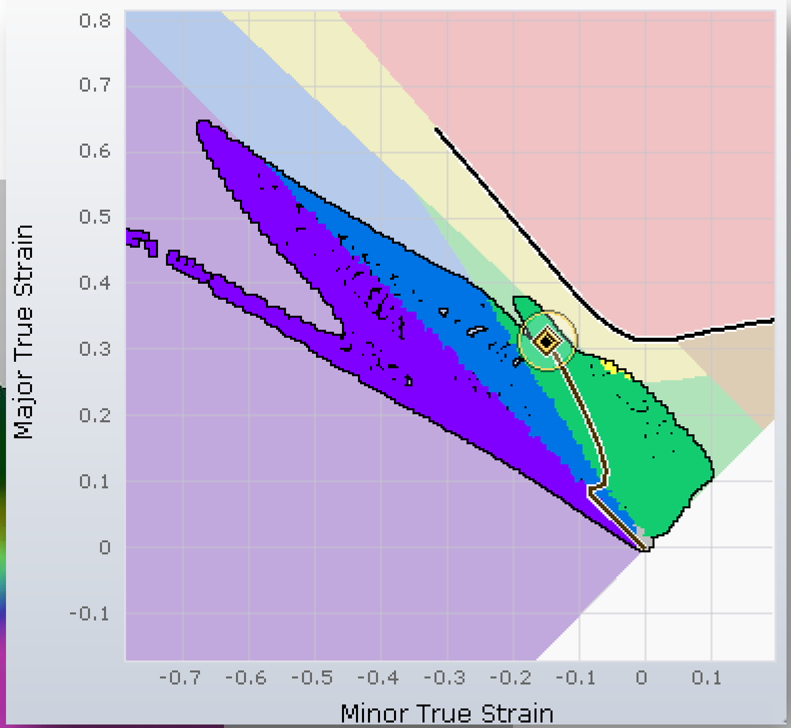

Major True Strain
Minor True Strain
0.8
0.7
0.6
0.5
0.4
0.3
0.2
0.1
0
-0.1
-0.7
-0.6
-0.5
-0.4
-0.3
-0.2
-0.1
0
0.1

Example 1

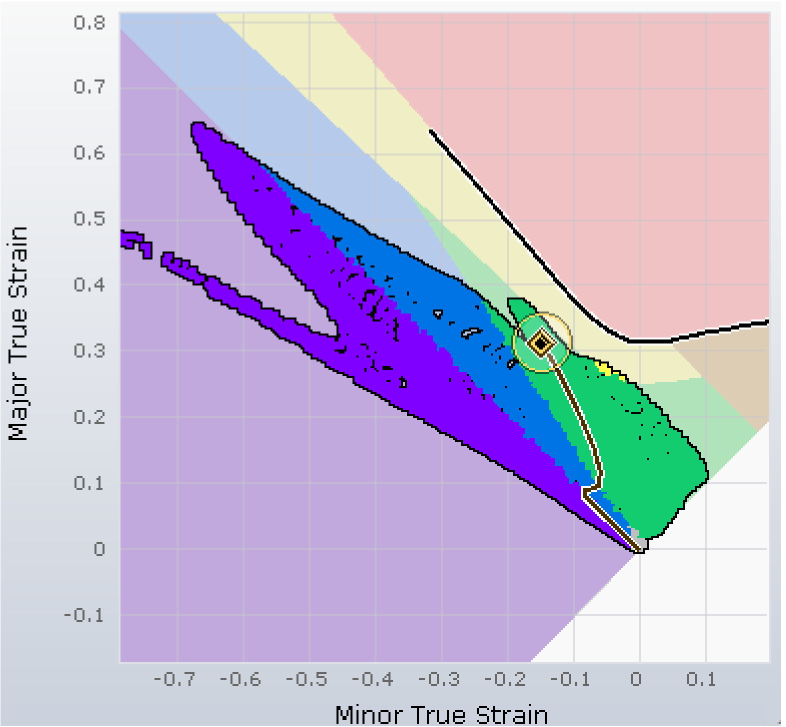
0.8
0.7
0.6
0.5
0.4
0.3
0.2
0.1
0
-0.1
Major True Strain
-0.7 -0.6 -0.5 -0.4 -0.3 -0.2 -0.1 0 0.1
Minor True Strain

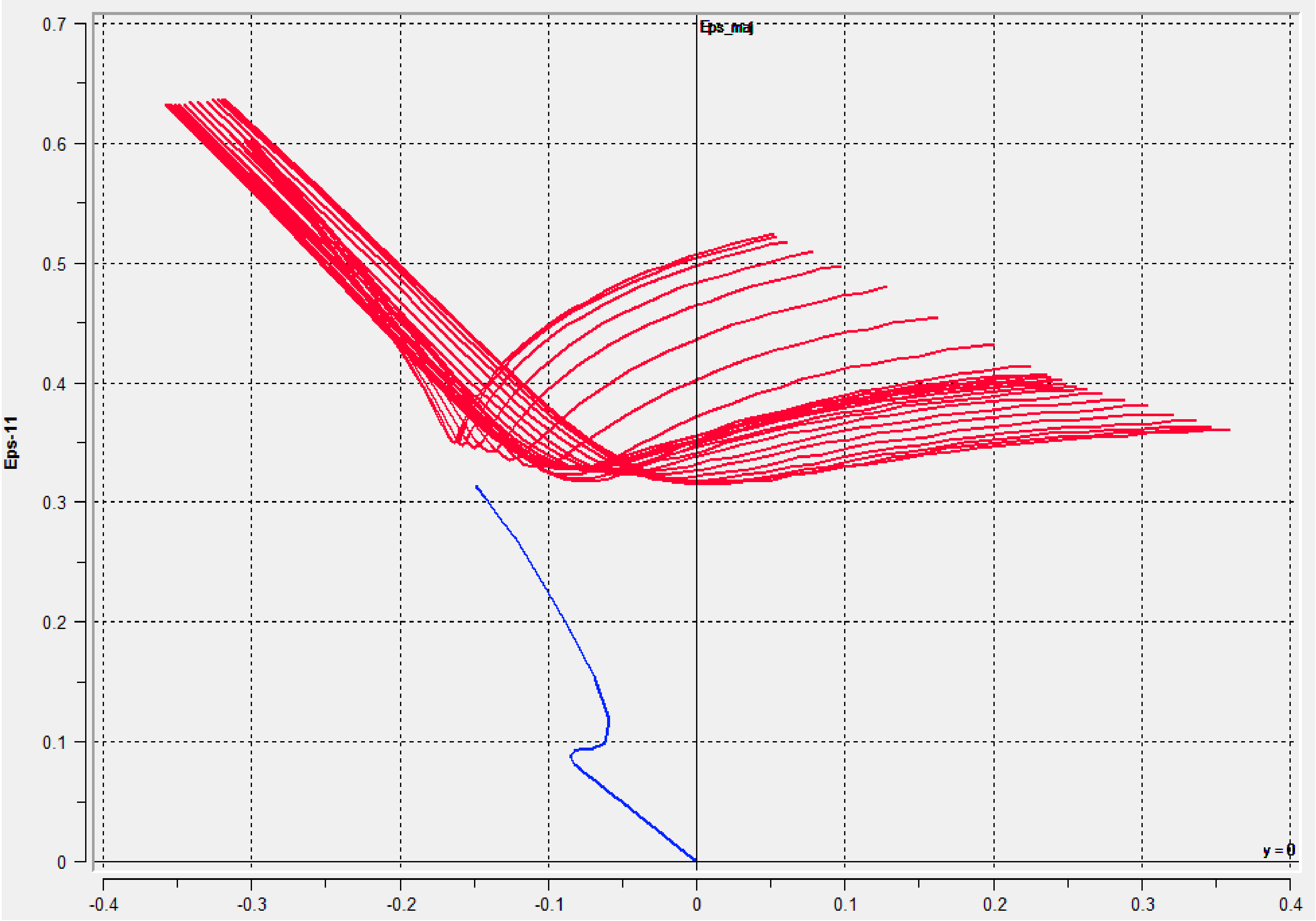
Eps_maj
Eps-11
0.7
0.6
0.5
0.4
0.3
0.2
0.1
0
-0.4 -0.3 -0.2 -0.1 0 0.1 0.2 0.3 0.4
y = 0

Example 2

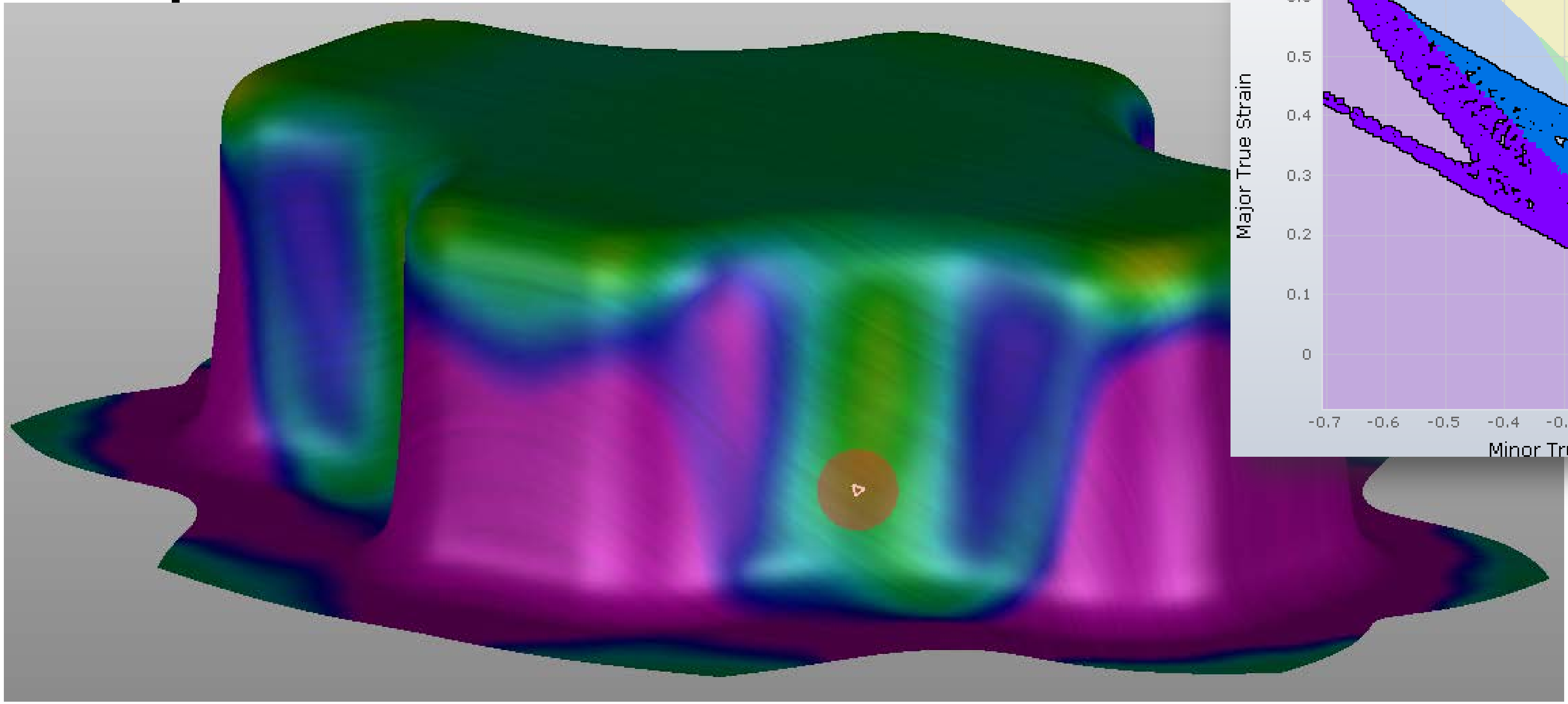

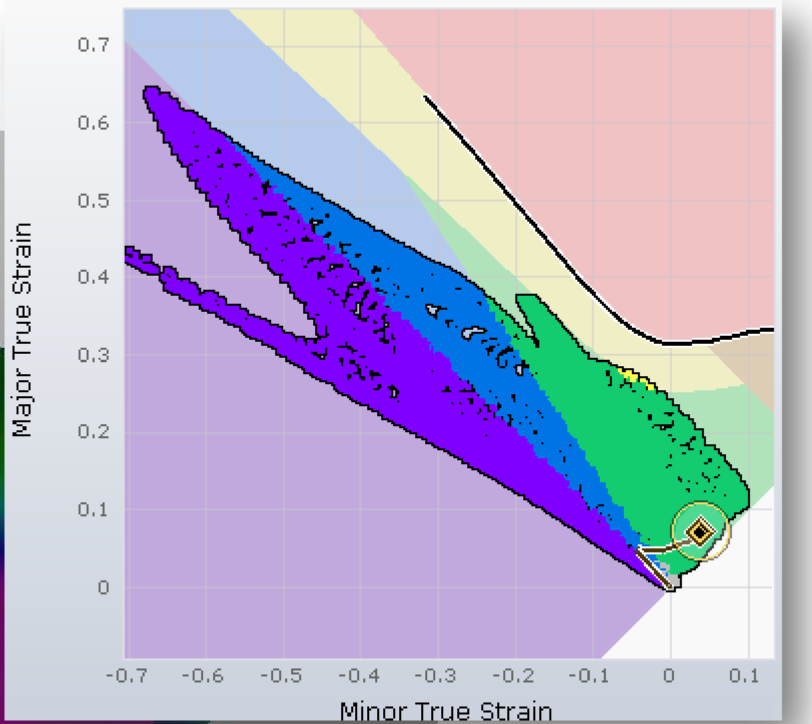
Major True Strain
Minor True Strain
0.7
0.6
0.5
0.4
0.3
0.2
0.1
0
-0.7
-0.6
-0.5
-0.4
-0.3
-0.2
-0.1
0
0.1

Example 2

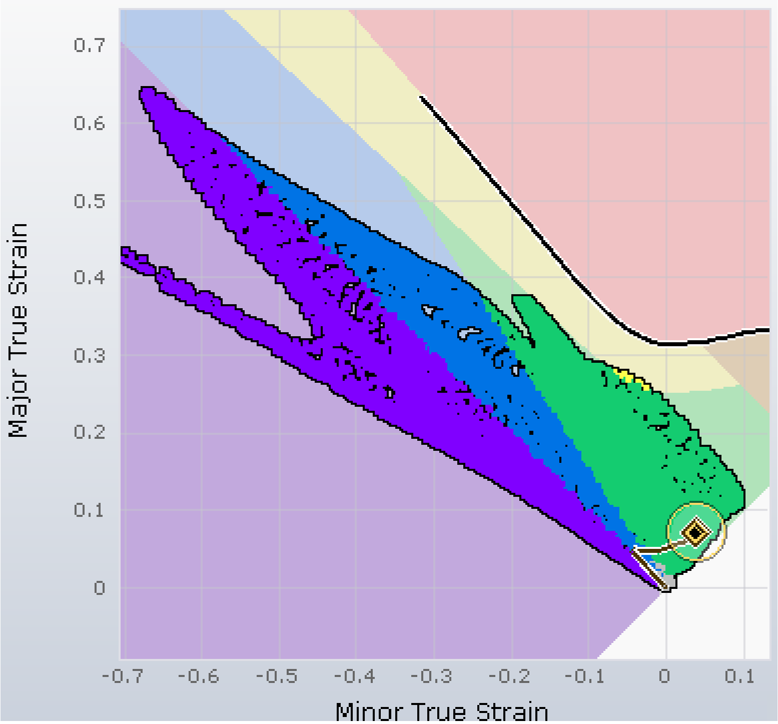
Major True Strain
Minor True Strain
0.7
0.6
0.5
0.4
0.3
0.2
0.1
0
-0.7
-0.6
-0.5
-0.4
-0.3
-0.2
-0.1
0
0.1

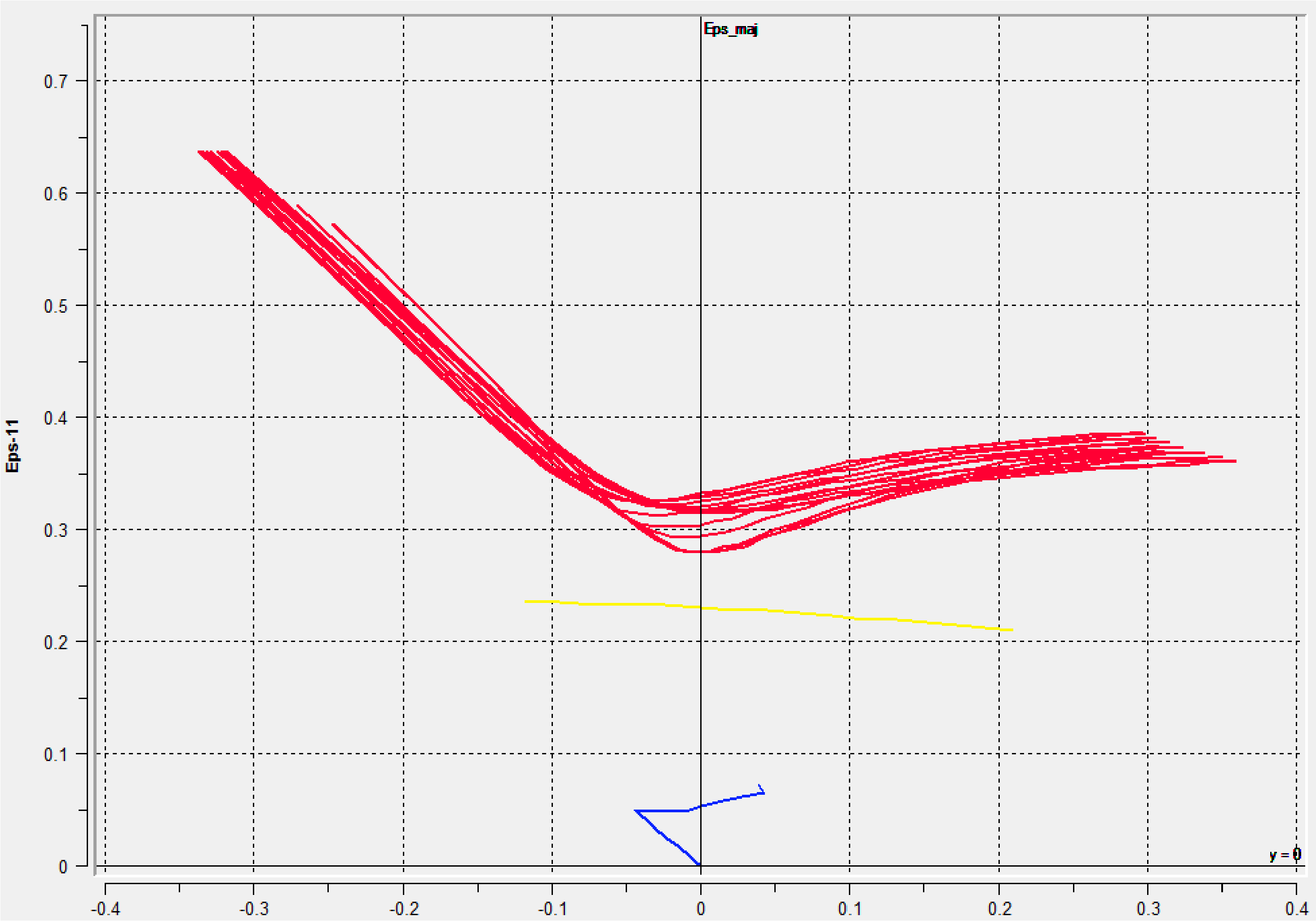
Eps_maj
Eps-11
y = 0
0.7
0.6
0.5
0.4
0.3
0.2
0.1
0
-0.4
-0.3
-0.2
-0.1
0
0.1
0.2
0.3
0.4

Example 3

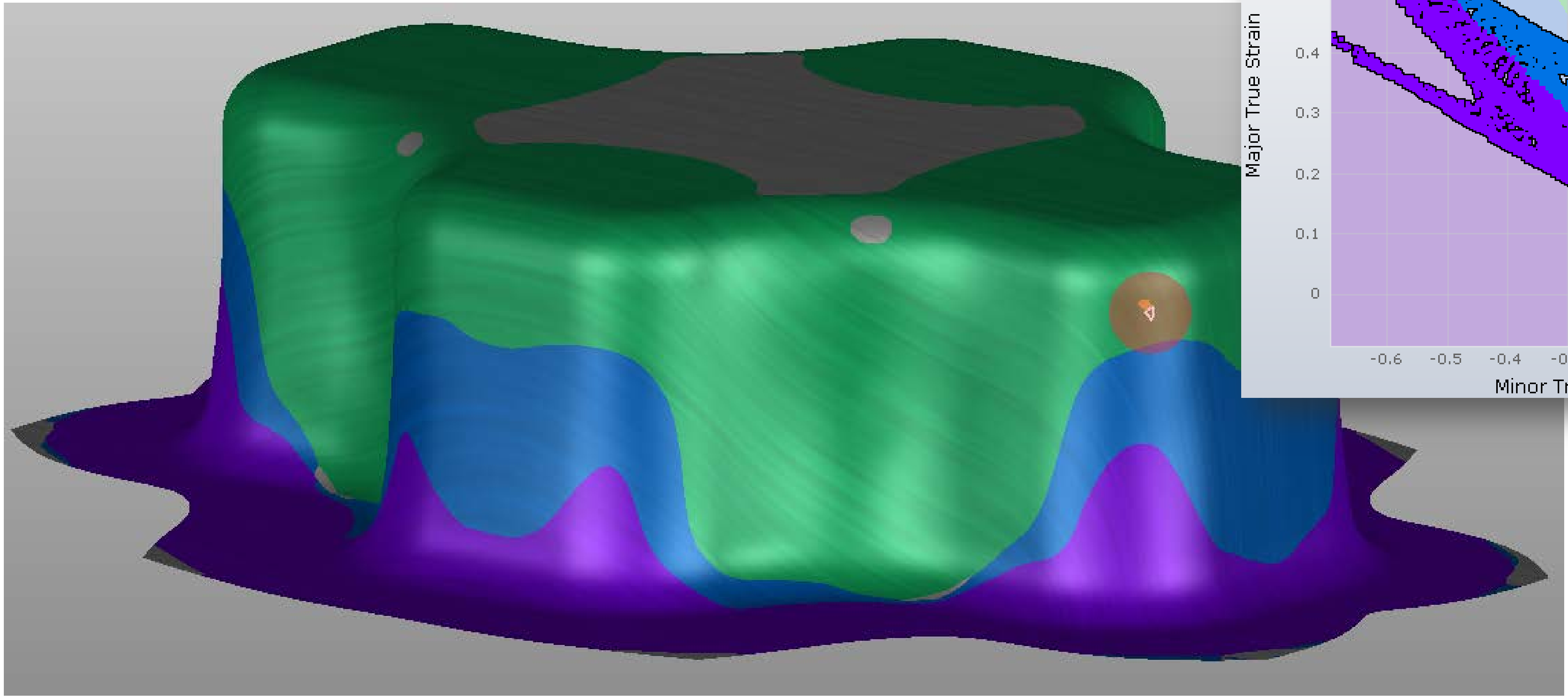

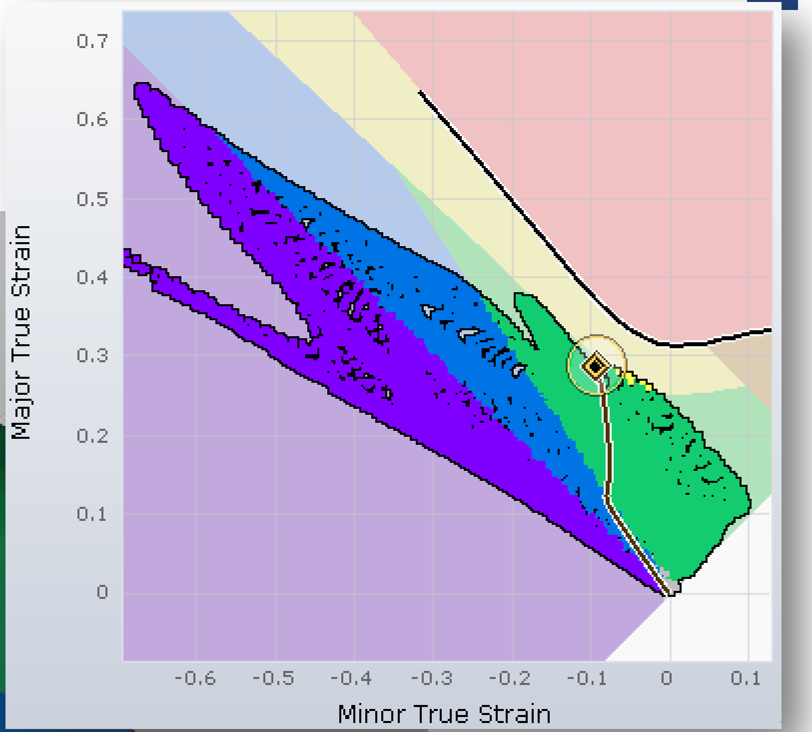
0.7
0.6
0.5
0.4
0.3
0.2
0.1
0
Major True Strain
-0.6
-0.5
-0.4
-0.3
-0.2
-0.1
0
0.1
Minor True Strain

Example 3

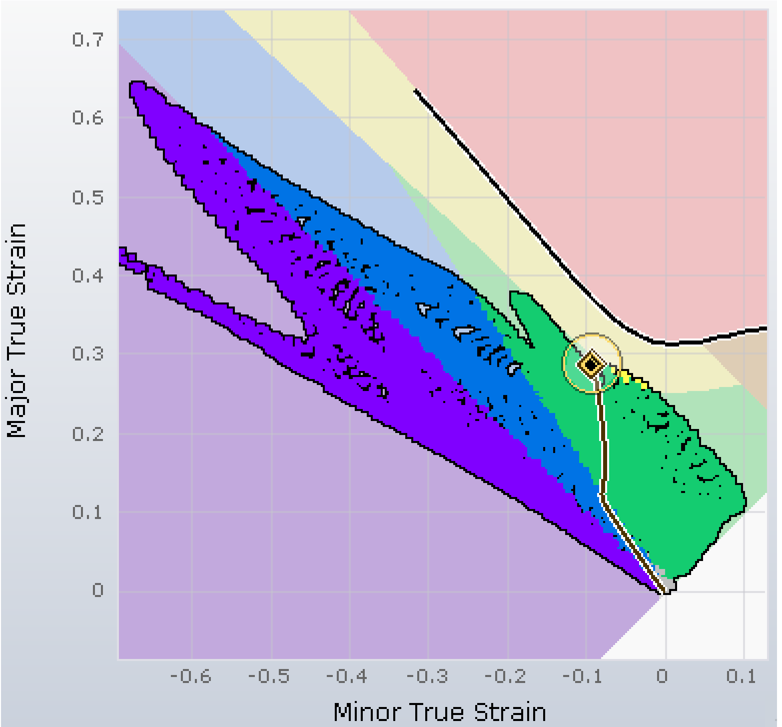
Major True Strain
Minor True Strain
0.7
0.6
0.5
0.4
0.3
0.2
0.1
0
-0.6
-0.5
-0.4
-0.3
-0.2
-0.1
0
0.1

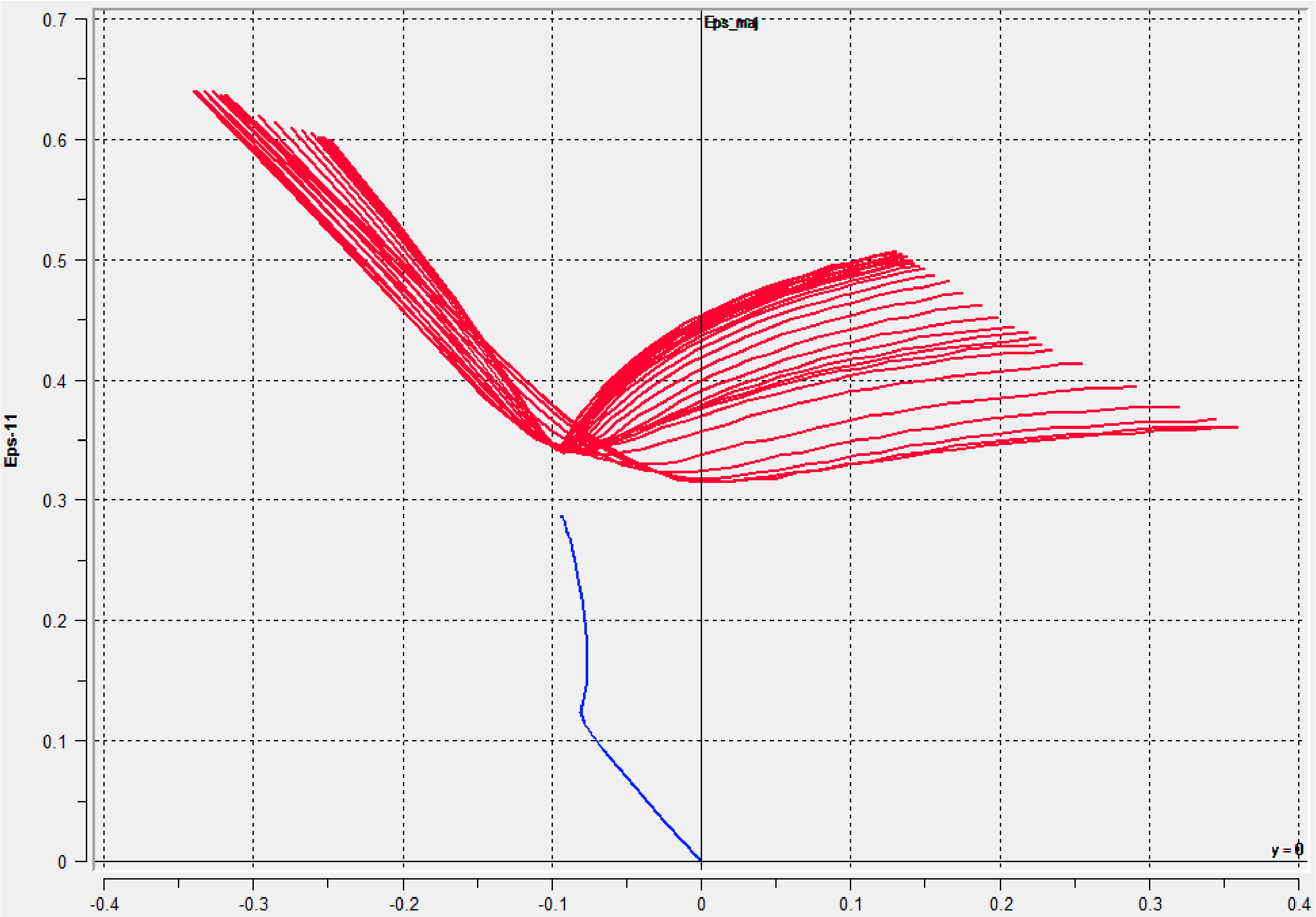
Eps_maj
Eps-11
y = 0
0.7
0.6
0.5
0.4
0.3
0.2
0.1
0
-0.4
-0.3
-0.2
-0.1
0
0.1
0.2
0.3
0.4

PART I
NECKING PREDICTION

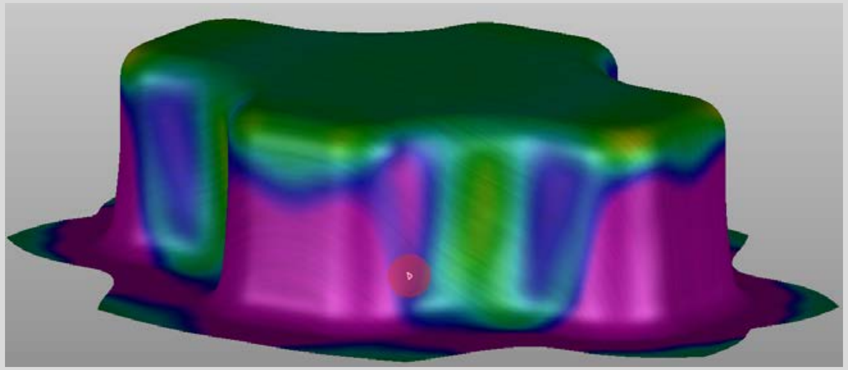

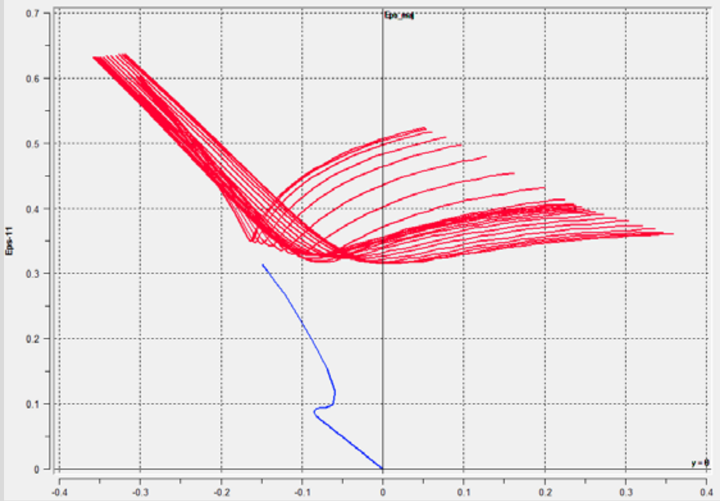

PART II
CRACK PREDICTION

Shear crack

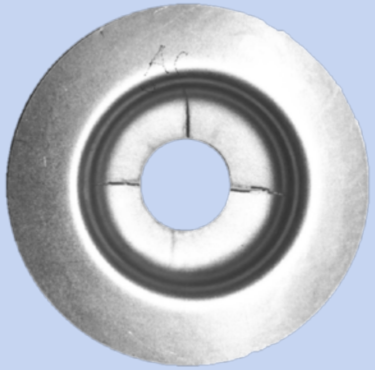

Edge crack

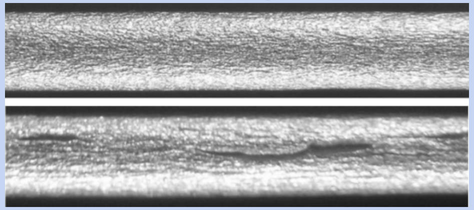

Bending crack

Content

1 **General topics in constitutive modeling**

2 **Necking prediction**

- Limitations of classical FLC based prediction methods
- FLC Limitations of Nakajima testing methods
- Advanced FLC methods (eMMFC)
- Prediction of non-linear strain-paths

3 **Crack prediction - Sheet specific fracture methods (X-FLC)**

- Different experimental methods
- Nakajima based experimental detection of crack (fracture) limits
- Application of X-FLC methods

4 **Conclusions**

Experimental tests for ε^f

Sheet

Instability by necking

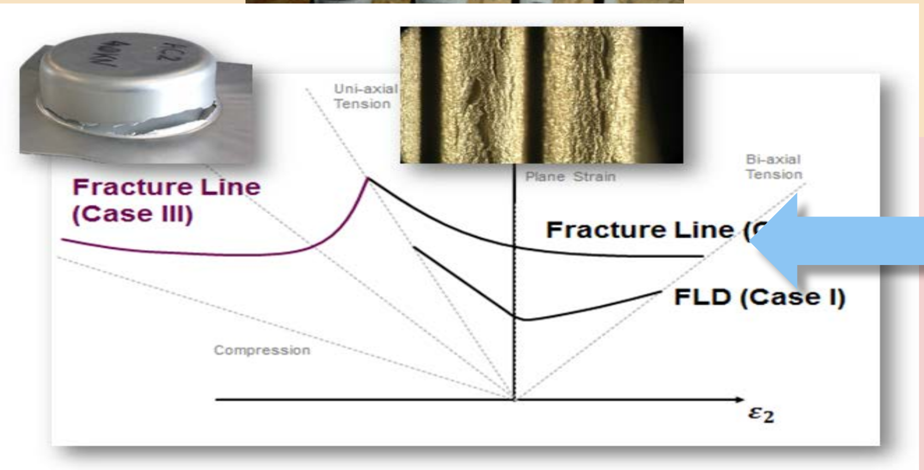

Fracture

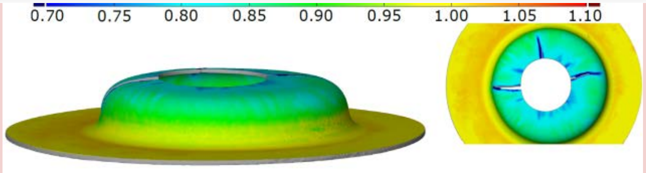

?

Bulk and sheet

Johnson-Cook: $\varepsilon^f(\sigma_H/\sigma_V)$

Triaxiality: $\varepsilon^f(\sigma_H/\sigma_{V,}$ Lode)

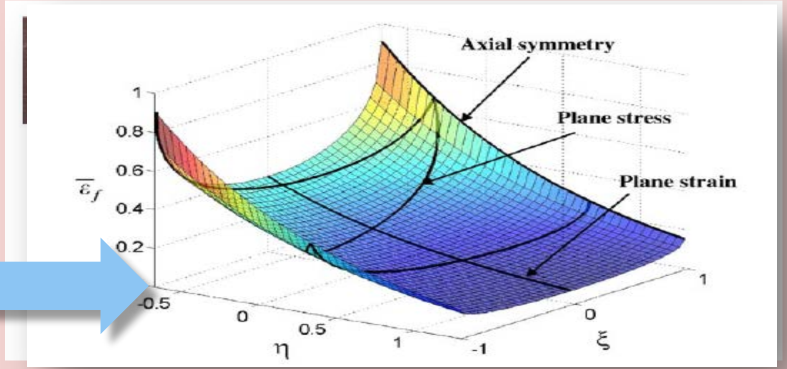

MD: Voids nucleation and growth

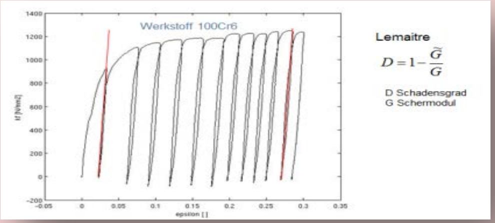

Influence of slight β>0 prestreching of Nakajima tests

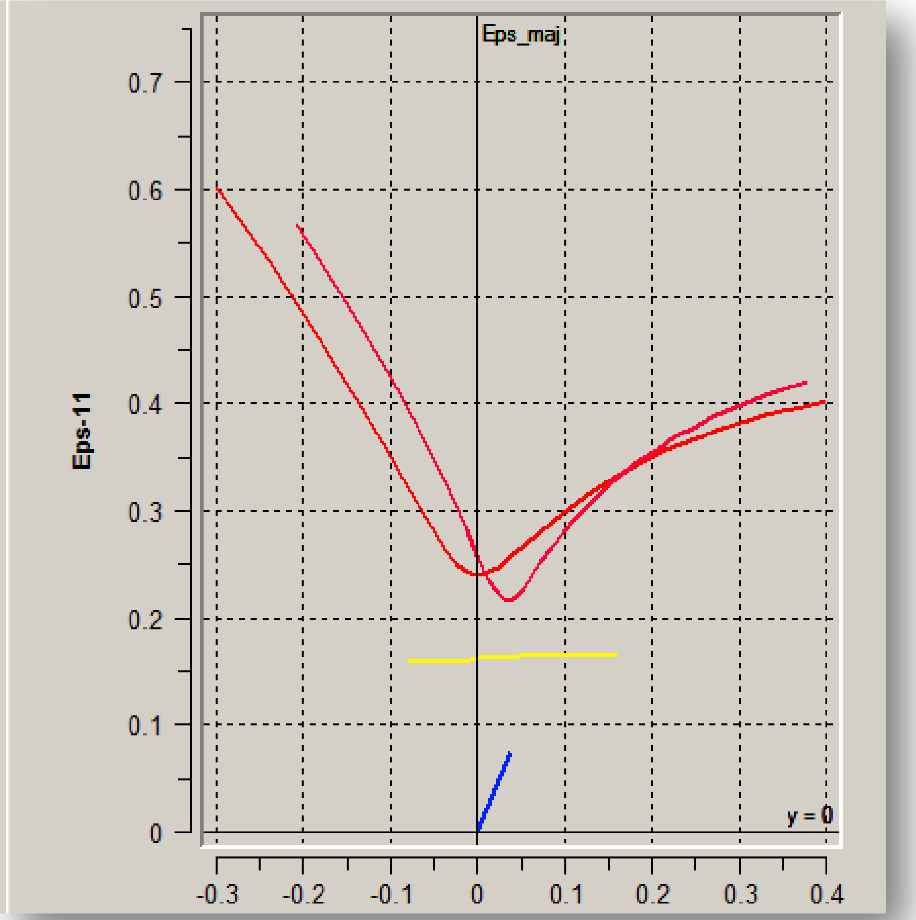

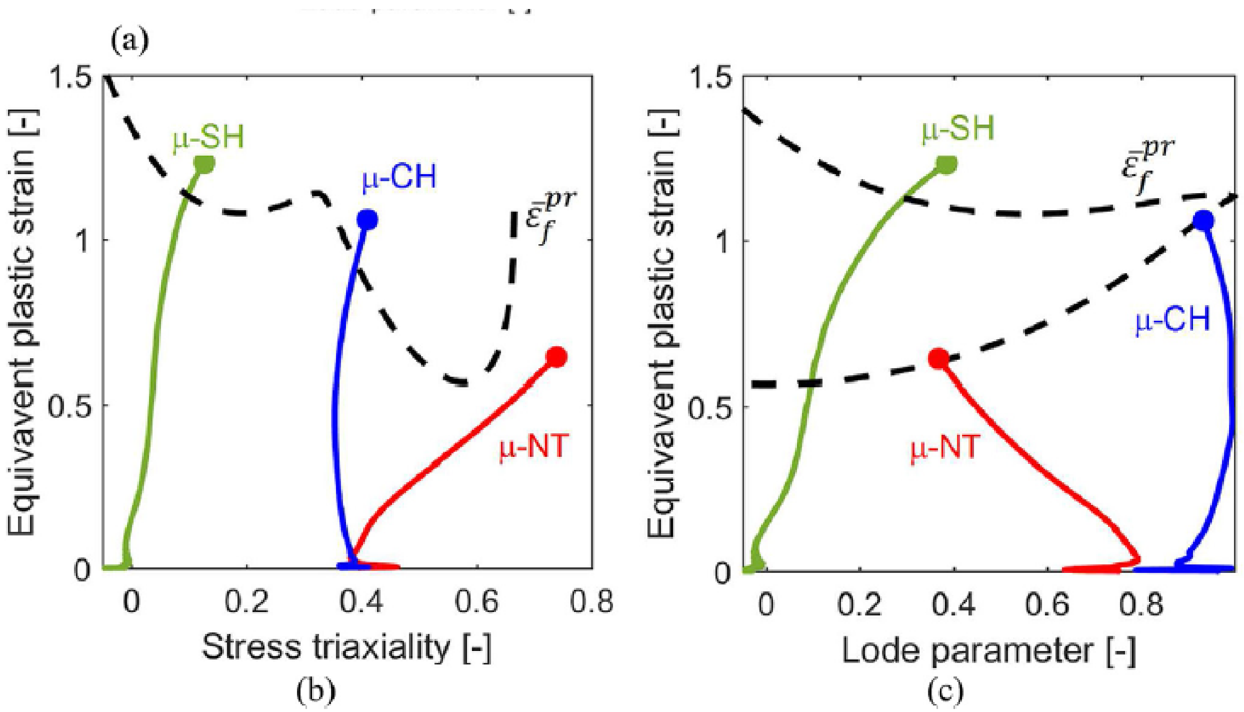

Sheet specific evaluation of fracture strains:

Thinning method

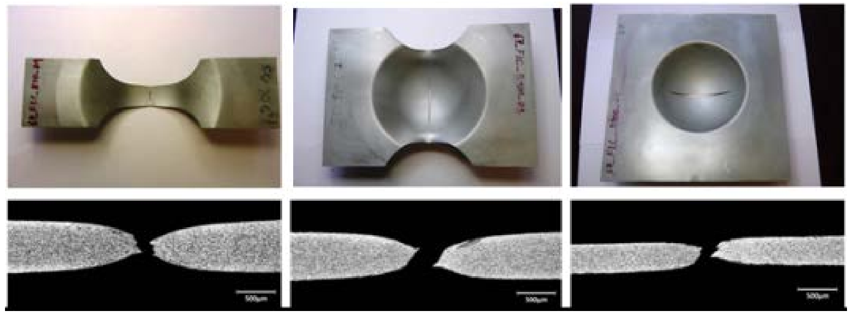

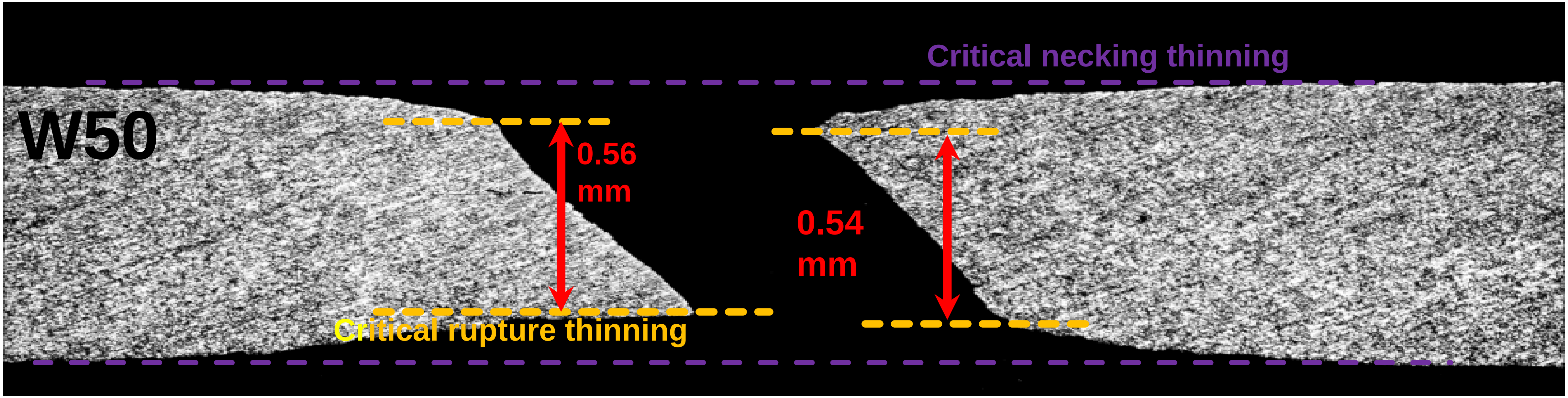

Source: M. Gorji, B. Berisha, P. Hora, F. Barlat. Modeling of Localization and Fracture Phenomena in Strain and Stress Space for Sheet Metal Forming, International Journal of Material Forming, 2015

Thinning method: Nakajima

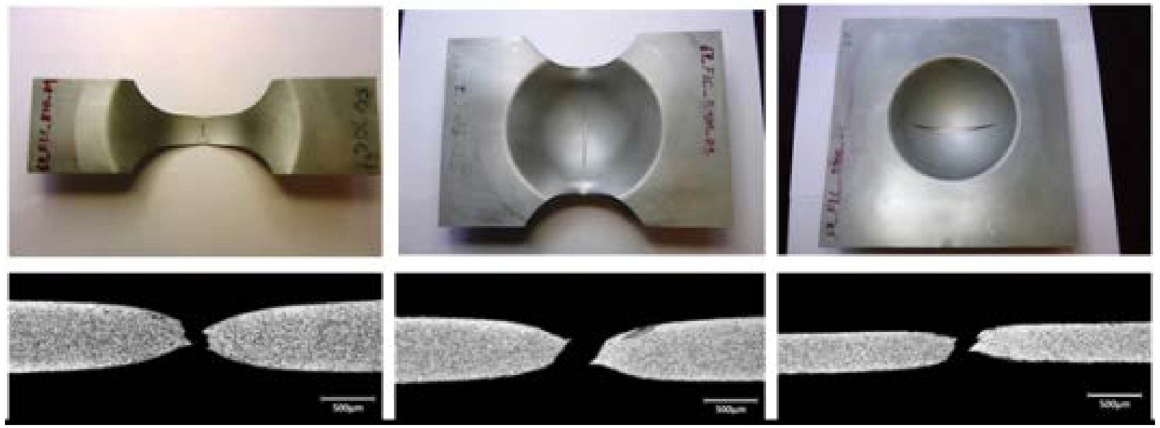

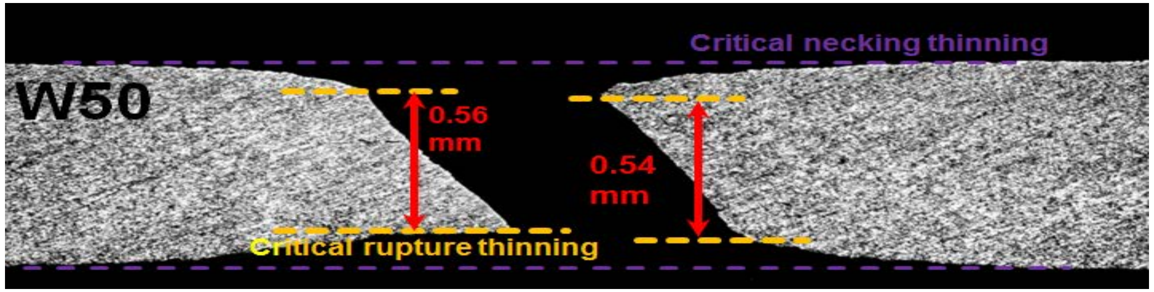

Cup drawing test

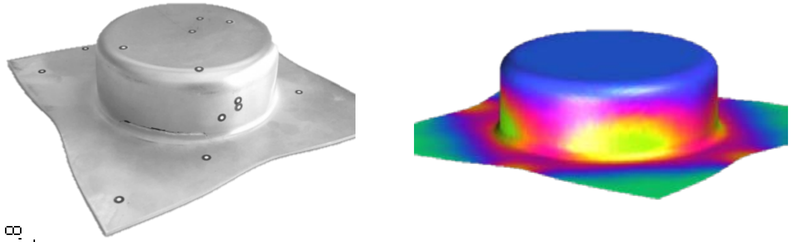

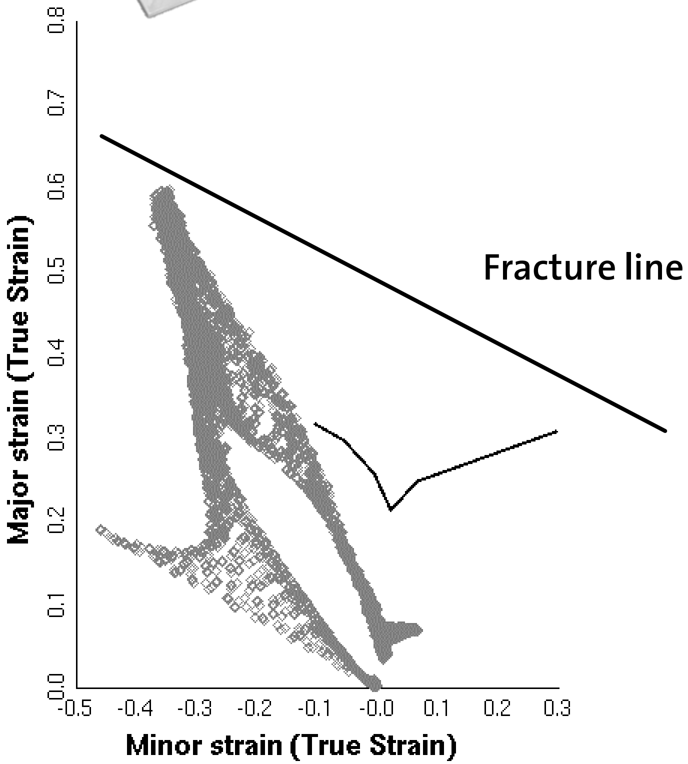

… how to deal with in-plane shear cracks ?

Out-of-plane and in-plane shear cracks on sheets

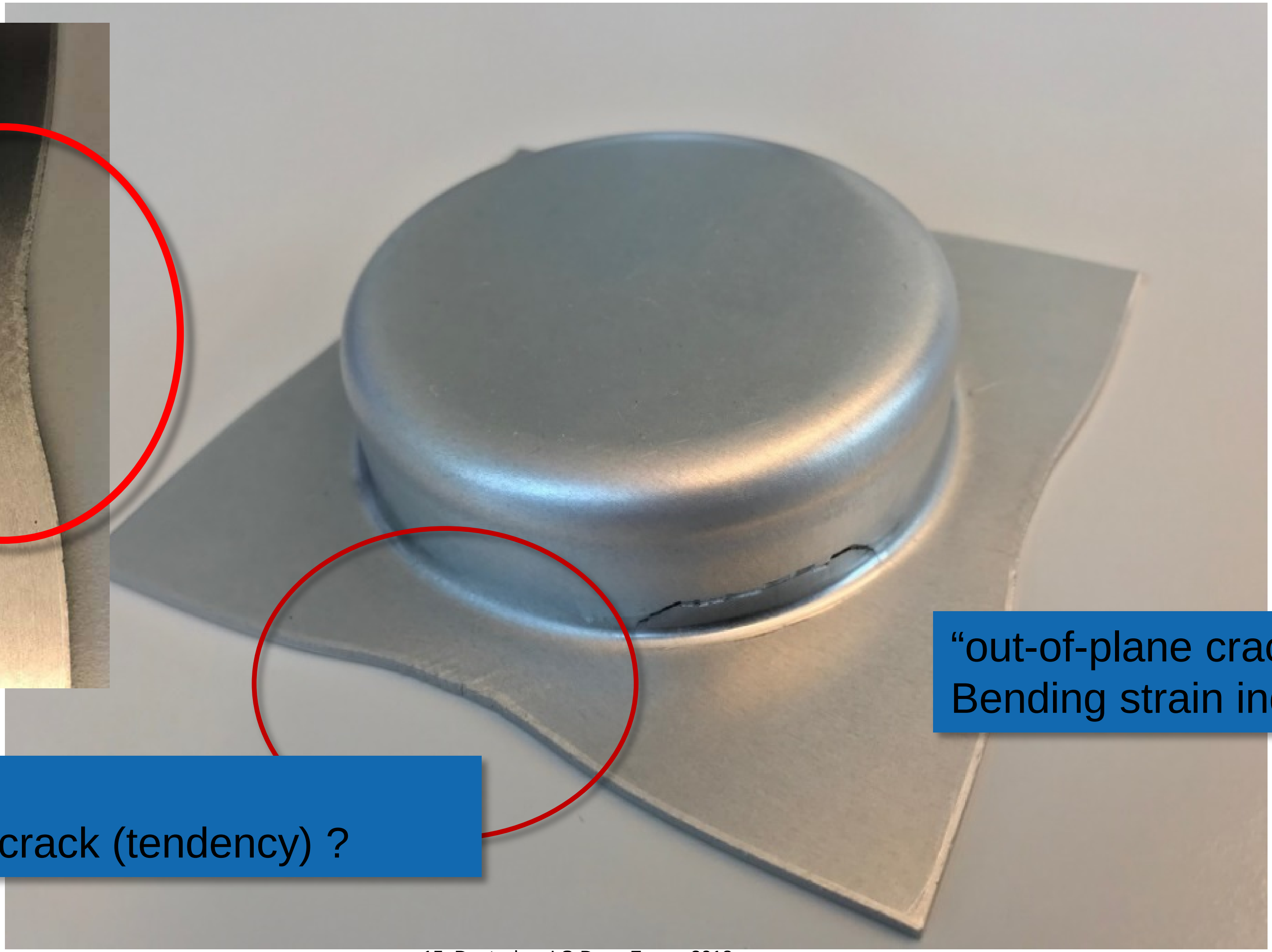

“out-of-plane crack”
Bending strain induced shear crack

“in-plane crack”
Outer line shear crack (tendency) ?

Cup Drawing
Results

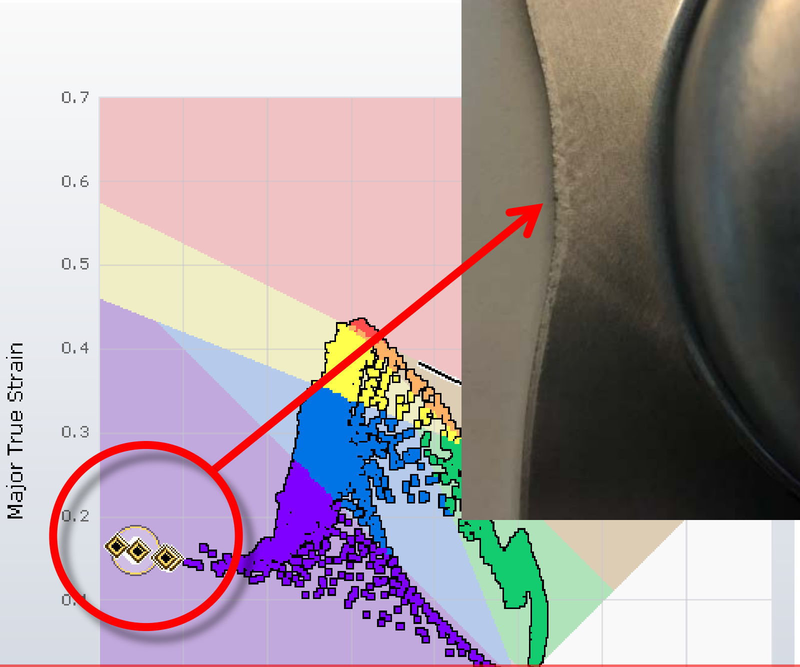

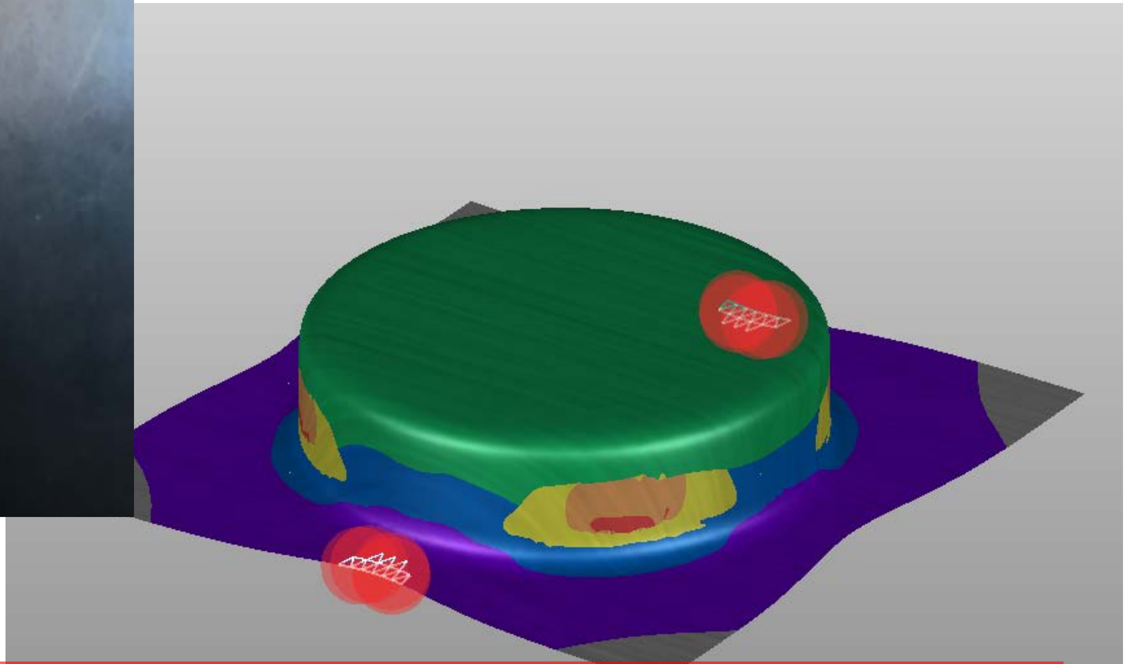

Edge cracks: strain limits strongly influenced by the edge quality

Application of the thinning method

Diss. M. Gorji ETH 2015

Development of combined neckig-crack failure models for multilayer Al-sheets (FUSION)

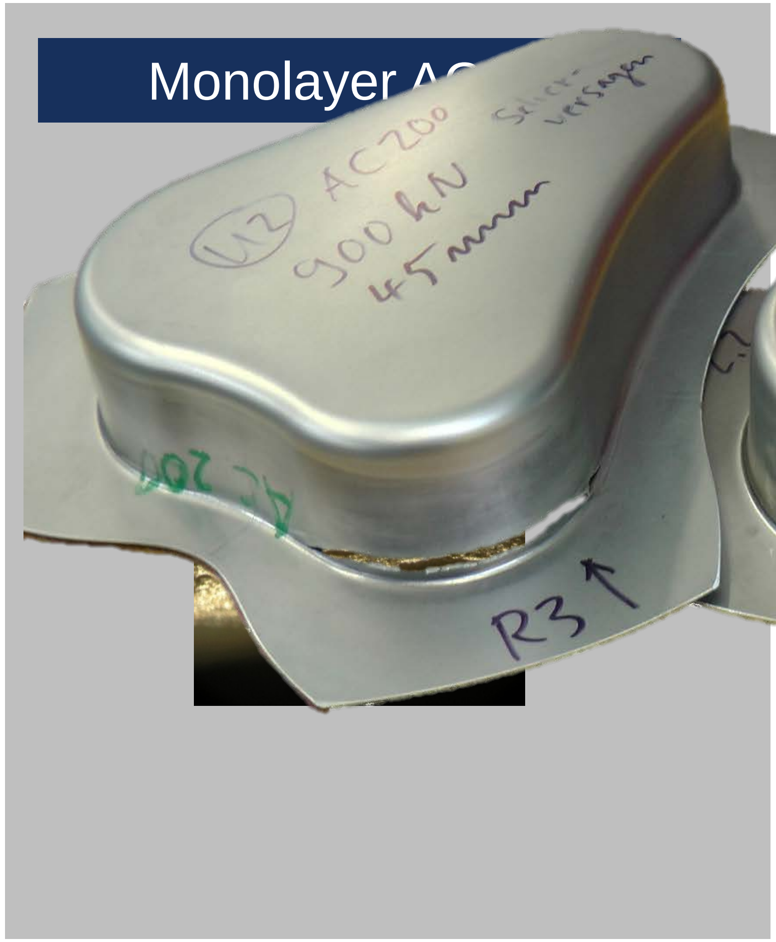

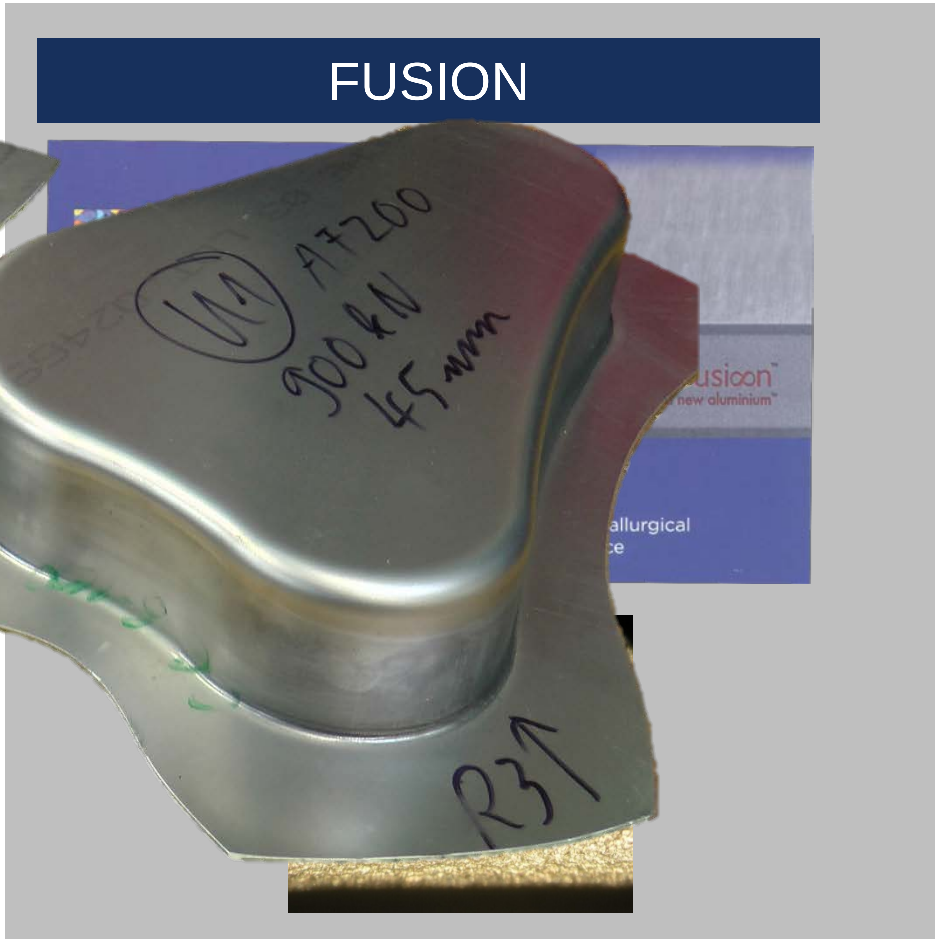

Source: M.Gorji Diss. ETH 2015

Fracture Strain based on Thinning Method

Source: M. Gorji, B. Berisha, P. Hora, F. Barlat. Modeling of Localization and Fracture Phenomena in Strain and Stress Space for Sheet Metal Forming, International Journal of Material Forming, 2015

Clad material AA5005

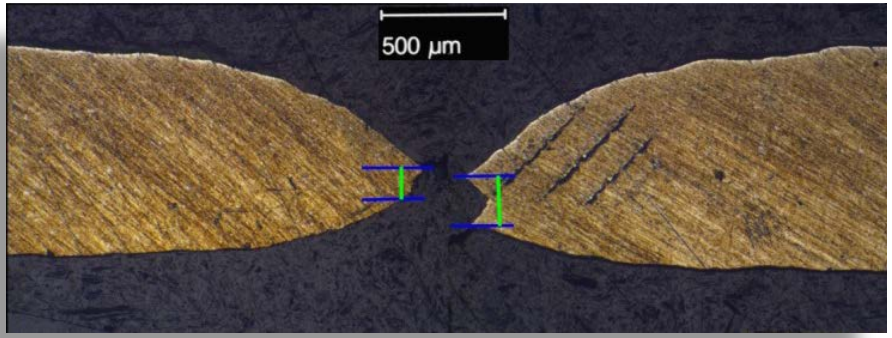

Core material AA6016

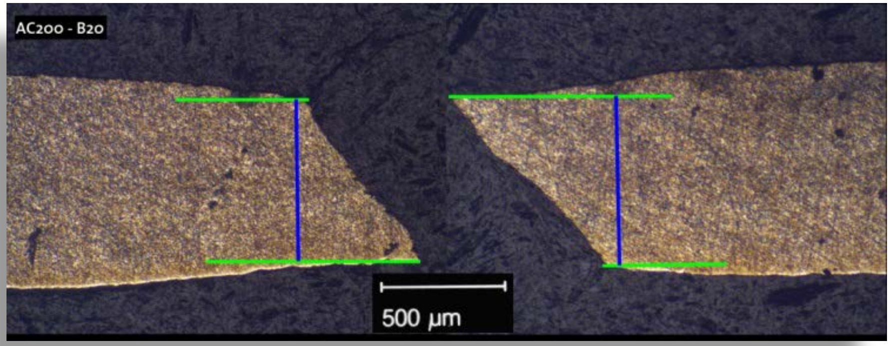

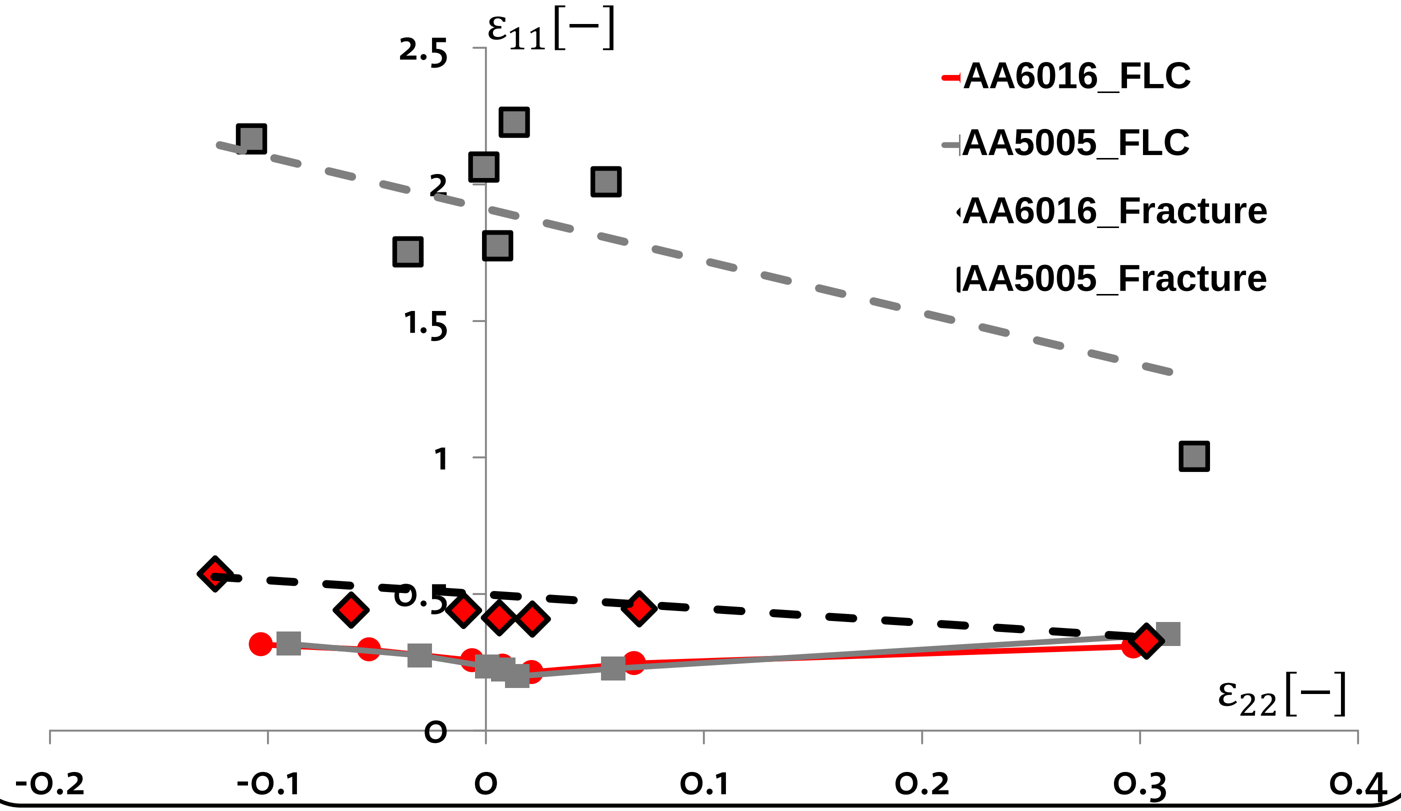

For Fusion, both materials (core and clad) lead to similar FLCs. This means that uniform elongation and FLC do not improve by soft cladding.

FEM evaluation method (LS-Dyna)

In the LS-Dyna code the implementation was done by the subroutine **UMAT41**.

The ***PART COMPOSITE** functionality of FE-code LS-Dyna has been employed instead of the regular shell element.

Based on this element formulation the mechanical properties and thickness distribution of each layer can be described separately.

Published in IDDRG 2016, Linz
P. Hora, M.Gorji, B.Berisha: Modelling of fracture effects in the sheet metal forming based on an extended FLC evaluation method in combination with fracture criterions

Model IV) Linear fracture line – AA6016

Drawing depth 35 mm

Lower layer

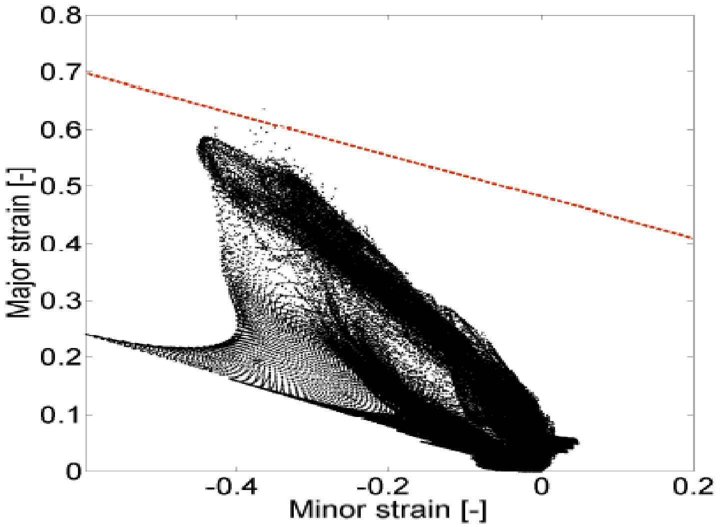

Middle layer

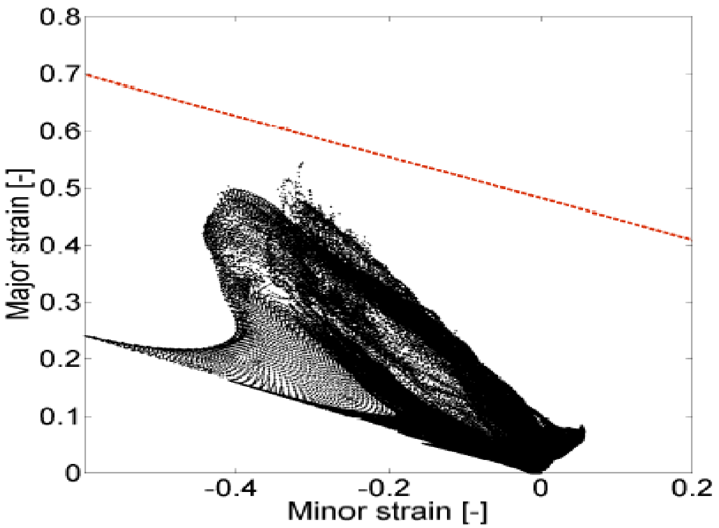

Upper layer

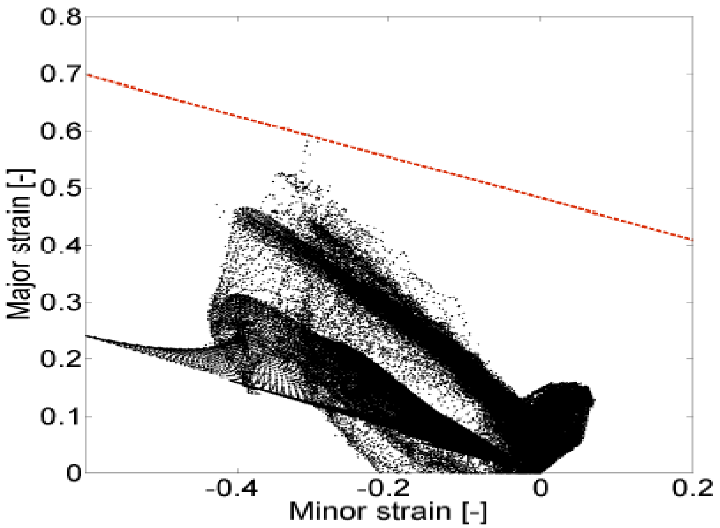

Fracture line is measured based on the thinning method (by using Nakazima test) and cup drawing experiment

Model IV) Linear fracture line – AA6016

Drawing depth **40 mm**

Lower layer	Middle layer	Upper layer

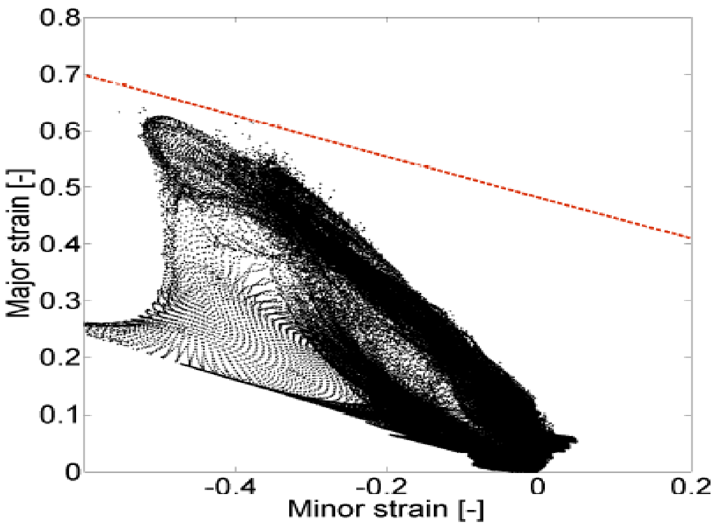

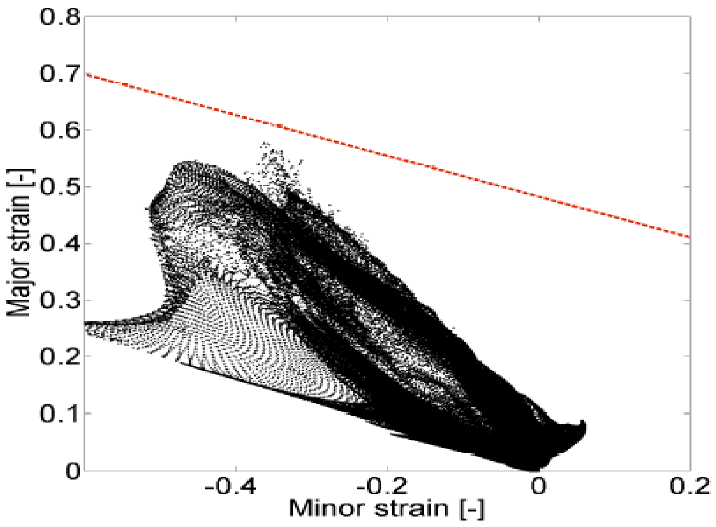

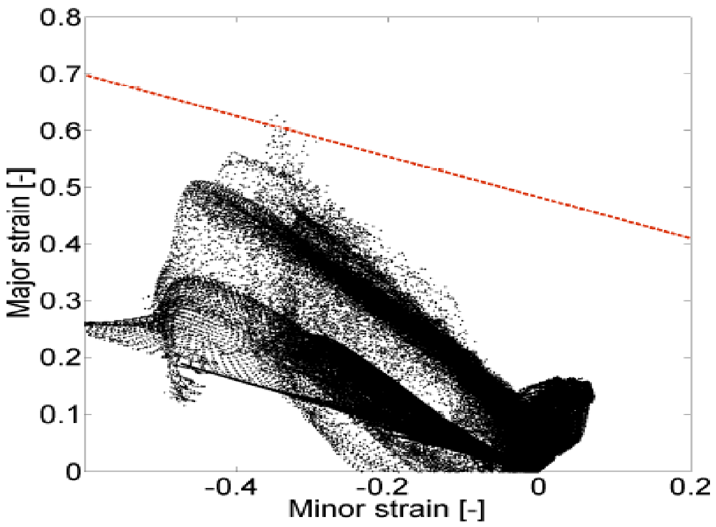

Fracture line is measured based on the thinning method (by using Nakazima test) and cup drawing experiment

Model IV) Linear fracture line – AA6016

Drawing depth 45 mm

Lower layer	Middle layer	Upper layer
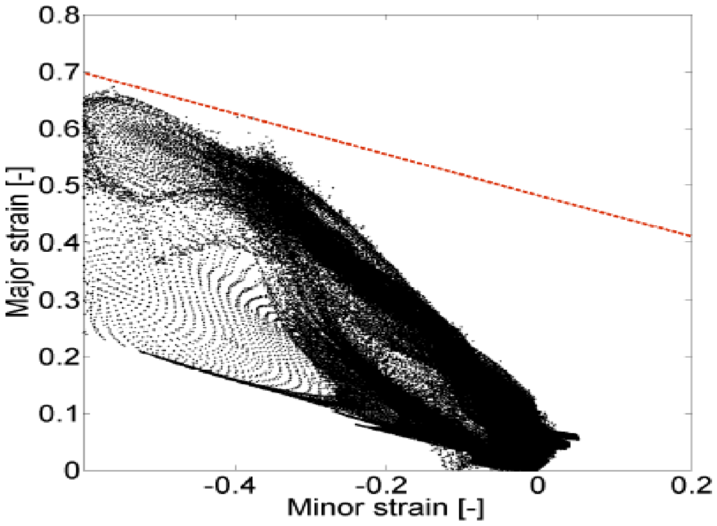	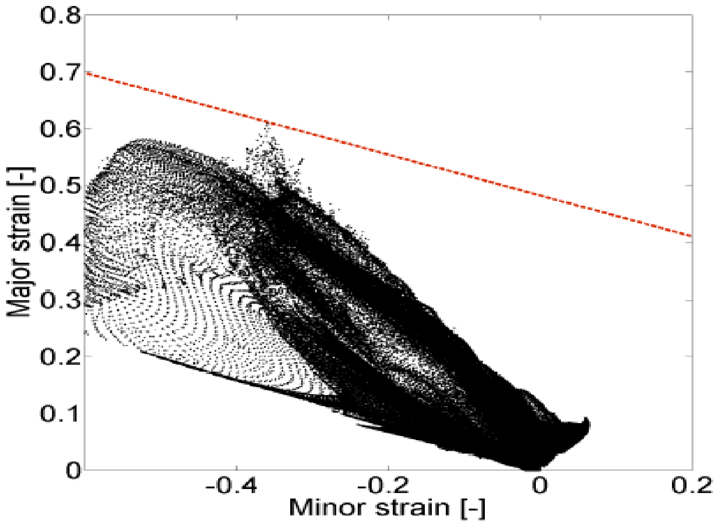	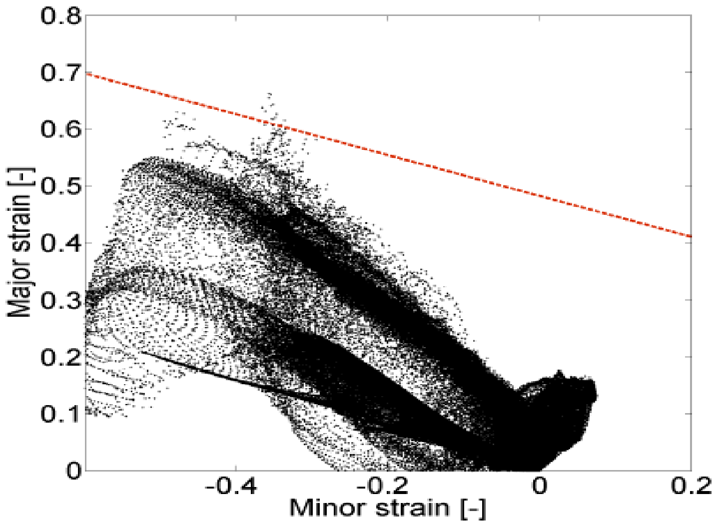

Fracture line is measured based on the thinning method (by using Nakazima test) and cup drawing experiment

Monolayer AC170

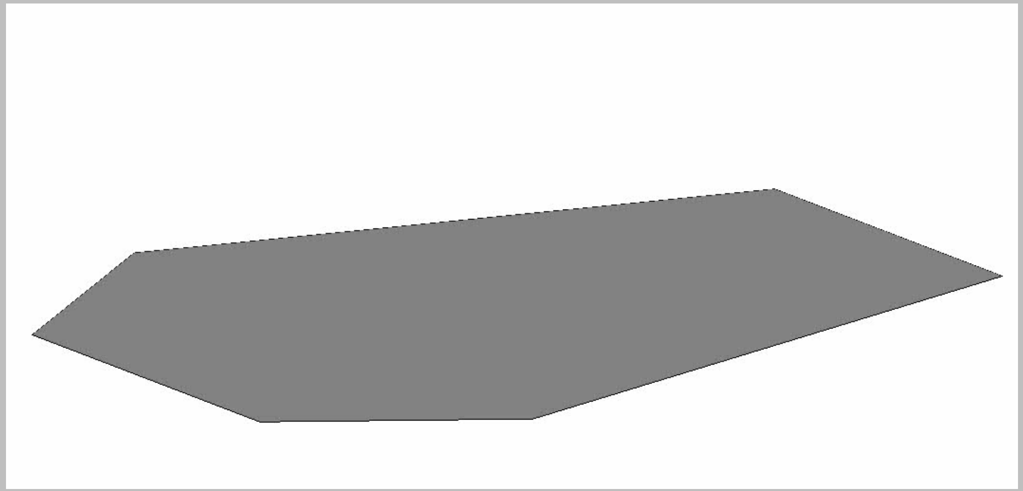

FUSION

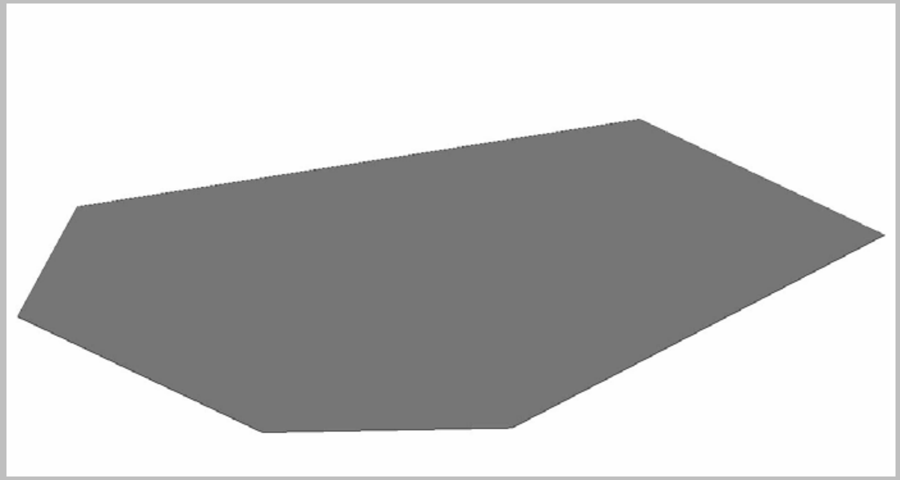

Source: M.Gorji Diss. ETH 2015

Content

Summary and Conclusion

Influence of Curvature

- FLC for small bending radii may change significantly compared to the classical FLC
- Stretch bending test proves such dependencies.
- A possible theoretical prediction is given with the eMMFC criterion

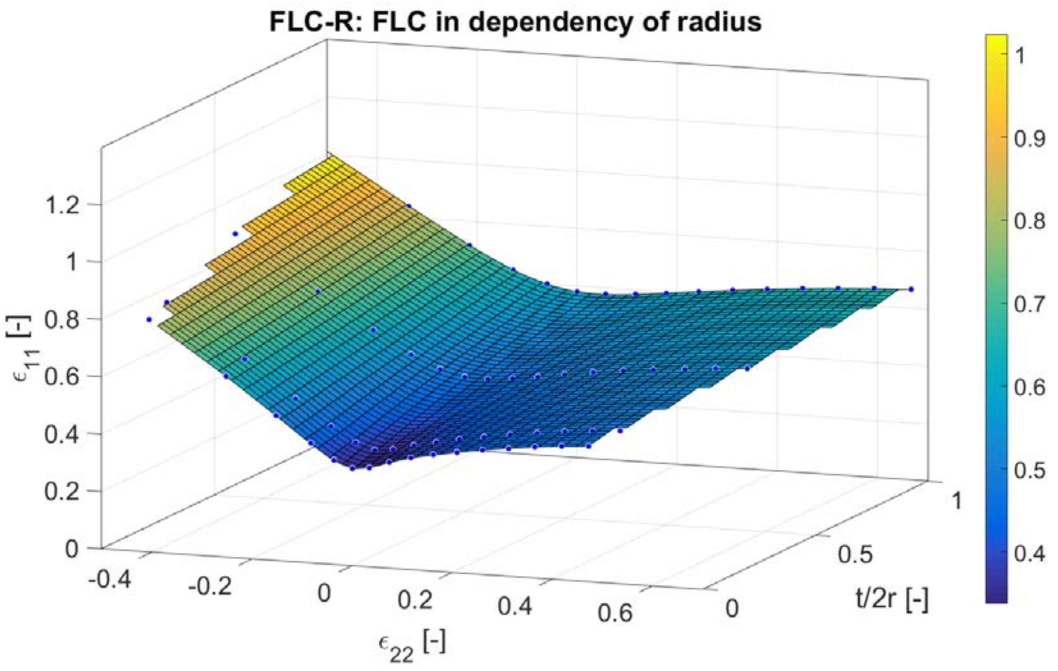

Summary and Conclusion (2)

Necking prediction – non-linear FLC

- The eMMFC based FLC prediction seems to deliver reasonable FLC curves.
- It can be simply applied for the visualization of the non-linear path influence on the FLC shape.

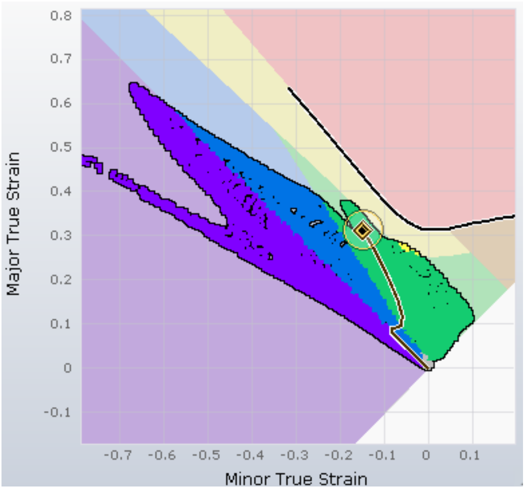

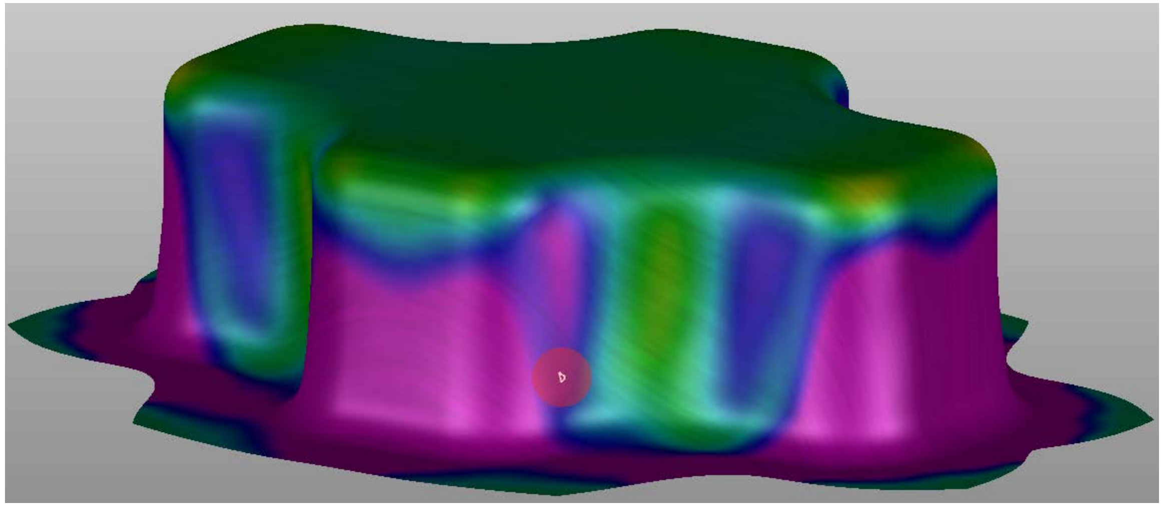

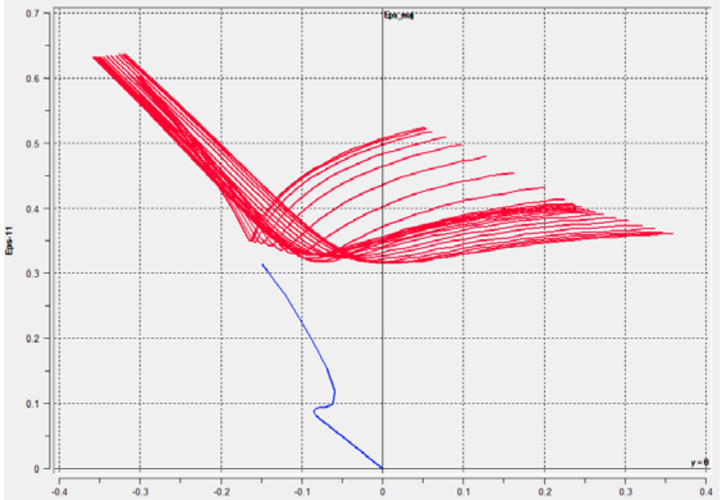

Summary and Conclusion (3)

Prediction of cracks

- For the detection of the fracture line ε^f (β) specimens of the classical Nakajima test and a special designed cup drawing test have been used.
- The proposed "thinning evaluation method" in combination with an additional cup drawing test allow a very accurate detection of fracture strains ε^f.
- The combined method allows the prediction for multilayer materials too

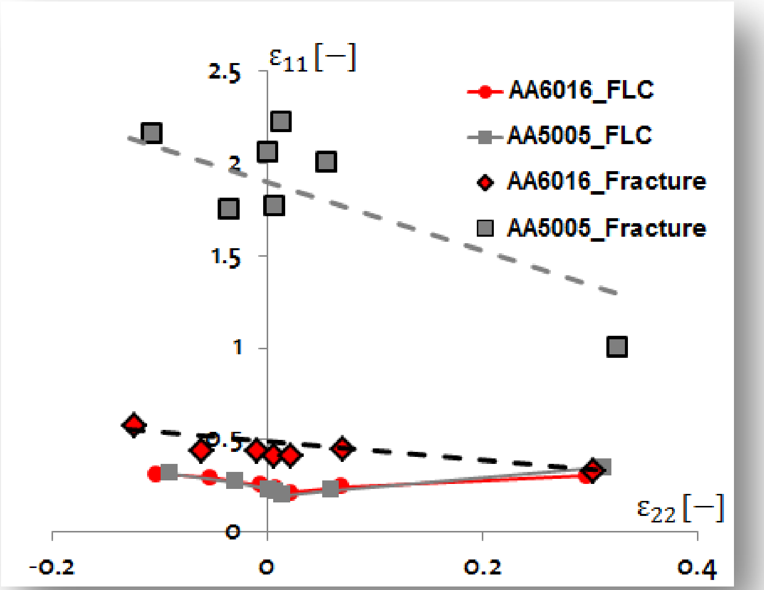

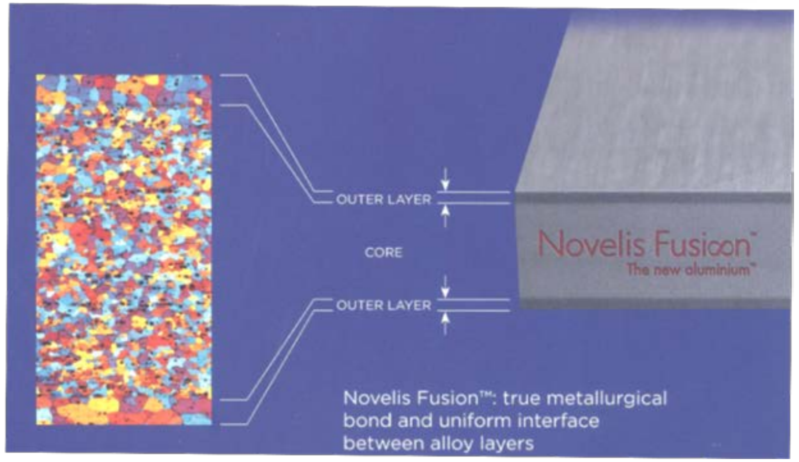

15. Deutsches LS-Dyna Forum 2018

Integration neuer graphischer Auswertemethoden zur verbesserten Erkennung von Blechversagen unter dem Einfluss nicht-linearer Dehnungspfade

P. Hora, L. Tong, N. Manopulo, M. Gorji, R. Schober + Prof. W. Volk, Ch.Gaber , UTG

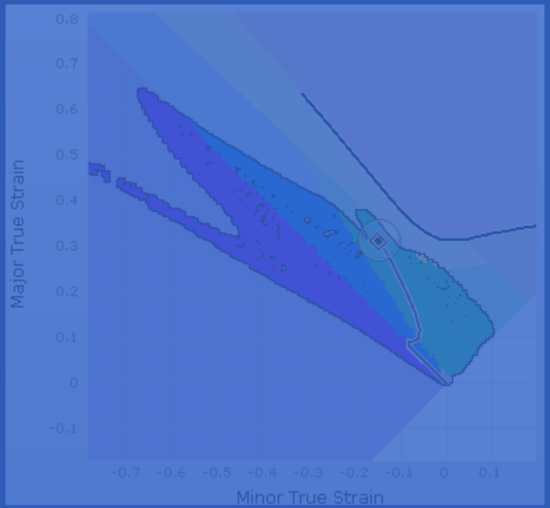

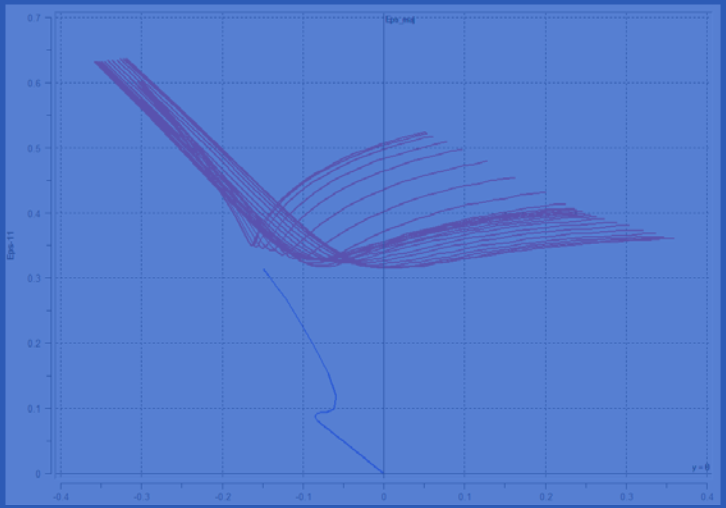

Thank you for your attention

www.ivp.ethz.ch